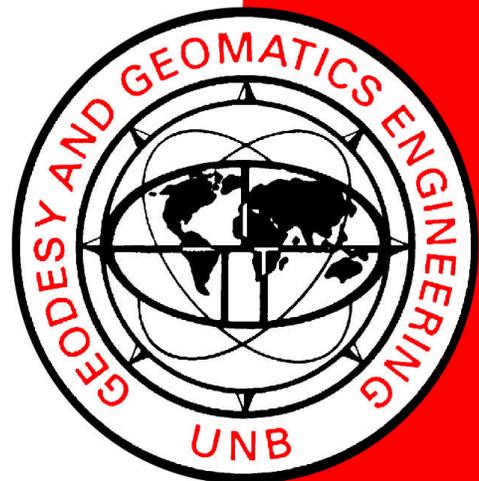# AN INVESTIGATION ON THE USE OF GPS FOR DEFORMATION MONITORING IN OPEN PIT MINES

JASON BOND

March 2004

AN INVESTIGATION ON THE USE OF GPS FOR DEFORMATION MONITORING IN OPEN PIT MINES

Jason Bond

Department of Geodesy and Geomatics Engineering
University of New Brunswick
P.O. Box 4400
Fredericton, N.B.
Canada
E3B 5A3

March 2004

PREFACE

This technical report is an unedited reproduction of a thesis submitted in partial fulfillment of the requirements for the degree of Master of Science in Engineering in the Department of Geodesy and Geomatics Engineering, March 2004. The research was supervised by Dr. Adam Chrzanowski and co-supervised by Dr. James Secord, and funding was provided by NSERC, the Natural Sciences and Engineering Research Council of Canada.

As with any copyrighted material, permission to reprint or quote extensively from this report must be received from the author. The citation to this work should appear as follows:

Bond, J. (2004). *An Investigation on the Use of GPS for Deformation Monitoring in Open Pit Mines.* M.Sc.E. thesis, Department of Geodesy and Geomatics Engineering Technical Report No. 222, University of New Brunswick, Fredericton, New Brunswick, Canada, 140 pp.

ABSTRACT

In order to implement GPS for deformation monitoring purposes, sub-centimetre displacements must be detected in all three directional components. These results must be attained with such frequency as to provide sufficient warning of impending danger. In applications such as open pit mining where unfavourable conditions exist for GPS, this requirement is particularly challenging to meet.

This research determines what accuracy can be expected in an unfavourable GPS environment. GPS data which have been collected in a large open pit mine are analyzed using optimal software settings determined from a nearly ideal scenario.

It is shown that GPS can be used to augment the current robotic total station deformation monitoring system used at this mine site to obtain sub-centimetre accuracy displacement values at 95%. The potential of improving these results through processing strategies and new technology is also investigated.

TABLE OF CONTENTS

LIST OF FIGURES

LIST OF TABLES

ACKNOWLEDGEMENTS

1 INTRODUCTION

Safety and profit are two primary concerns of the mining industry. A well-operated mine maximizes profit without sacrificing the safety of its workers. Implementing a deformation monitoring system to monitor the stability of the mine is a rational approach to addressing both of these needs.

Over the last two decades, the Global Positioning System (GPS) has been perhaps the most influential positioning technology to emerge. GPS offers several advantages over other types of technology: it requires minimal user interaction (and therefore can be cost effective); it provides 3-dimensional position information; GPS equipment can be much less expensive than other sensors; and it can be easily customized for automation. It is not surprising, then, that mining operations are looking to implement GPS as a stand alone or augmenting deformation monitoring system for their mine site.

As the mining industry looks to GPS as a tool for deformation monitoring, the expertise of geomatics engineers specializing in geodetic surveys is sought. Unfortunately, at the present time, there is not a wealth of information available on this particular application in the mining industry. The Canadian Centre for Geodetic Engineering (CCGE) at UNB has conducted significant research into designing and implementing a fully automated deformation monitoring system which uses GPS and robotic total stations to monitor deformations [Wilkins *et al*., 2003a].

Since the uncertainty in the vertical component of a GPS solution is about three times worse than in the horizontal, applications requiring precise vertical solutions (monitoring ground subsidence, deformation monitoring of bridges, dams and buildings and slope stability monitoring) push GPS to the limits of its abilities. In order to obtain high precision position solutions, meticulous efforts must be made to contain all GPS error sources.

Several methods have been put forth for implementing GPS for monitoring sub-centimetre displacements [Radovanovic, 2000; Wubbena *et al.,* 2001; Dai *et al.,* 2001]. Unfortunately, many of these techniques have been tested experimentally in ideal conditions. Real-world situations that have limited satellite coverage, high multipath environments or large height differences between reference and rover stations will generally yield poorer results than in ideal conditions.

This research focuses on evaluating the potential of GPS as a tool in a high precision deformation monitoring system in large open pit mines. This topic stems from one of the Canadian Centre for Geodetic Engineering's current projects at Highland Valley Copper (HVC) mine, British Columbia, Canada. HVC, which may be considered a harsh GPS environment, is used as an example. Although the GPS conditions at HVC are unfavourable, they are realistic and represent conditions that are likely to exist in other mining operations. The desired accuracies for this application are most demanding: +/- 5 mm in each solution component (N, E, H) at a 95% confidence level.

2

1.1 <u>Purpose</u>

This research is part of the ongoing efforts at the Canadian Centre for Geodetic Engineering at the University of New Brunswick to develop techniques for deformation monitoring. The underlying motivation was to determine whether or not GPS can, in practice, be used to monitor sub-centimetre displacements in three dimensions (N, E, H) in an unfavourable environment. By testing GPS and GPS processing techniques in a real-world situation, a realistic picture of achievable results was attained. More specifically, the following objectives were presented in order to achieve this goal:

1.   To compare the flexibility, user friendliness and solution reliability of commercial and scientific GPS processing software.

2.   To determine the settings and variables which optimize the GPS vertical component solution with regard to:

      a.   Session Length;

      b.   Tropospheric Model;

      c.   Observation Sample Rate;

      d.   Elevation Cut-off Angle; and

      e.   Time of Day of Observations.

3.   To evaluate the effectiveness of processing techniques used to improve the GPS solution in high precision surveys.

4.   To investigate the benefits of augmenting GPS systems with:

a)   Pseudolites; and

b)   GPS+GLONASS receivers;

5.   To provide guidelines and recommendations, from this research, on how to optimize the GPS height solution for deformation monitoring.

6.   To gain an appreciation for the highest level of precision that can be expected at the present time based upon the above mentioned research.

Having met the above objectives, this research would:

1.   Provide an indication as to the capabilities of GPS for monitoring vertical displacements in both best and worse case scenarios;

2.   Serve as a guide for those wishing to optimize vertical solution results; and

3.   Benefit engineering disciplines (e.g, geotechnical, geomatics and mining) by providing a clearer picture of the potential of GPS in this area.

1.2   Methodology

The basic idea behind this research was quite simple: collect GPS data in a harsh environment and determine what accuracy and precision can be expected.   Although simple in description, proper analysis and assessment required rigorous efforts to draw sound conclusions.

To achieve the objectives of this report, GPS data were collected continuously over several days at HVC mine for this analysis. Additionally, three days worth of data were collected in an ideal scenario simulating the same baseline lengths that were observed at HVC. From this ideal data set, optimal software processing settings (with respect to sample rate, elevation cut-off angle, tropospheric model) were determined which were used in the analysis of the HVC data. An optimal setting was defined as that which produced the greatest accuracy and precision over the sample. Since it was possible that the GPS stations were moving at HVC, it would have been difficult to determine the optimal settings using that data set.

Commercial and scientific software were compared to determine which one yields the highest accuracy and precision in GPS solutions. Using this software, the impacts of session length and time of day of observations were investigated. The HVC data were processed using the software and settings determined to produce the best results. As a result of this analysis, an

appreciation for the accuracy that can be attained in a harsh GPS environment was acquired.

Several strategies have been devised for improving the results attained through standard GPS processing techniques (correlating the day-to-day repeatability of multipath, estimating residual tropospheric delay parameters, and recording and using meteorological data). The potential of improving the results through using these techniques was investigated. Similarly, with respect to hardware, new technologies (e.g., pseudolites, GPS+GLONASS enabled receivers) have been introduced to improve GPS results. These technologies were also investigated and assessed for their potential benefits in this situation.

Finally, based upon the findings of this research, conclusions and recommendations have been drawn. These conclusions and recommendations address the objectives stated in the previous section.

1.3 Report Structure

Chapter 2 of this report is dedicated to providing the reader with an understanding of the error sources involved in using GPS which limit the performance of the system. This discussion is important for obtaining insight into the results and analysis that are later presented. The third chapter is concerned

with providing details of the HVC project, and the challenges it poses with respect to deformation monitoring.

Chapter 4 analyzes GPS data collected in a nearly ideal scenario to determine optimal software settings. These settings are then used to quantify what accuracy and precision can be expected at HVC, as presented in Chapter 5.

Chapter 6 evaluates the potential of other techniques that can be used to improve GPS results. Recommendations and conclusions drawn from this research are presented in Chapter 7.

The structure of this report can be broken down into three main components:

1. Background

2. Analysis and assessment

3. Recommendations and conclusions

Figure 1.1 indicates where each chapter fits into the thesis and the purpose it sets out to achieve.

Chapter	Purpose
	Background
1	Describes the motivation and purpose of this research
2	Describes the limitations of GPS
3	Describes the challenges faced at HVC
	Analysis and Assessment
4	Analyzes GPS data from a near ideal scenario to determine optimal software settings
5	Analyzes GPS data from HVC to determine what accuracy and precision can be expected
6	Evaluates the effectiveness of processing techniques and augmentation technology used to improve GPS results.
	Recommendations and Conclusions
7	Draws conclusions and recommendations based upon the results of this research

Figure 1.1   Report Structure

2 GPS LIMITATIONS

To gain an appreciation for the accuracy and precision that is presently achievable using GPS, it is necessary to understand its limiting factors. This research focuses on baselines which are less than 3 km in length, are observed in static mode, and may have height differences of several hundred metres. This discussion will address limitations and error sources that are pertinent to this investigation. Thus, errors and biases such as ionospheric delay, satellite clock errors and orbital errors are assumed to be mitigated through differencing of the observables, and will not be mentioned. For further reading on these issues, see Kleusberg and Langley [1990], Seeber [1993] or Hofmann-Wellenhof *et al*., [2001].

2.1 Tropospheric Delay

Tropospheric delay is caused by signal refraction in the non-ionized atmospheric layer called the troposphere [Langley, 1995; Rizos, 2001; Seeber, 1993]. The troposphere varies in thickness, extending 8 to 16 km above the Earth's surface (Figure 2.1). It is thickest near the equator. Atoms and molecules in the stratosphere (the layer directly above the troposphere, extending to about 50 km above the Earth's surface) also affect signal propagation. However, since

the largest portion of the neutral atmosphere exists in the troposphere, the whole

neutral atmosphere is often loosely called 'troposphere' [Langley, 1995].
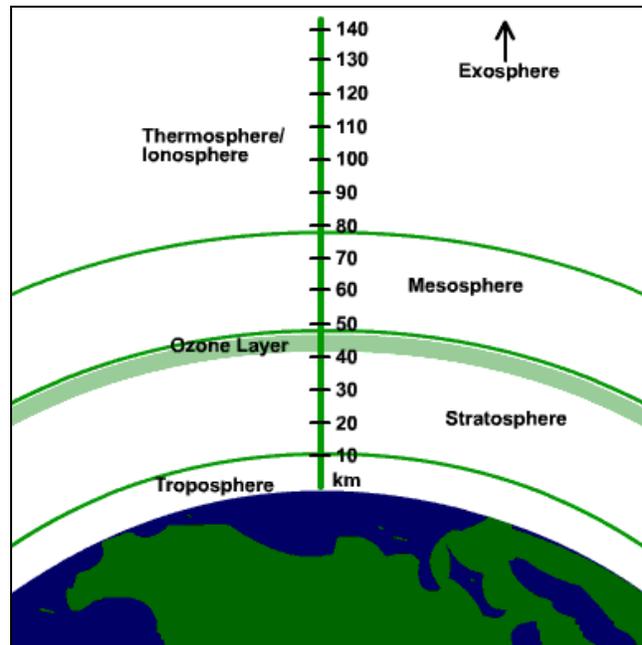
Figure 2.1   Layers of Earth's Atmosphere [MiStupid, 2003]

Unlike the ionosphere, the troposphere is a non-dispersive medium for the

microwave spectrum. Thus, refractive effects on microwaves (which include the

L-Band of GPS signals) are frequency independent. The troposphere affects both

the code modulation and carrier phases in the same way [Leick, 1995].

Consequently, its impact cannot be calculated using signal combinations having

different frequencies, as is the case with ionospheric delay [Seeber, 1993].

Mitigation of residual tropospheric delay effects therefore poses some interesting challenges in precise GPS positioning.

A tropospheric delay value for a GPS observable is dependent upon satellite elevation angle and the altitude of the receiver [Rizos, 2001]. It is a measure of the influence of refractivity on a GPS signal as it travels through the troposphere. Temperature (T), pressure (P) and water vapour pressure (e) all influence refractivity and thus the quantity of tropospheric delay [Rüeger, 1990]. For a spherically symmetric atmosphere for which the refractive index varies only as a function of radius, tropospheric delay can be expressed in first approximation as [Langley, 1995]:

$$d_{trop} = \int_{r_s}^{r_a} [n_{trop}(r) - 1] \csc \theta(r) dr + [\int_{r_s}^{r_a} \csc \theta(r) dr - \int_{r_s}^{r_a} \csc \varepsilon(r) dr] \quad (2.1)$$

Where:

n_{trop} refractive index of the troposphere
r geocentric radius with r_s the radius of the earth's surface and
r_a the radius of the top of the neutral atmosphere
θ refracted (apparent) satellite elevation angle
ε non-refracted (true) satellite elevation angle

The first integral in equation (2.1) accounts for the difference in the electromagnetic and geometric lengths of the refracted transmission path. The bracketed integrals take into account the path curvature [Langley, 1995].

For tropospheric delays in the zenith direction, equation (2.1) becomes [Langley,1995]:

$$d_{trop}^z = \int_{r_s}^{r_a} [n_{trop}(r)-1]dr \quad (2.2)$$

or, in terms of refractivity where N = 10^6(n-1):

$$d_{trop}^z = 10^{-6}\int_{r_s}^{r_a} N_{trop}(r)dr \quad (2.3)$$

Zenith delay values at sea level are typically between 2.3 and 2.6 metres [Langley, 1995] (e.g., assuming a constant refractivity of N_{trop} = 300 and a path length, r_a - r_s = 8000 m, then $d_{trop}^z \approx 10^{-6}$ * 300* 8000 m = 2.4 m). At 10 degrees above the horizon, total tropospheric delay values can reach 20 metres [Wells *et al.*, 1987].

Tropospheric refractivity consists of both a wet and dry component:

$$N_{trop} = N_{wet} + N_{dry} \quad (2.4)$$

Therefore, the total tropospheric delay can be expressed as:

12

$$d_{trop} = d_{dry} + d_{wet}$$ (2.5)

About 90% of the magnitude of the total tropospheric delay arises from the dry component, and the other 10% from the wet component [Langely, 1995], [Leick, 1995], [Rizos, 2001]. The dry component can be accurately modeled to about 0.2% using surface pressure data [Wells *et al*., 1987]. Water vapour content cannot be accurately predicted and modeled and as a result the wet component is much more difficult to quantify [Leick, 1995]. This was shown in Chrzanowski *et al*. [1989] by comparing weather balloon data with the Hopfield model wet and dry refractivity values (Figures 2.2 and 2.3). Wet delay along the total satellite signal path is in the range of 5-30 cm in continental mid-latitudes. It can be modeled to about 2-5 cm [Leick, 1995]. Combined models for dry and wet delays are used to predict the time delays caused by the troposphere.
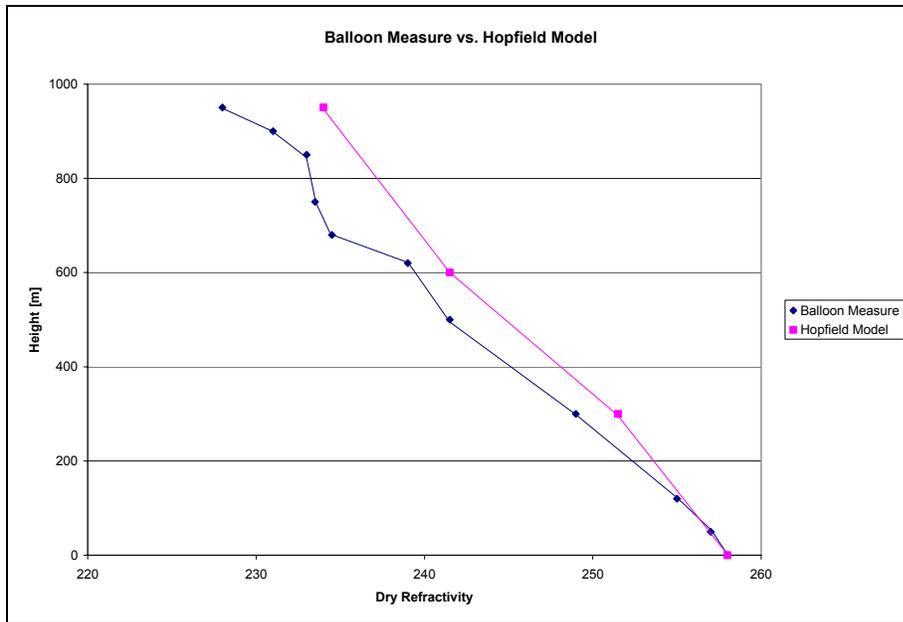
Figure 2.2   Balloon Measure vs. Hopfield Model Dry Refractivity
[Chrzanowski *et al*., 1989]
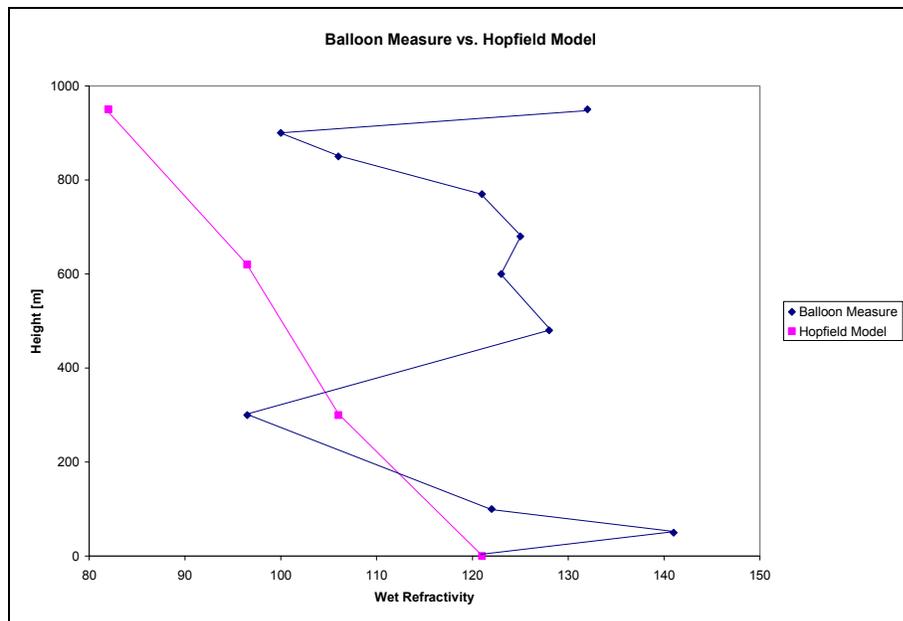
Figure 2.3   Balloon Measure vs. Hopfield Model Wet Refractivity
[Chrzanowski *et al.*, 1989]

Much effort has been devoted to developing tropospheric refraction models to compute the tropospheric delay along the GPS signal propagation path [e.g, Hopfield, 1969; Saastamoinen, 1972; Goad and Goodman, 1974; Black, 1978] as well as to mapping vertical delay with elevation angle. The available tropospheric models, even with real-time meteorological data, appear to reduce the combined tropospheric effects by 92% to 95% depending on the amount of atmospheric information available to the user [Wells *et al*., 1987].

2.1.1 Residual Tropospheric Delay Implications

Accounting for tropospheric delay is critical for precise position and baseline determination, especially in the height component [Seeber, 1993]. When post-processing dual frequency carrier phase data, the residual tropospheric delay (the tropospheric error that remains in the solution after being 'accounted' for) can easily be the largest remaining error source [Collins and Langley, 1997]. Centimetre level biases in height can easily be introduced into the height solution by this error, even if meteorological data are used [Collins and Langley, 1997]. This is primarily a result of the inability to accurately represent the water vapour profile in tropospheric delay models [Collins and Langley, 1997].

For differential observations, differences in tropospheric effects between the two ends of the baseline lead directly to a degradation in the GPS solution for

height. Generally, baselines having longer lengths have more poorly correlated tropospheric parameters than shorter ones. Similar is the case for height differences [Seeber, 1993].

If tropospheric conditions are alike at the two stations (which typically occurs when the stations are close together), the residual tropospheric errors are almost entirely removed by differencing the observations from the two sites [Seeber, 1993]. The magnitude of the error introduced into baseline components will typically be in the order of 1 ppm [Rizos, 2001]. In situations which are not so favourable, some other means must be used to account for this bias.

Beutler *et al.*, [1988] have shown that the effect of the differential troposphere can be written in a first approximation for local networks as:

$$\boxed{\Delta h_e = \Delta d_{trop}^z \sec(\Psi_{max})} \quad (2.6)$$

Where:

Δd_{trop}^z difference in zenith delay between co-observing stations
Ψ_{max} maximum zenith angle observed

Equation 2.6 implies that neglecting the differential troposphere causes a 3 to 5 mm relative height error for every millimetre difference in zenith delay between stations (with an elevation mask of 10 to 20 degrees). In other words, *a 1 mm differential tropospheric bias causes a height error of about 3 mm*. The effect on latitude and longitude is minimal [Beutler, 1988].

In GPS software, the differential troposphere delay is not neglected. Using one of the several tropospheric models available and a mapping function, the tropospheric delay is taken into account at each station. The bias in the solution, caused by the residual tropospheric delay, will be a function of how well the model is able to reflect actual tropospheric conditions.

An example of a tropospheric model is the Hopfield model. The Hopfield model uses the models for dry and wet refractivity at the surface of the Earth, introduced by Essen and Froome [1951]:

$$N_{dry,0} = 77.64 \cdot \frac{P}{T}$$

$$N_{wet,0} = -12.96 \cdot \frac{e}{T} + 3.718E5 \cdot \frac{e}{T^2}$$

(2.7a and b)

Where:

P   atmospheric pressure (mbars)
e   partial pressure of water vapour (mbars)
T   temperature (K)

The variation of dry refractivity as a function of height, h (in metres), is calculated as [Hopfield, 1969]:

$$N_d^{Trop}(h) = N_{d,0}^{Trop} \left[\frac{h_d - h}{h_d} \right]^4$$

(2.8)

Where:

$h_d =$ 40136 + 148.72(T - 273.16) [m]

The dry part of the tropospheric delay can be computed using equation (2.3) by solving the integral along the zenith path where the variation in N_{dry} along the signal path is calculated using equation (2.8). Neglecting curvature of the signal path leads to the following expression for the dry zenith delay:

$$d_{dry}^z = \frac{10^{-6}}{5} \cdot N_{d,0} \cdot h_d \quad (2.9)$$

Due to the lack of a better alternative, the Hopfield model takes a similar approach in modelling the highly variable wet component of refractivity [Hopfield, 1969]:

$$N_w^{Trop}(h) = N_{w,0}^{Trop} \left[\frac{h_w - h}{h_w} \right]^4 \quad (2.10)$$

Where:

$h_w =$ a mean value of 11 000 m (sometimes 12 000 m is used).

Integration of equation (2.3) for the wet component of the zenith delay occurs in the same fashion as was done for equation (2.9), yielding [Hofmann-Wellenhof *et al.*, 2001]:

$$d_{wet}^z = \frac{10^{-6}}{5} \cdot N_{w,0} \cdot h_w \quad \text{(2.11)}$$

Zenith delay values obtained from equations (2.9) and (2.10) are scaled using an appropriate mapping function for the wet and dry components to account for the elevation angle of the satellite [Hofmann-Wellenhof, 2001]:

$$d_{dry} = \frac{1}{\sin(\sqrt{E^2 + 6.25})} \cdot d_{dry}^z$$

$$d_{wet} = \frac{1}{\sin(\sqrt{E^2 + 2.25})} \cdot d_{wet}^z \quad \text{(2.12 a and b)}$$

Where:

E   the satellite elevation angle in degrees

In many tropospheric models (Hopfield, Saastamoinen, Lanyi, Chao, Marini and Murray) measured values of meteorological parameters are assumed to be available at the GPS receiver site [Rizos, 2001]. If meteorological data are not available, profile functions are often used to express temperature, pressure and water vapour pressure as a function of height above mean sea level [Rizos, 2001]. Examples of profile functions are [Gurtner *et al.*, 1989]:

$$p = p_0 \cdot (1 - 0.0226 \cdot H)^{5.225}$$
$$T = T_0 - 6.5 \cdot H$$
$$e = e_0 \cdot 10^{H \cdot (1 + H/8)/8}$$
$$H = H_0^{-0.6396 \cdot H}$$

(2.13)

Where:

p_0 standard pressure (e.g., 1013.25 mb)
T_0 standard temperature (e.g., 291.15 K)
e_0 standard water vapour pressure (e.g., 15 mb)
H_0 standard relative humidity (e.g., 50%)

Typically, results obtained using profile functions are good when atmospheric conditions are similar between receiver sites. Rizos [2001] points out surface meteorological observations are rarely used in GPS processing since experience indicates that baseline results are often worse when they are used. Janes *et al*. [1991] advises that modeling of the differential troposphere should only be undertaken when the meteorological gradients between co-observing stations exceed the accuracy to which surface meteorological parameters can be measured.

Rüeger [1990] assesses the effects of errors in T, P, and e on the refractive index for microwaves. Under normal conditions, the following conclusions are drawn:

    1. An error of 1 C in temperature, T, causes an error of 1.4 ppm in n and therefore in distance.

2. An error of 1 mb in the atmospheric pressure, P, causes an error of 0.3 ppm in n or distance.

3. An error of 1 mb in the partial water vapour pressure, e, causes an error of 4.6 ppm in n or distance.

The critical parameter in the case of refractive index of microwaves is the partial water vapour pressure. The partial water vapour pressure can be determined using an aspiration psychrometer which is typically accurate to 0.2 ºC. However, an error of 0.22 ºC in the dry bulb temperature or an error of 0.14 ºC in the wet bulb temperature causes an error of 1 ppm in n. An accuracy of better than +/- 3 ppm in n cannot easily be achieved [Rüeger, 1990].

2.1.2 <u>Techniques for Mitigating Residual Tropospheric Delay</u>

There are several different techniques that have been proposed and tested for mitigating the effects of residual tropospheric delay. Each of these has its advantages and disadvantages. The following subsections discuss these strategies. It should be pointed out that for most short baselines, there will be a high degree of correlation in tropospheric conditions between sites, and the tropospheric bias will largely be eliminated through differencing the observables. The following techniques are typically used in special cases where one cannot

assume a laterally homogenous atmosphere, such as in valleys or mountainous regions.

2.1.2.1   Estimation of a Tropospheric Zenith Delay Parameter

A powerful method of determining zenith tropospheric delays involves their estimation through a least squares solution of the GPS phase observations. Gurtner *et al*. [1989] claim that using this technique, it is possible to produce GPS solutions with accuracies better than 1 cm in height in a local network of the size of several kilometres and height differences up to 1000 m. Different estimation strategies have been developed. Estimation can take the form of a single scale bias, a residual zenith delay estimated for n (or n-1) observing stations spanning a certain period of time, or stochastic estimation using Kalman filtering [Langley, 1995].

Gurtner *et al*. [1989] suggest estimating one height-dependent tropospheric zenith correction (a scale parameter), dr_0, for each campaign, which can be defined as:

$$dr_0 = a_0 * (h - h_0) \quad (2.14)$$

Where:

a_0 parameter estimated
h   station height
h_0 reference height in the model

This approach does not sacrifice as much redundancy as estimating a parameter for each station. However, this approach assumes that the tropospheric delay varies uniformly throughout the area of interest. Estimating a tropospheric parameter for each point (n), or for each baseline (n-1), may potentially introduce a large number of additional unknowns. However, no assumptions concerning the behaviour of the troposphere are made. The type of approach that should be used will depend upon the conditions of the survey. Test results presented in Gurtner *et al*. [1989] indicated that both the scale and parameter approaches resulted in millimetre accuracies in height, with the scale parameter technique yielding slightly better results.

When estimating tropospheric delay parameters, the question that frequently arises is, "How many parameters should be estimated?" Brunner and McCluskey [1991] point out that there are two main competing solution strategies:

1. Solve for d_{trop} values at all n stations, or

2. Solve for the relative d_{trop} values at n-1 stations (all except the reference station).

From their analysis using scientific GPS software (Bernese), Brunner and McCluskey [1991] determined that the n-1 strategy always yields erroneous results, while the n strategy always gives correct results. Only for small networks with baselines shorter than approximately 50 km does the n-1 approach give errors which are negligibly small.

23

The coefficients of the normal equations will determine whether or not it is possible to solve for the d_{trop} values [Brunner and McCluskey, 1991]. These coefficients are determined by squaring and multiplying the cosecants of the elevation angles, and are summed for all epochs [Brunner and McCluskey, 1991]. Larger differences occur at lower elevation angles, which make the coefficients more numerically different [Brunner and McCluskey, 1991]. Therefore, an attempt to solve simultaneously for zenith delay and position will be aided by the inclusion of low elevation angle data (provided that the mapping function is reliable) [Langley, 1995].

The Kalman filter approach has also effectively demonstrated the ability to contain tropospheric delay biases. Tralli and Lichten [1990] have shown that stochastic estimation of total zenith path delays can potentially yield baseline repeatabilities of a few parts in 10^8, which is comparable or better than those results attained after path delay calibration using a water vapour radiometer. This will be discussed in the following section.

2.1.2.2   <u>Water Vapour Radiometer (WVR)</u>

As previously discussed, the wet component of the tropospheric delay can be modeled for the zenith direction with an accuracy of +/- 2-5 cm. Since there

are no models that precisely describe the variation of water vapour in the atmosphere, significant improvements cannot be expected.

For geodetic applications, it may be worthwhile to measure water vapour content directly along the signal propagation path with a water vapour radiometer (WVR) (Figure 2.4). WVRs are capable of determining the signal path delay with an accuracy estimate of +/- 1-3 cm [Seeber, 1993]. Perhaps the biggest drawback in using such devices for geodetic applications is the price - $115,000 USD [Ware, 2004]. For this reason, tropospheric parameter estimation techniques are a more welcome alternative.

Figure 2.4   UNB's Water Vapour Radiometer [Wert, 2003]

2.1.2.3   <u>Use of Surface Meteorological Data</u>

GPS results obtained using meteorological (met) data are often considerably worse than those obtained using meteorological values extrapolated from standard values [Rothacher *et al*., 1986; Rizos, 2001; Langley, 1995]. However, this does not imply that met data does not contain valuable information. Beutler *et al.* [1989] summarize the scenario as follows:

1. Baseline repeatabilities when using mets in the classical sense are typically poor (cm level), in both similar and variable weather conditions.

2. Baseline repeatabilities are very good when comparing results obtained under similar weather conditions using the same standard atmosphere model in processing.

3. Baseline repeatabilities are poor when comparing results obtained under different weather conditions using the same standard atmosphere model in processing.

Beutler *et al*. [1989] suggest that the classical approach of using meteorological data is inappropriate for small networks and that an alternative method should be used:

1. The entire set of surface meteorological data is used to derive a height dependent profile of the atmosphere (temperature, pressure and humidity) in the layer between the highest and lowest point of the

survey. Linear modelling should be sufficient.

2. The signal path between a station "A" and a satellite "S" is divided into two sections: the first between A and A_0 and the second between A_0 and S. A_0 is defined as the intersection of the signal path with the horizontal plane at height h_{A0} of the highest met station (Figure 2.5).

3. Atmospheric refraction is computed as the sum of refraction along A to A_0 using the standard formulae for terrestrial refraction [Rüeger,1990], and refraction along A_0S, using the standard Saastamoinen or Hopfield models (assuming a hypothetical station at A_0 having the same meteorological conditions as those at height h_{A0}).
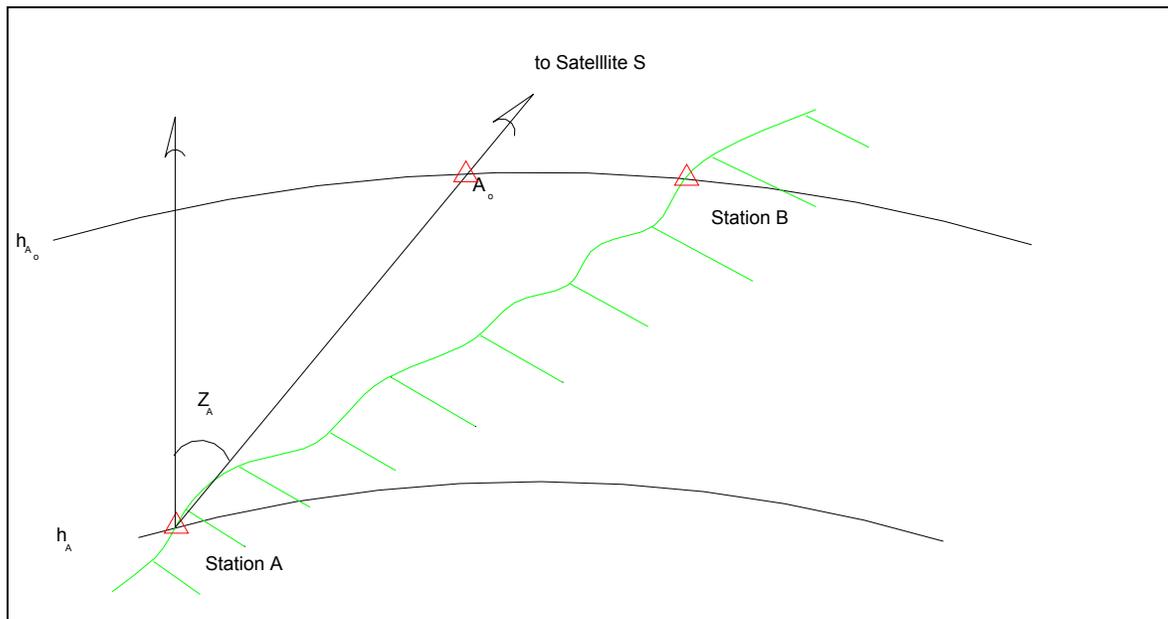
Figure 2.5   Differential Tropospheric Model (after Rothacher [1986, p. 985])

Height repeatabilities comparable to those obtained using standard atmospheres under similar weather conditions have been achieved using this procedure [Beutler *et al.*, 1989].

2.2 Multipath

Multipath is the phenomenon whereby a signal arrives at a receiver site via two or more different paths [Wells *et al.*, 1987]. The difference in path lengths causes the signals to interfere at the receiver. Multipath affects both code and carrier measurements. Its impact on P-code observations is two orders of magnitude larger than on carrier phase observations [Seeber, 1993].

2.2.1 Multipath Implications

Except in the rare case that both antennas are located in the same area and have the same multipath influences, multipath experienced at two or more independent antennas is not spatially correlated. Therefore, the effects of multipath can be significant in relative positioning (even on short-baselines) and cannot be cancelled by the double-differencing operation [Kim *et al.*, 2003].

The theoretical maximum multipath bias that can occur in pseudo-range data is about half the chip length (150 m for C/A and 15 m for P (Y) code ranges). However, multipath errors are typically much lower (<10 m). Carrier phase multipath does not exceed about one-quarter of the wavelength (5 to 6 cm for L1 or L2). As the receiver-satellite geometry changes, multipath exhibits a sinusoidal pattern, and generally averages out over a period from several minutes to a quarter of an hour, or more [Rizos, 2001].

2.2.2 Techniques for Mitigating Multipath Biases

Multipath biases can be significantly reduced through strategic planning, including [Rizos, 2001]:

1.   Carefully selecting the antenna site to avoid reflective objects;

2.   Using a receiver that internally filters multipath;

3.   Selecting an antenna that is multipath-resistant;

4.   Masking low-elevation satellites signals (which are easily

         contaminated by multipath); and

5.   Using longer session lengths.

Additionally, several multipath mitigation techniques have been proposed to mitigate the effects of multipath in GPS code and carrier phase

measurements. Although recent receiver technologies have significantly improved medium and long delay multipath performance, multipath mitigation techniques for short delays (due to close-by reflectors) are not at the same level [Weill, 2003], [Braasch and Van Dierendonck, 1999].

Radovanovic [2000] and Wubbena *et al.* [2001] illustrate how the day-to-day repeatability of multipath can be exploited to improve positioning accuracies. Given known coordinates of a point on a certain day, the multipath 'signature' at every epoch can be calculated. Since the GPS constellation repeats itself, this error can be subtracted from phase data collected from the corresponding epoch on a subsequent day.

Standard deviations of 5 mm in the height component are reported. The reliability of this technique is dependent upon the repeatability of the multipath signature and on the premise that the point being monitored is not changing position significantly enough (< 1 cm) to alter the multipath characteristics.

2.3   Antenna Phase Centre Variation

Antenna phase centre variation is caused by non-coincidence of the electrical and physical centre of both the receiver and GPS antennas. Phase centre variations are primarily the result of a non-spherical phase response pattern of the GPS antenna [Leica GeoSystems, 2002]. This is primarily a

manufacturing problem. The electrical centre varies with the direction and strength of the incoming signal.

There are two different types of phase centre variation (PCV) models: relative and absolute. In the first approach, a reference antenna is used from which offsets of the antenna of interest are measured. The International GPS Service standard reference antenna is JPL's Dorne Margolin Choke Ring antenna Model T [Leica GeoSystems, 2002]. Antenna correction models can be downloaded from the Astronomical Institute of the University of Bern website [Bern, 2003] and the National Geodetic Survey (NGS) web site [NGS, 2003]. Both correction models use the Dorne Margolin T as a reference, so models from both sources can be mixed [Leica GeoSystems, 2002]. Models which refer to different reference antennas should not be used together.

Absolute PCV models define offsets in an absolute sense. Absolute phase centre calibrations typically take place in an anechoic chamber. These models are only available for a few antenna models and therefore are not as commonly used [Leica GeoSystems, 2002].

2.3.1 Implications of Antenna Phase Centre Variation Biases

Ignoring antenna phase center variations can lead to serious (up to 10 cm) vertical errors [Mader, 2002]. For precise geodetic applications, it is critical that this bias is modelled and taken into account when mixing antenna types.

2.3.2 Mitigation of Antenna Phase Centre Variation Biases

The following options exist for mitigating antenna phase centre variations [Rizos, 2001]:

1. Orient antennas in the same direction, so that the impact on the groundmark-to-groundmark solution will be a systematic shortening or lengthening of the baseline;

2. Avoid mixing antenna types (using the same antennae on a baseline will cancel out this error).

3. Use models of antenna phase centre variations, which are available from the NGS and the Astronomical Institute of Bern.

2.4   Satellite Geometry / Visibility

In addition to errors in the ranges measured by a GPS receiver, the configuration of GPS satellites being measured to will also impact the quality of the solution. A GPS solution is essentially a resection problem. A well distributed system of control stations or, in this case, GPS satellites, will lead to a stronger solution than having the satellites bunched together in the sky (see Figure 2.4).

Dilution of precision (DOP) values are used to measure the geometric strength of the GPS satellite configuration contributing to a solution. These values change with time as the satellites travel along their orbits. A small DOP value indicates favorable satellite geometry [Wells *et al.*, 1987].
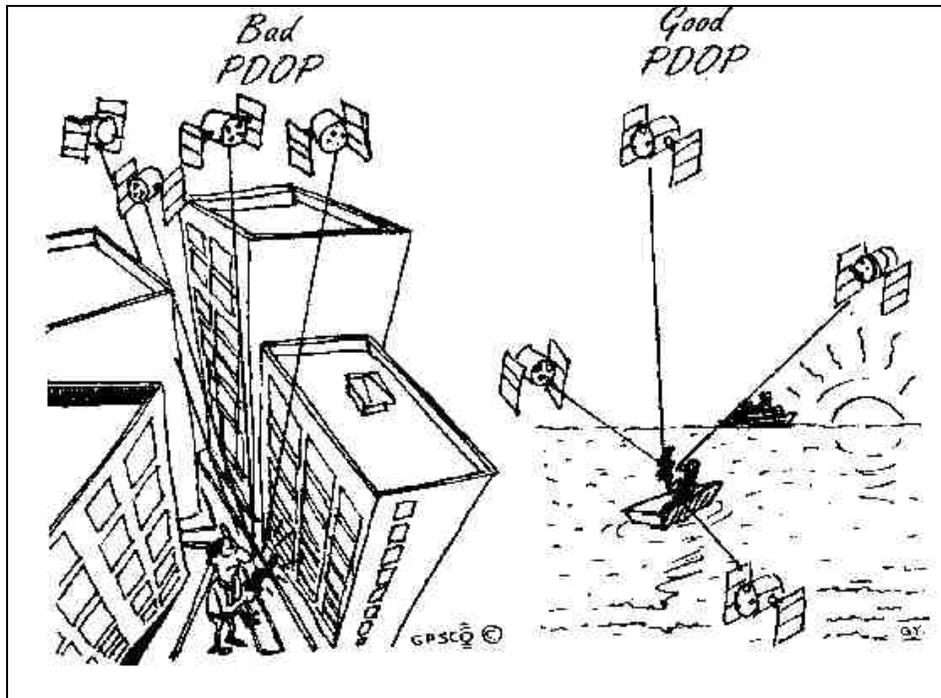
Figure 2.6   Bad Satellite Geometry vs Good Satellite Geometry [Rizos, 2001]

2.4.1   Impact of Poor Satellite Geometry / Visibility

During certain periods of the day, the receiver site location may be such that the DOP values are much larger than normal. Any constraints on satellite visibility will diminish the potential quality of the results and may lead to such a situation. In extreme cases, it may not be possible to obtain a solution.

2.4.2 <u>Improving Satellite Geometry / Visibility</u>

Since it is not possible to control the space segment of the GPS system, one is limited to making a wise selection for the GPS antenna site. Ensuring a clear view of the sky will help address this issue. Unfortunately, in some cases the station of interest is located in an area with restricted satellite visibility, and one has very little control over antenna site location.

In recent years, receivers capable of tracking both GPS and GLONASS satellites have become commercially available. This helps to improve the redundancy of the solution. Additionally, the use of pseudolites (from 'pseudo-satellite') as a ground based augmentation system to the GPS constellation has offered some hope of improving GPS results in areas with restricted satellite visibility [Wang, 2002].

3 HIGHLAND VALLEY COPPER PROJECT

Highland Valley Copper (HVC) mine is a unique environment which poses some interesting challenges when trying to implement a deformation monitoring system. This chapter focuses on describing the mining environment at HVC, the current deformation monitoring system that is in place and its limitations, and the proposed solution for improving the current system.

HVC represents an unfavourable GPS scenario, as will be discussed. It is a real-world operation that can take advantage of a deformation monitoring system augmented with GPS. Rather than simply testing in an ideal environment and providing false hopes of GPS capabilities, it was decided to look at the other extreme. The premise being that one would be hard pressed to find an environment that would place any higher demands on the deformation monitoring system and therefore the results should only get better for other applications.

3.1 Investigation Site: Highland Valley Copper Mine, Logan Lake, British Columbia

Highland Valley Copper mine is situated within the Canadian Rockies, 75 km south west of Kamloops, British Columbia, Canada (Figure 3.1) [Mining Technology, 2003]. The Valley pit has yielded more than 1000 mega-tonnes of ore in its lifetime. About 89% of the ore comes from the Valley Pit, which is the focus area of this investigation [Mining Technology, 2003]. The remainder comes from the Lornex Pit. The Highland Valley mill is the world's third largest copper concentrator.

Figure 3.1   HVC Mine Location [Venture Kamloops, 2004]

The Valley Pit extends over 2 km wide and over 0.6 km deep (Figure 3.2). The southern wall of the pit is a majestic series of benches, while in the north the slope is less steep. A roadway terraces its way down to the bottom of the pit so that haul trucks can transport ore.
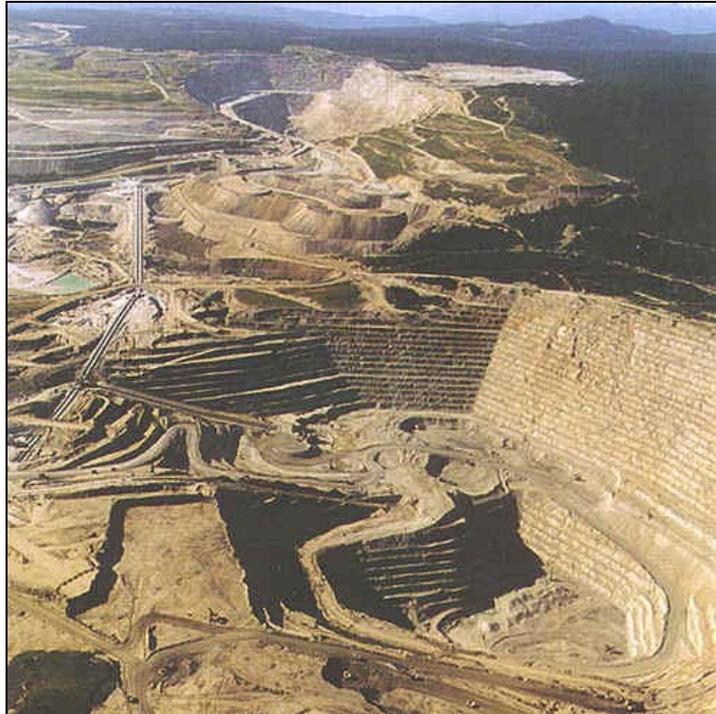
Figure 3.2   Valley Pit (foreground) and Lornex Pit (background)
[Mining Technology, 2003]

Mining occurs by open pit methods at the Lornex and Valley pits. Three drills prepare blast hole patterns while nine P&H electric shovels load ore into a fleet of Komatsu haul trucks for transport to in-pit crushers (Figure 3.3). Water trucks, road graders and bulldozers provide additional operations support. The

mine uses two semi-mobile, in-pit crushers to minimize haul distances to the mill

(Figure 3.4) [Mining Technology, 2003].

Figure 3.3   Shovel and Truck Fleet [Mining Technology, 2003]

Figure 3.4   Crushers and Conveyor System [Mining Technology, 2003]

There are significant differences in modes of instability, deformation characteristics of the rock mass, and magnitudes of displacements between the two pits. The Lornex Pit is excavated in a relatively poor quality, deformable rock mass, with sections of its pit walls being subject to toppling instability and relatively high magnitudes of deformation [Newcomen *et al*., 2003]. The Valley Pit walls, on the other hand, are excavated in a fair to good quality, relatively brittle, rock mass. The pit walls experience toppling, planar and wedge types of instability with significantly smaller displacements than those observed in the Lornex Pit [Newcomen *et al*., 2003]. Consequently, each pit requires different levels of accuracy in pit wall monitoring.

Since the equipment used at HVC is human operated, it is critical that the stability of the benches is monitored to warn of impending danger. A reliable deformation monitoring system not only serves as an important safety measure for the mining operation, but also allows management to make informed decisions about how to proceed with operations.

Differences in the potential modes of instability between the two pits, the deformation characteristics of the rock mass, the pit wall angles and the nature and magnitude of the slope movements were taken into consideration when quantifying displacement rate thresholds under which mining could safely be carried out [Newcomen *et al*., 2003].

For example, displacements due to toppling instability are generally large, with associated ongoing moderate movement rates. At the other end of the instability spectrum, planar failures can occur suddenly at very low strains with very little indication of accelerating movements. Therefore movement thresholds for the Lornex Pit (pit wall angles between 26º and 37º from vertical) are larger than for areas of the Valley pit (pit wall angles between 39º and 45º from vertical) [Newcomen *et al*., 2003]. The Valley Pit is the focus of this research. The following section discusses the deformation monitoring system requirements for the Valley Pit as requested by HVC.

3.2 HVC Deformation Monitoring System Accuracy / Precision Requirements

The principle objective in implementing a deformation monitoring system at HVC is to monitor the stability of the benches which form the massive walls encompassing the pit. This is achieved through monitoring prisms which are mounted to the pit walls. By determining the position of the prism at successive epochs, the stability of the wall can be monitored.

For this project, sub-centimetre accuracy is required for detecting displacements, with an ultimate goal of achieving +/- 5 mm in all three directional components of the solution (N, E, H). In order to attach a certain degree of confidence to the results provided by the system, a statistical expansion factor must be applied to the standard deviations of the position solutions. Horizontal and vertical solution components are treated separately. A 95% confidence level has been chosen for this project (2D expansion factor for horizontal: 2.4477, 1D expansion factor for height: 1.9600). Thus, a standard deviation of about +/- 2 mm in detecting the displacements of the targets is desired.

3.3 Current Deformation Monitoring System: ALERT

The Canadian Centre for Geodetic Engineering's (CCGE) fully automated displacement monitoring system, ALERT, is currently used at HVC [Wilkins *et al.,* 2003b]. This system draws upon robotic total stations (RTSs) as its primary sensors to obtain three-dimensional displacements with millimetre accuracy (Figure 3.5). Currently, Leica TCA 1800 [Leica Geosystems, 2004] RTSs are used. The scheduling, control, processing and quality assessment/quality control of the RTS measurements are fully automated.

At a specified time, the RTSs will measure angles and distances to a series of prisms mounted around the pit. In effect, polar coordinates are determined for each point of interest. By performing the same sequence of observations at a subsequent epoch, displacements from a reference epoch can be determined.

Figure 3.5 Sheltered Robotic Total Station (RTS) at HVC

A series of time-tagged coordinate values which are stored in the project database are produced by ALERT [Wilkins *et al.,* 2003b]. When plotted, these coordinate values allow for rapid visualization of displacement trends. The database allows for easy extraction of coordinate information using Structured Query Language (SQL) and analysis tools to meet specific project needs.

3.4 Error Sources Limiting RTS Performance

Refraction and pointing errors are the two main error sources affecting the RTS instruments used by ALERT. Neither error source is a systematic error that can be mitigated through field techniques.

For the purpose of measuring displacements, RTS distance measurements are more robust than angular measurement, since they are less susceptible to refraction biases. A standard deviation of about 1.6 mm or better can be expected for distances less than 1 km. [Leica GeoSystems, 2004]. As a result, the accuracy of displacement measurements along the line of sight will generally be much better than those in the direction perpendicular to it (affected by errors of angle measurements).

Therefore, to significantly improve the accuracy of a deformation monitoring system, the CCGE recommended using two or more RTSs so that distance intersections dictate horizontal solutions. Unfortunately, RTSs do not help much in the determination of vertical displacements which are dependent upon the accuracy of the vertical angle [Wilkins *et al*., 2003a].

3.4.1 Effects of Refraction on an RTS

Refraction is caused by non-homogeneous atmospheric conditions along the profile perpendicular to the line of sight. If the air temperature gradient (dt/dz) across the line of sight is constant at all points across the line, the refracted path follows a circular curve with the radius, r, producing a pointing error, e, between the real position, B, and the apparent position, B' of the target (Figure 3.6) [Chrzanowski, 1999]:

$$e = \frac{S^2}{2r} = k\frac{S^2}{2R} \quad (3.1)$$

Where:

        k   coefficient of refraction (k = R/r)
        S   distance to target
        R   Earth's radius
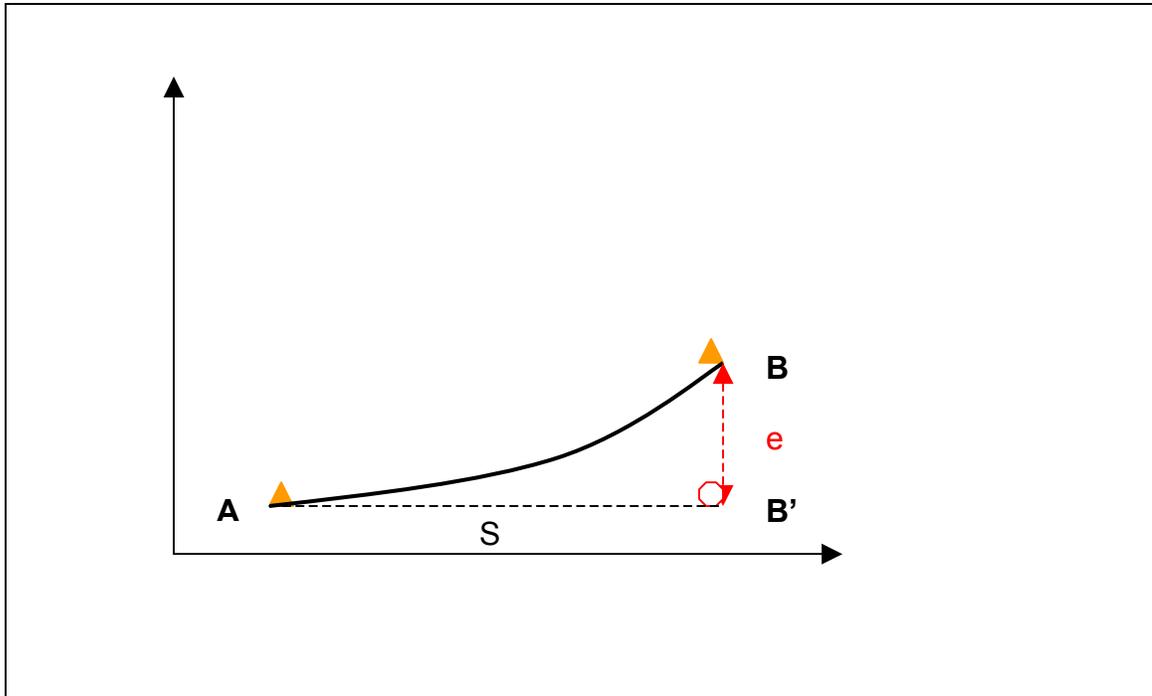
Figure 3.6   Refracted Line of Sight (after Chrzanowski [1999])

The influence of refraction on a direction measurement, dγ, has been shown to be (Figure 3.7) [Chrzanowski, 2002]:

$$d\gamma('') = 8'' \frac{P \bullet S}{T^2} \bullet \frac{dT}{dy} \quad (3.2)$$

Where:

S   distance to target [m]
P   pressure (usually average value) [mb]
T   temperature (usually average value) [K]
dT/dx   temperature gradient (usually average value) [C/m]

The position error, e, in the direction caused by refraction is calculated as

[Chrzanowski, 2002]

$$e = 8" \frac{S^2 P}{T^2 \rho"} \frac{dT}{dy}$$ (3.3)

Where:

S   distance to target [m]
P   pressure (usually average value) [mb]
T   temperature (usually average value) [K]
dT/dy   temperature gradient (usually average value) [C/m]
ρ   206265 "
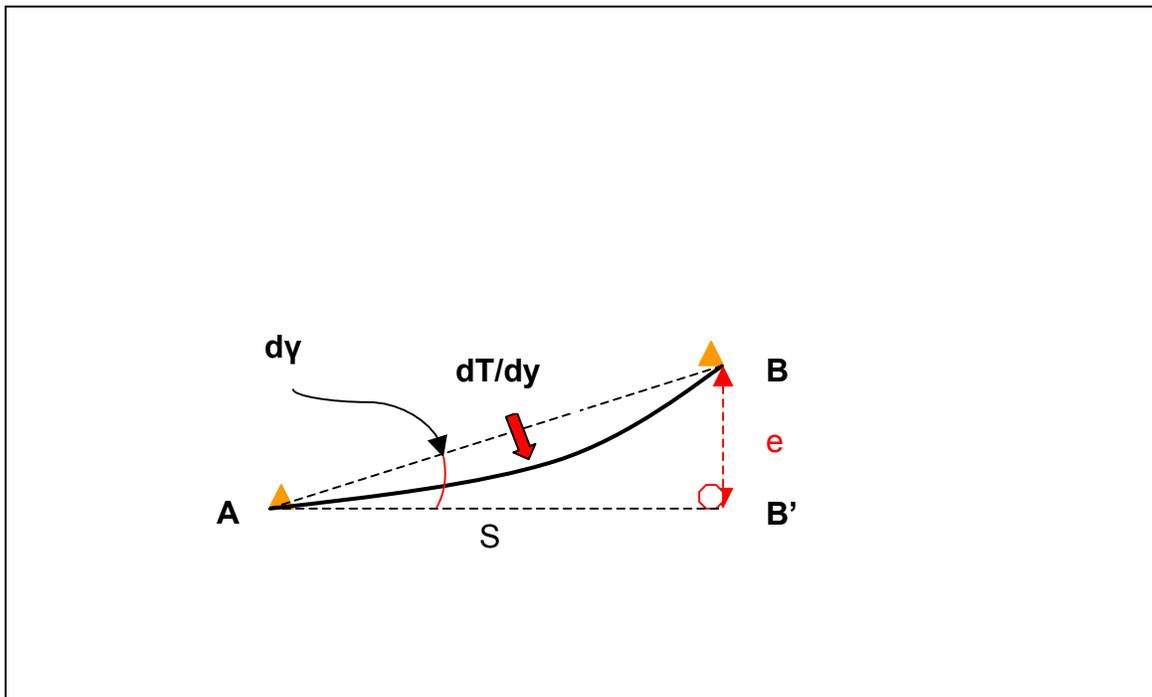
Figure 3.7   Influence of Refraction on a Direction Measurement
(after Chrzanowski [1999])

To gain an appreciation for the contribution of refraction to angular errors, consider the following example using standard values for pressure and temperature, a sight length of 1000 m (which can be easily reached at HVC) and assuming a temperature gradient as small as 0.05 C/m:

Given:

$S = 1000$ m, $P = 1013$ mb, $T = 293.15$ K, $dT/dx = 0.05$ C/m

Then:

$d\gamma = 4.7$"   and $e = 23$ mm

From equation (3.3) it can be seen that a positional error caused by refraction is directly proportional to the square of the distance observed. If, for example, a distance of 2000 m is observed (an extreme case at HVC), under the same atmospheric conditions described above, then:

$$d\gamma = 9.4\text{"}   \text{and}   e = 91 \text{ mm}$$

3.4.2 Effects of Pointing Errors on an RTS

Leica TCA1800 robotic total stations come equipped with Automatic Target Recognition (ATR) technology. An infrared light bundle is sent by the

instrument and returned by the prism. The instrument interprets the center of light of the light bundle and the servo-motors turn the telescope to home in on the prism center [Leica GeoSystems, 2004]

The manufacturer's specified accuracy for direction measurements using the TCA1800 is 1" per pointing, under average atmospheric conditions (for angles, this value increases by a factor of $\sqrt{2}$ to approximately 1.5") [Leica GeoSystems, 2004]. The range of this instrument using ATR mode is 1000 m [Leica GeoSystems, 2004]. The contribution to the positional error, e, in the direction perpendicular to the line of sight of a directional error of 1.0" observed over a distance of 1000 m, is:

$$e = 1.0\text{ "} \times 1000 \text{ m} / 206265\text{ "} = 0.0048 \text{ m}$$

Since displacements are being determined (the difference between two positions) the error shown increases by a factor of $\sqrt{2}$:

$$0.0048 \text{ m} \times \sqrt{2} = 0.0068 \text{ m}$$

This value is larger than the desired +/- 5 mm accuracy in detecting displacements. Thus, some mitigating measures must be considered.

3.4.3 Mitigation of Refraction and Pointing Errors

The effects of refraction on RTS measurements may be minimized by making observations in consecutive epochs in similar atmospheric conditions. However, this is not likely possible and therefore not feasible in practice. The effects of refraction may be randomized and minimized by designing lines of sight to be several metres away from sources of heat radiation (e.g., the pit walls) and by observing angular observations in several sets spread out over several hours.

The effects of random pointing errors may be reduced by a factor of $1/\sqrt{n}$ where n is the number observation sets [Chrzanowski, 2002]. There is a limit to the amount of improvement that can be achieved. It is not reasonable to think that observing 100 sets of angles will result in a standard deviation of 0.15" due to systematic effects of refraction.

Summarizing, in order to decrease the effects of both refraction and random pointing errors, it is recommended to [Duffy *et al*., 2001]:

1. Maintain short distances from the RTS stations to the target prisms;

2. Take observations in several sets;

3. Spread the observations over long periods to randomize the effects of refraction; and

4. Keep lines of sight away from strong sources of heat radiation.

In practice, if these precautions are taken, then a standard deviation of about +/- 0.5" can be expected for horizontal directions and +/- 0.7" for vertical angles [Chrzanowski, 2004].

As stated above in the first recommendation, in order to use RTS instruments effectively for the purpose of deformation monitoring surveys, sight lengths to targets must be limited to reduce the effects of refraction. As shown in the previous section, sight lengths must be kept within a few hundred metres. However, an interesting problem arises in the open pit mine environment. If sight lengths must be short, then the RTS will have to be placed in an unstable environment at the bottom of the pit. Additionally, visibility to stable reference points located beyond the rim of the open pit becomes obscured. Without any means to monitor the stability of the instrument, the whole monitoring system becomes unreliable.

3.5   Proposed Solution: RTS+GPS System

Suppose it were possible to locate the RTSs within the zone of deformation while constantly monitoring their stability. Sight lengths to the wall targets can now be reduced without concern for RTS instability. This is the approach taken by the CCGE to address the challenges associated with deformation monitoring in an open pit environment [Wilkins *et al.,* 2003a].

In order to implement such a system, it is necessary that two requirements are fulfilled:

1. The stability of the RTS stations and the wall-mounted prisms are monitored at sub-centimetre level in all 3 components (N, E, H) with 95% confidence.

2. The corrections to the RTS stations are derived in fully automated mode.

This research attempts to address the issue of whether or not this first requirement above can be satisfied using GPS. This is not an easy task, as will be discussed in the following section. The second requirement has already been met by the research team at the CCGE.

3.6 System Requirements: Pre-Analysis

To gain an appreciation for what level of accuracy is required from GPS in order to achieve the accuracy requirements for this project, a pre-analysis investigation was conducted. The use of term 'accuracy' (the proximity of the observations to the true value) rather than precision (the proximity of the observations to one another) in this discussion warrants some explanation. The quantities of interest are the displacement values of the target points. Since displacements are determined by differencing subsequent epochs of measurements over a relatively short period of time (hours), any biases affecting the measurements should be removed. Therefore, the differences in positions determined should accurately represent the true displacement values.

For this pre-analysis, two robotic total stations (RTS1 and RTS2) were situated as depicted in Figure 3.8. In order to decrease the distances to the monitored targets, it was proposed to locate a RTS in the pit, as indicated by RTS3 in Figure 3.8. Since the RTSs are located in an unstable environment (in particular, RTS3, since it is proximate to the mining operation) augmenting the RTS stations with GPS observations was considered. Point 987 is a reference station, located in a 'stable' location. Table 3.1 presents the local coordinate values used for this pre-analysis. Stations '100m' to '700m' represent target points subsequently described.
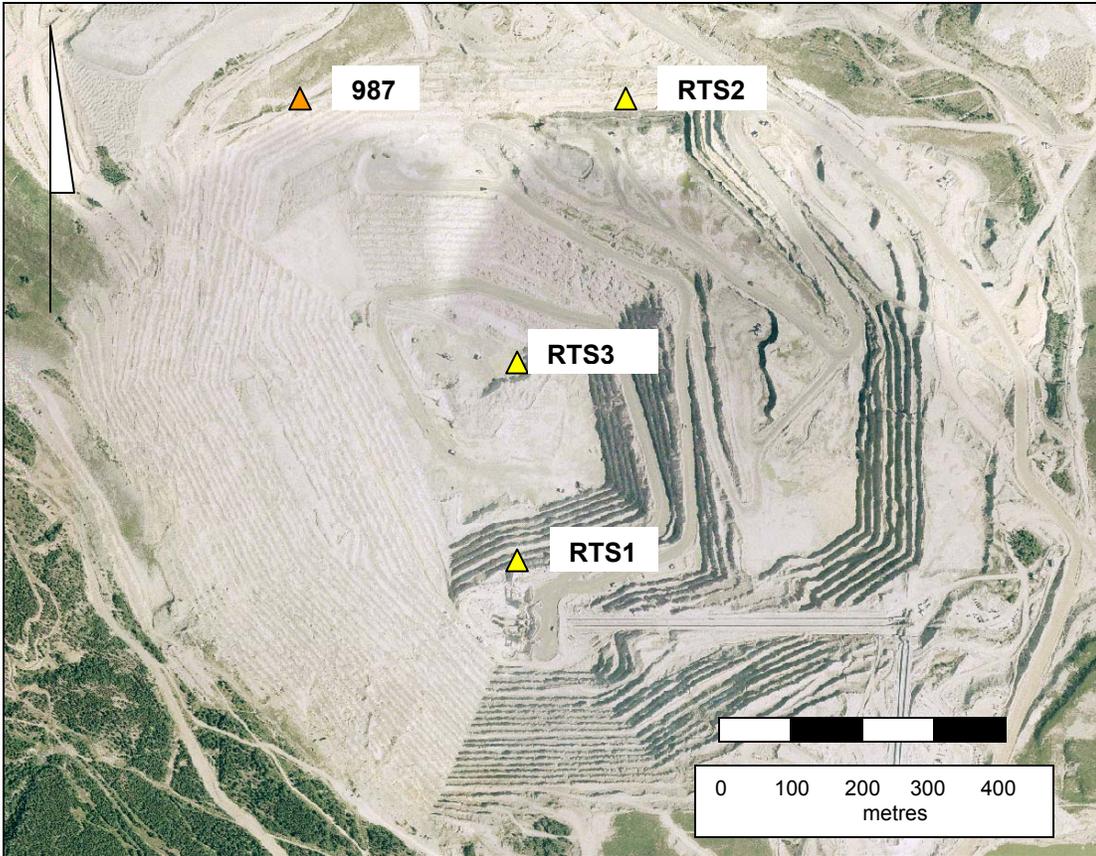
Figure 3.8   Pre-Analysis Station Configuration

Table 3.1   Pre-Analysis Local Coordinate Values

Station	N [m]	E [m]	H [m]
987	5516.165	-1879.122	1213.500
RTS1	4345.535	-2660.666	1016.781
RTS2	5114.781	-1596.424	1168.818
RTS3	4695.078	-2325.027	852.376
100m	4695.078	-2425.027	902.376
200m	4695.078	-2525.027	902.376
300m	4695.078	-2625.027	902.376
400m	4695.078	-2725.027	902.376
500m	4695.078	-2825.027	902.376
600m	4695.078	-2925.027	902.376
700m	4695.078	-3025.027	902.376

Two scenarios were considered to simulate conditions at HVC. In the first scenario, GPS was used to monitor stations RTS1 and RTS3, with 987 being the reference station (Figure 3.9). Direction, zenith angle and distance measurements were measured from RTS3 to target prisms, with reference to RTS1. Target prisms have been placed at 100 m increments away from RTS3 at a height of 50 m above RTS3, to illustrate how errors propagate as sight lengths increase.
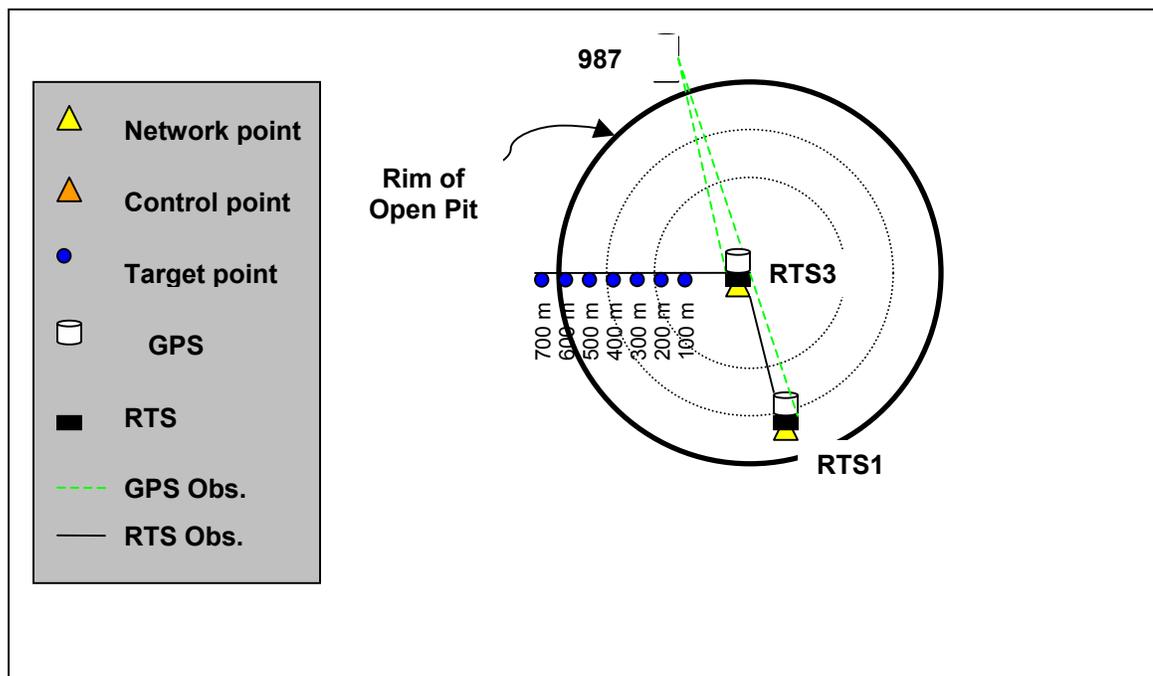
Figure 3.9   Pre-Analysis Scenario I

In the second scenario, GPS was used to monitor stations RTS1 and RTS2, with 987 being the reference station (Figure 3.10). In this case, RTS3 was

56

not augmented with GPS since it is located at the bottom of the pit and it is doubtful that good GPS results can be achieved at this station. Alternatively, RTS2 was enabled with GPS so that it could serve as a back sight for RTS1. RTS3 was monitored by means of conventional measurements from RTS1. As in Scenario I, direction, zenith angle and distance measurements were measured from RTS3 to target prisms.
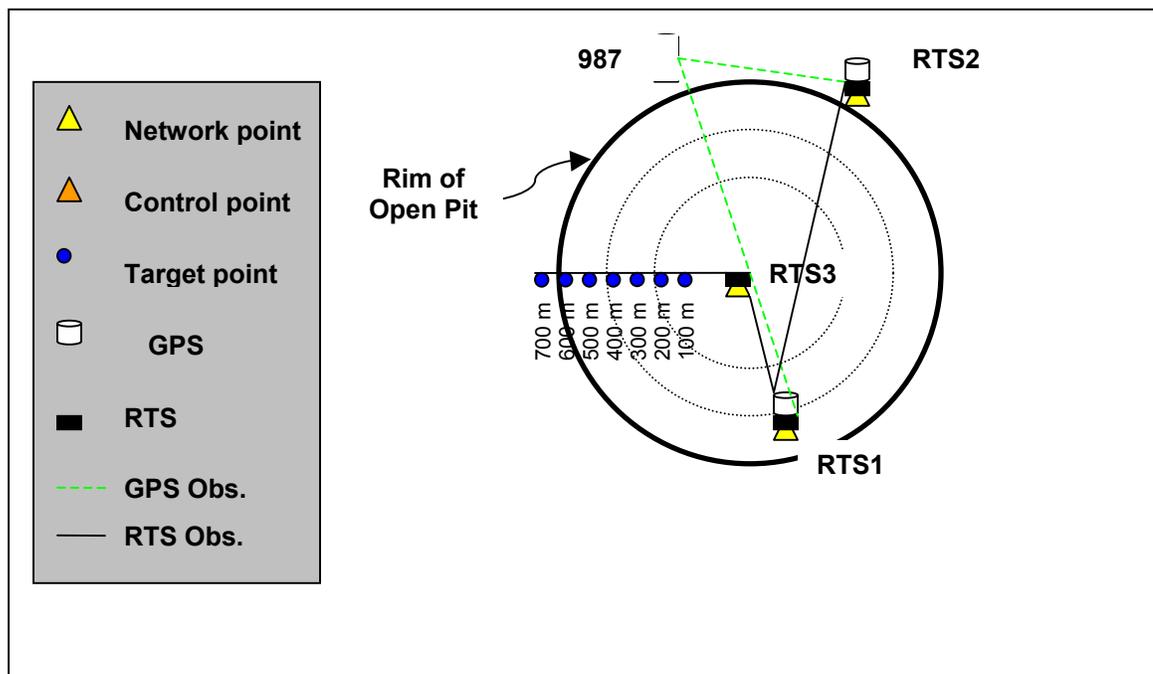
Figure 3.10   Pre-Analysis Scenario II

The pre-analyses of these two scenarios were performed by propagating the expected measurement errors (standard deviations) as indicated in Table 3.2

to obtain displacement error estimates. In order to achieve the angular measurement and distance accuracies cited, a high precision total station, such as Leica's TCA 1800 will have to be used. When observing network points, several sets of angular measurements will have to be observed. The precisions of the GPS solutions were varied to determine at what point the project requirements are met. Three levels of GPS accuracy were considered, as indicated in Table 3.2.

Table 3.2   Expected Standard Deviation of Observations

Observation Type	Standard Deviations
Directon	0.5"
Zenith Angle	0.7"
Distance	+/-1 mm +/- 2 ppm
GPS Horizontal	A) 0.5 B) 1 C) 2 mm
GPS Vertical	A) 1 B) 2 C) 3 mm

The confidence regions at 95% (2.4477 expansion factor applied) as well as the vertical confidence interval at 95% (1.9600 expansion factor applied) were calculated using GeoLab®. Since displacements between two epochs are determined by the deformation monitoring system, the station values calculated in GeoLab® were multiplied by $\sqrt{2}$.   Table 3.3 summarizes the results for Scenario I, Cases A-C.

Table 3.3   Scenario I, Cases A-C 95% Confidence Values

Scenario:	A) 0.5 mm & 1 mm		B) 1 mm & 2 mm		C) 2mm & 3 mm	
Station	Major Semi-Axis [m]	Vertical [m]	Major Semi-Axis [m]	Vertical [m]	Major Semi-Axis [m]	Vertical [m]
100m	0.004	0.003	0.006	0.006	0.008	0.008
200m	0.004	0.003	0.006	0.006	0.008	0.008
300m	0.004	0.004	0.006	0.006	0.008	0.008
400m	0.004	0.004	0.006	0.007	0.010	0.008
500m	0.006	0.006	0.007	0.007	0.011	0.010
600m	0.007	0.006	0.008	0.007	0.013	0.010
700m	0.008	0.007	0.010	0.008	0.016	0.010
RTS1	0.001	0.003	0.003	0.006	0.007	0.008
RTS3	0.001	0.003	0.003	0.006	0.007	0.008

The following conclusions can be drawn from Table 3.3:

1. *Sub-centimetre* results can be achieved if standard deviations of 2 mm in horizontal and 3 mm in vertical GPS components are obtained with respect to 987 and sight lengths are restricted to 400 m or less.

2. *Sub-centimetre* results can be achieved if standard deviations of 1 mm in horizontal and 2 mm in vertical GPS components are obtained with respect to 987 and sight lengths are restricted to 700 m or less.

3. If standard deviations of 0.5 mm in horizontal and 1 mm in vertical GPS components are achieved with respect to 987 (not likely), than the goal of achieving +/- 5 mm displacement solutions at 95% confidence can be met with RTS sight lengths of up to 400 m.

Table 3.4 summarizes the results for Scenario II, Cases A-C:

Table 3.4   Scenario II, Cases A-C 95% Confidence Values

Scenario:	A) 0.5 mm & 1 mm		B) 1 mm & 2 mm		C) 2mm & 3 mm	
Station	Major Semi-Axis [m]	Vertical [m]	Major Semi-Axis [m]	Vertical [m]	Major Semi-Axis [m]	Vertical [m]
100m	0.006	0.004	0.006	0.006	0.007	0.007
200m	0.006	0.004	0.006	0.006	0.007	0.007
300m	0.006	0.006	0.006	0.006	0.007	0.007
400m	0.006	0.006	0.006	0.007	0.007	0.007
500m	0.006	0.006	0.007	0.007	0.008	0.008
600m	0.007	0.007	0.008	0.007	0.010	0.008
700m	0.008	0.007	0.008	0.008	0.010	0.008
RTS1	0.001	0.003	0.003	0.004	0.007	0.006
RTS2	0.001	0.003	0.003	0.003	0.004	0.004
RTS3	0.004	0.004	0.004	0.006	0.006	0.007

From Table 3.4, the following conclusion can be drawn:

1. *Sub-centimetre* level results can be achieved if standard deviations of 2 mm in horizontal and 3 mm in vertical GPS components are obtained with respect to 987 and sight lengths are restricted to 700 m or less.

2. The goal of achieving +/- 5 mm displacements at 95 % confidence level can not be met in this scenario; the RTS observations limit achievable accuracy.

3.7 GPS Limitations at HVC

The majestic walls encompassing the open pit at HVC cause poor satellite visibility. The implications of poor satellite visibility have been discussed in Chapter 2 Section 4. To repeat, the quality of a GPS solution is dependent upon the distribution of satellites in the sky. Obstructions limiting satellite visibility dilute the quality of the solution. Any GPS antenna placed in the pit will have a natural elevation mask imposed upon it, caused by the pit walls. The south wall of the pit is particularly troublesome, blocking out satellites up to 30 degrees in elevation. These lower elevation satellites are important for obtaining robust GPS solutions and for estimating tropospheric delay parmameters [Langley, 1995].

Another characteristic of this site that makes it difficult to obtain repeatable results is the depth of the mine itself. Just as it is necessary to locate the RTS points in a stable area, it is also necessary to locate the reference GPS receiver outside the deformation zone. This inevitably means that the reference will have to be stationed outside of the pit, while the rover receivers will be within it. As discussed in Chapter 2 Section 1, residual tropospheric delay can bias the results since atmospheric conditions vary between receivers. These limitations are depicted in Figure 3.11.
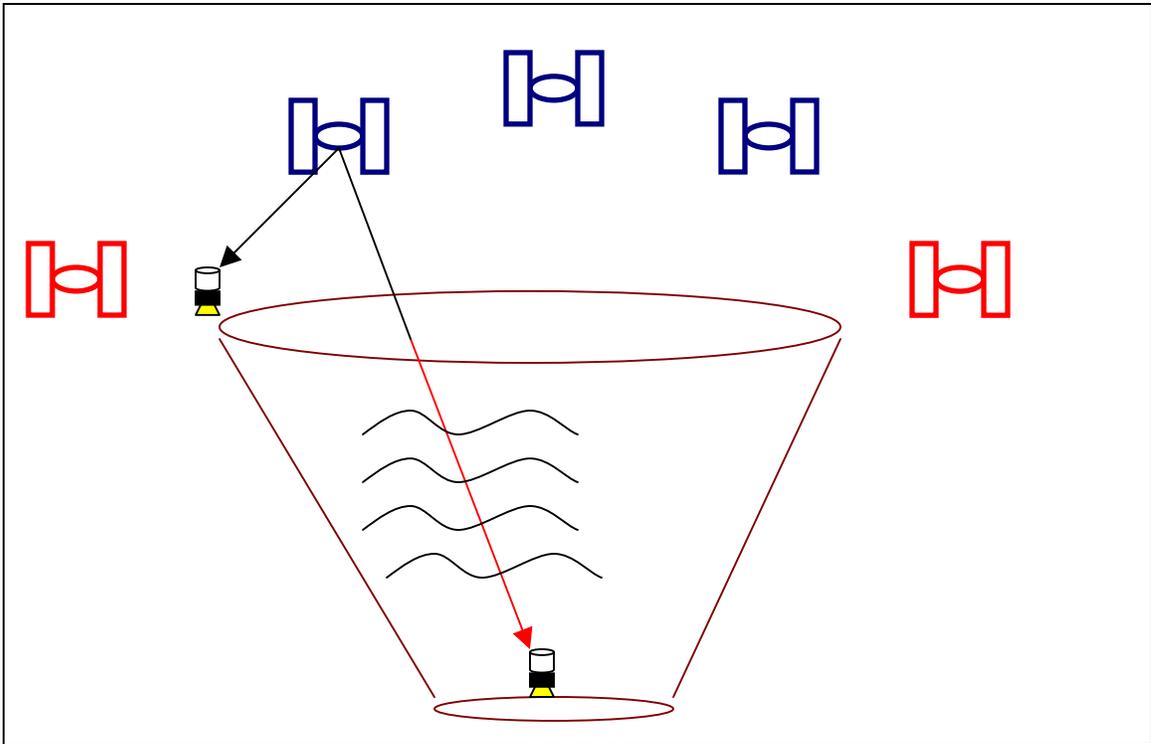
Figure 3.11   Major GPS Limitations at HVC: Satellite Visibility and Residual Tropospheric Delay

4 IDEAL SCENARIO DATA ANALYSIS

This chapter analyzes GPS data collected in a nearly ideal scenario to determine optimal software settings. For this research, the optimal setting is considered to be that which produces the greatest accuracy and precision over the sample. Since it is possible that the GPS stations are moving at HVC, it would be difficult to determine the optimal setting using this data set (as it would be uncertain if the degradation in results was caused by instability of the point or by the setting).

4.1 Ideal Scenario Investigation

In choosing a site for this particular investigation, there were certain characteristics that were desirable:

1.   Rover and reference antennas are located in low multipath environments;

2.   Rover and reference antennas have good visibility of the sky;

3.   Rover and reference antennas are located in a secure place so that they can be left unattended for several days without having to worry about theft;

4.   The height difference between stations is minimal; and

5.   The baseline length is similar to those measured at HVC.

Two setups located on the roofs of buildings were chosen. The reference antenna was located on the roof of Head Hall, at the University of New Brunswick and is shown in Figure 4.1. The rover station was located on the roof of the Hugh John Flemming Forestry Complex, as shown in Figure 4.2.

Figure 4.1   Head Hall Reference Station

Figure 4.2   Hugh John Flemming Forestry Centre Rover Station

The baseline length for this experiment was 2191.696 m, in the vicinity of what was expected to be typically measured at HVC. The height difference between stations was 87.591 m, sufficiently small so that residual tropospheric delay would not cause any major biases. Figure 4.3 depicts the baseline layout.

As shown in Figures 4.1 and 4.2, both roofs on top of which the GPS receivers are set up are covered with crushed rock. This reduces reflection of GPS signals in the vicinity of the antenna, thereby minimizing multipath. To confirm that multipath was not causing any significant biases in the solutions obtained over this baseline, the residuals of the double difference observations were analyzed. From the plots of the residuals (Figure 4.4), it can be seen that

the residuals were distributed about a zero mean, were small in magnitude and, for the most part, did not exhibit any upward or downward trends.
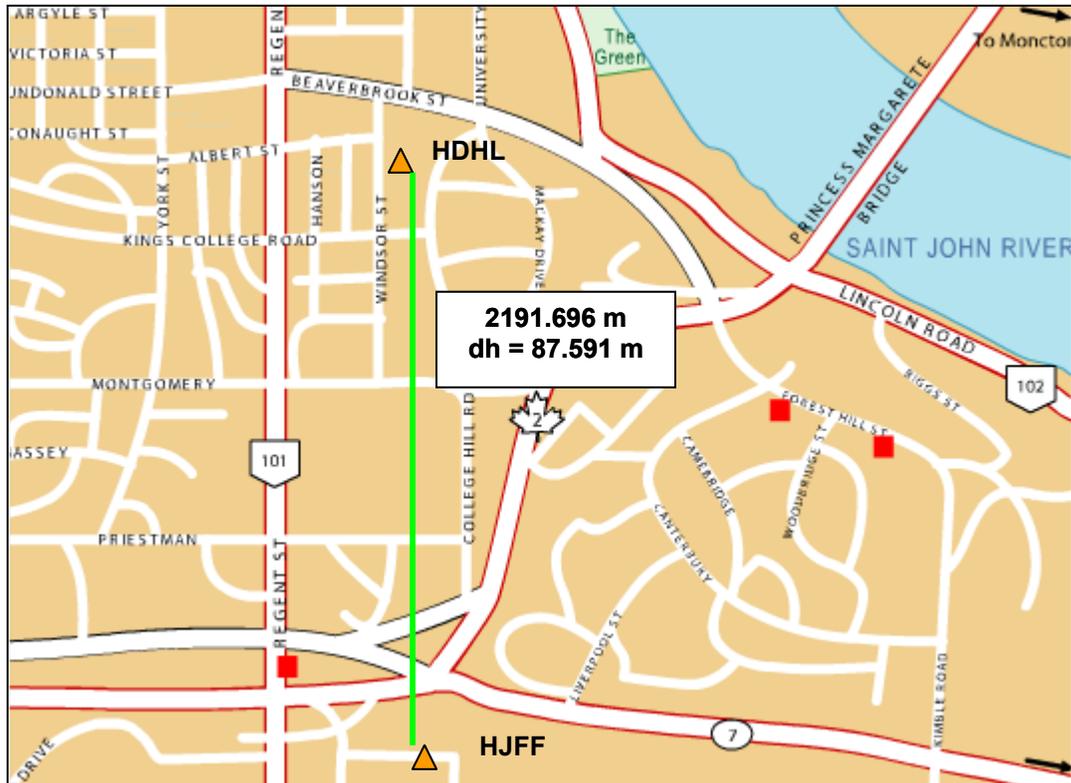
Figure 4.3   Ideal Baseline Location, Fredericton, NB, Canada
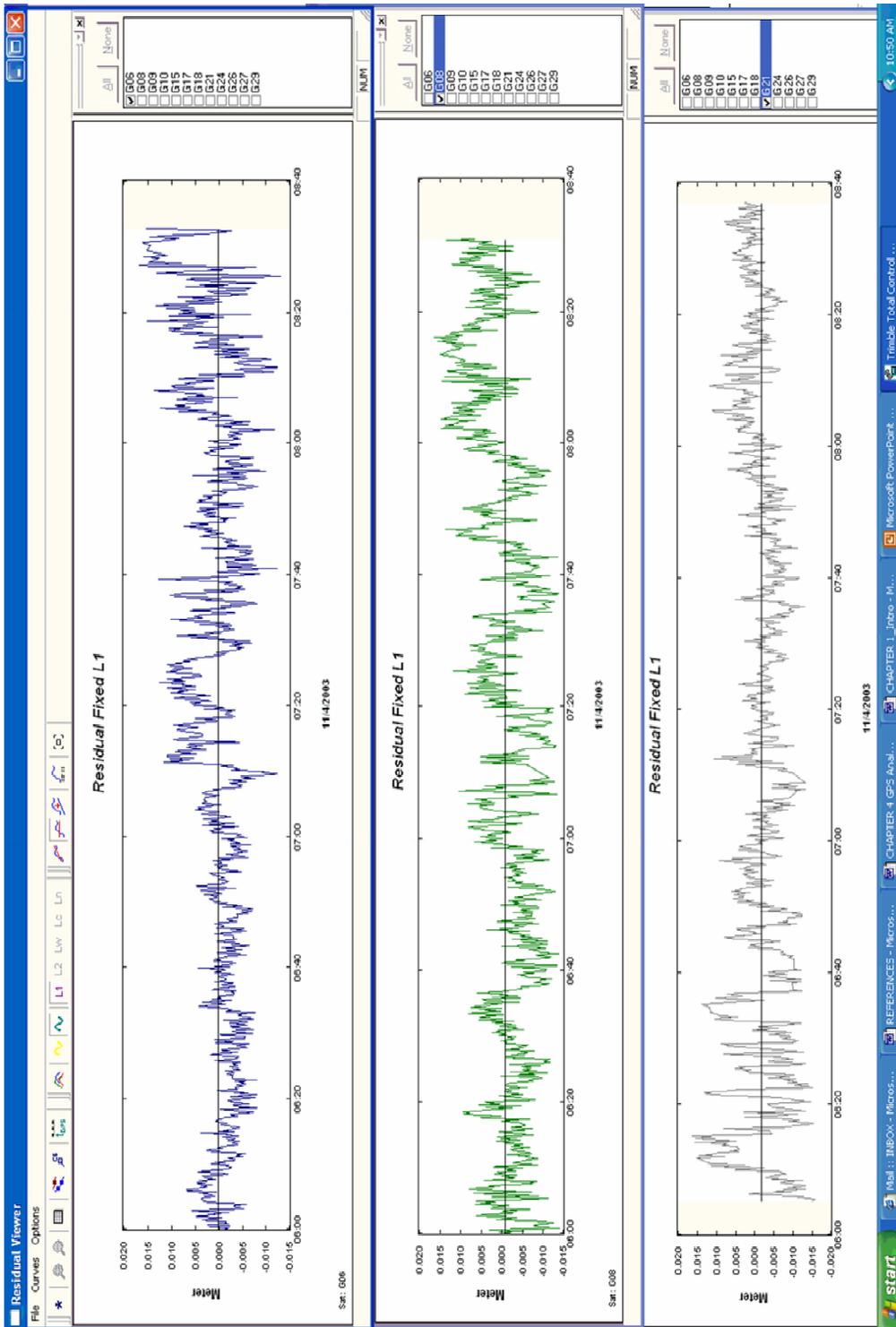
Figure 4.4 Double Difference Residuals for Selected PRNs

As can be seen in Figures 4.1 and 4.2, there are very few obstructions limiting satellite visibility. Figures 4.5 and 4.6 confirm that satellite coverage over the duration of this session was very good.
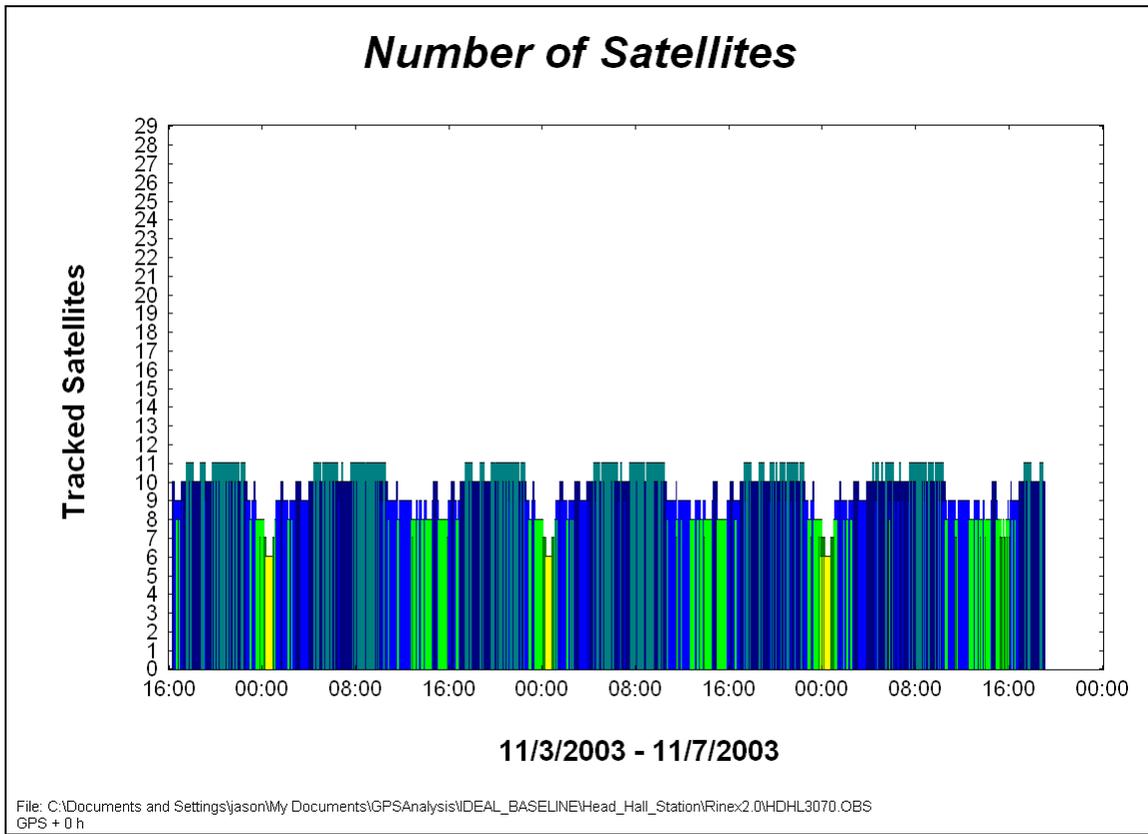
Figure 4.5   Satellite Availability at Head Hall Setup

Number of Satellites

Tracked Satellites (y-axis)

29 28 27 26 25 24 23 22 21 20 19 18 17 16 15 14 13 12 11 10 9 8 7 6 5 4 3 2 1 0

08:00   16:00   00:00   08:00   16:00   00:00   08:00   16:00   00:00   08:00   16:00   00:00

11/3/2003 - 11/7/2003

File: C:\DOCUMENTS AND SETTINGS\JASON\MY DOCUMENTS\GPSANALYSIS\IDEAL_BASELINE\HJFFC_Station\Rinex2.0\HJFF307x.OBS
GPS + 0 h
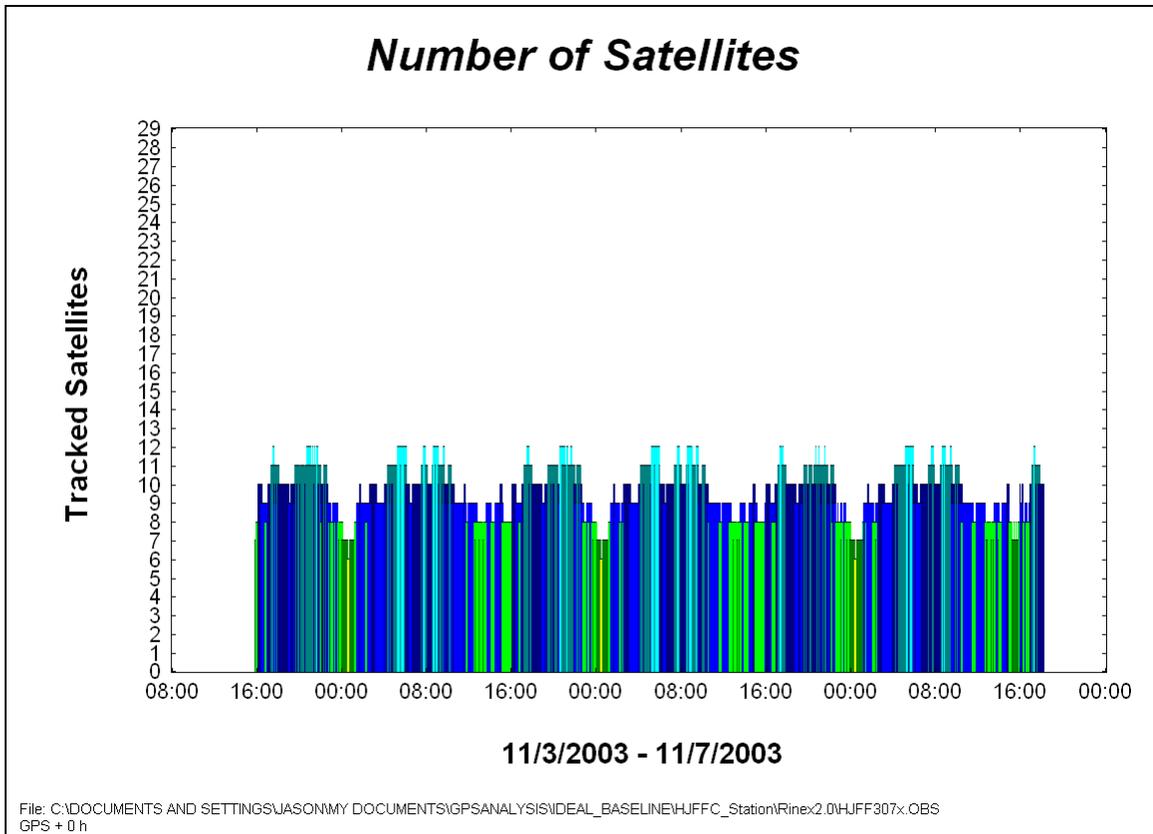
Figure 4.6   Satellite Availability at Hugh John Flemming Forestry Centre Setup

4.2   Procedure

Data were collected over a 3 day period beginning on November 3rd of 2003. Two Novatel DL4 receivers with multipath mitigating, Pinwheel 600 antennas were used. A 1 Hz sample rate and 0 degree cut-off angle were applied to the receiver settings.

In order to analyze the data, it was necessary to decide upon software that would allow for thorough analysis of the data. Both commercial and scientific

69

packages were tested including: Leica SkiPro, Ashtech WinPrism, Topcon Pinnacle, Trimble Geomatics Office, Trimble Total Control, UNB's DIfferential POsitioning Program (DIPOP) and a modified version of UNB RTK software. Since the end goal of this research was to determine if the desired displacement accuracy can be achieved, the accuracy of the solutions provided by each package ultimately dictated whether or not it would be used. The software packages were tested on a sample data set. The mean solution was found for the sample and the deviation of each session from the mean was calculated.

Software producing deviations:

1. Less than 5 mm were graded 'excellent';

2. Less than 10 mm were graded 'good'; and

3. Greater than 10 mm were graded 'poor'.

User-friendliness and flexibility in processing options also had some influence. Table 4.1 presents a summary of what was found.

Table 4.1   Comparison of Software Tested

Software	User-Friendliness	Flexibility	Speed	Accuracy
Leica SkiPro	Poor	Good	Excellent	Good
Ashtech Prism	Poor	Good	Poor	Good
Topcon Pinnacle	Good	Good	Good	Good
Trimble Total Control	Good	Excellent	Excellent	Excellent
Trimble Geomatics Office	Good	Good	Good	Good
DIPOP	Poor	Excellent	Poor	Good
UNB RTK	Poor	Good	Good	Good

4.3   Processing Results

Based on the findings listed in Table 4.1, data were processed using Trimble Total Control (TTC) software to determine which processing settings produced the best results. The effects of varying sample rate, elevation cut-off angle, tropospheric model, session length and time of day of the session were investigated. The results are presented in the following subsections.

4.3.1 Sample Rate

Sample rate is the frequency at which observations are logged by the GPS receiver. A higher sample rate will result in more observations being logged, but this does not necessarily imply a better solution for static applications. Logging large quantities of data makes file manipulation cumbersome and data processing slower.

A base sample rate of 1 s was chosen. In TTC, the sample rate was changed to 10 s and 30 s to determine what impact this would have on the final solution. The results of the vertical component are presented in Figure 4.7 a-c. Plotted are the deviations from the 3 day mean value of the height.

71

a) **HJJFC wrt HDHL: TTC L1 Height Values**
1s Sample Rate

b) **HJJFC wrt HDHL: TTC L1 Height Values**
10s Sample Rate

c) **HJJFC wrt HDHL: TTC L1 Height Values**
30s Sample Rate

Figure 4.7 a-c   1s, 10s and 30s Sample Rate Comparison

From Figure 4.7, it can be concluded that decreasing the sample rate to 30 s did not cause any loss of accuracy in the vertical component over this 3 day period. In fact, the deviations from the mean became smaller at the lower sample rate. Similar results were seen with the horizontal position solutions.

A 24 hour RINEX file collected at a 1 s sample rate can easily reach 70 megabytes of data, as compared to a 2 megabyte file when collected at 30 s. Processing 24 hours of 1 s data with a 2.20 GHz processor takes several minutes to complete in TTC, as compared to several seconds with the 30 s data. Unless software is being used that takes advantage of the information contained in high frequency data (e.g., for multipath mitigation), a 10 s or 30 s sample rate is recommended.

4.3.2 Elevation Cut-Off Angle

An elevation cut-off angle is used to mask low elevation satellite observations which are likely to contain tropospheric and multipath related biases. Although more susceptible to biases, these observations provide stronger geometry to the solution and also make it easier to solve for tropospheric parameters. So, although it is good to mask out poor quality observations that degrade the accuracy of the solution, it is important that observations which contribute to a stronger solution are not omitted.

A base elevation cut-off angle of 0 degrees was chosen. In TTC, the cut-off angle was altered to 10, 15, 20, and 30 degrees to determine what impact this would have on the final solution. The results of the vertical component are presented in Figures 4.8 a-e. Plotted are the deviations from the 3 day mean value of the height.
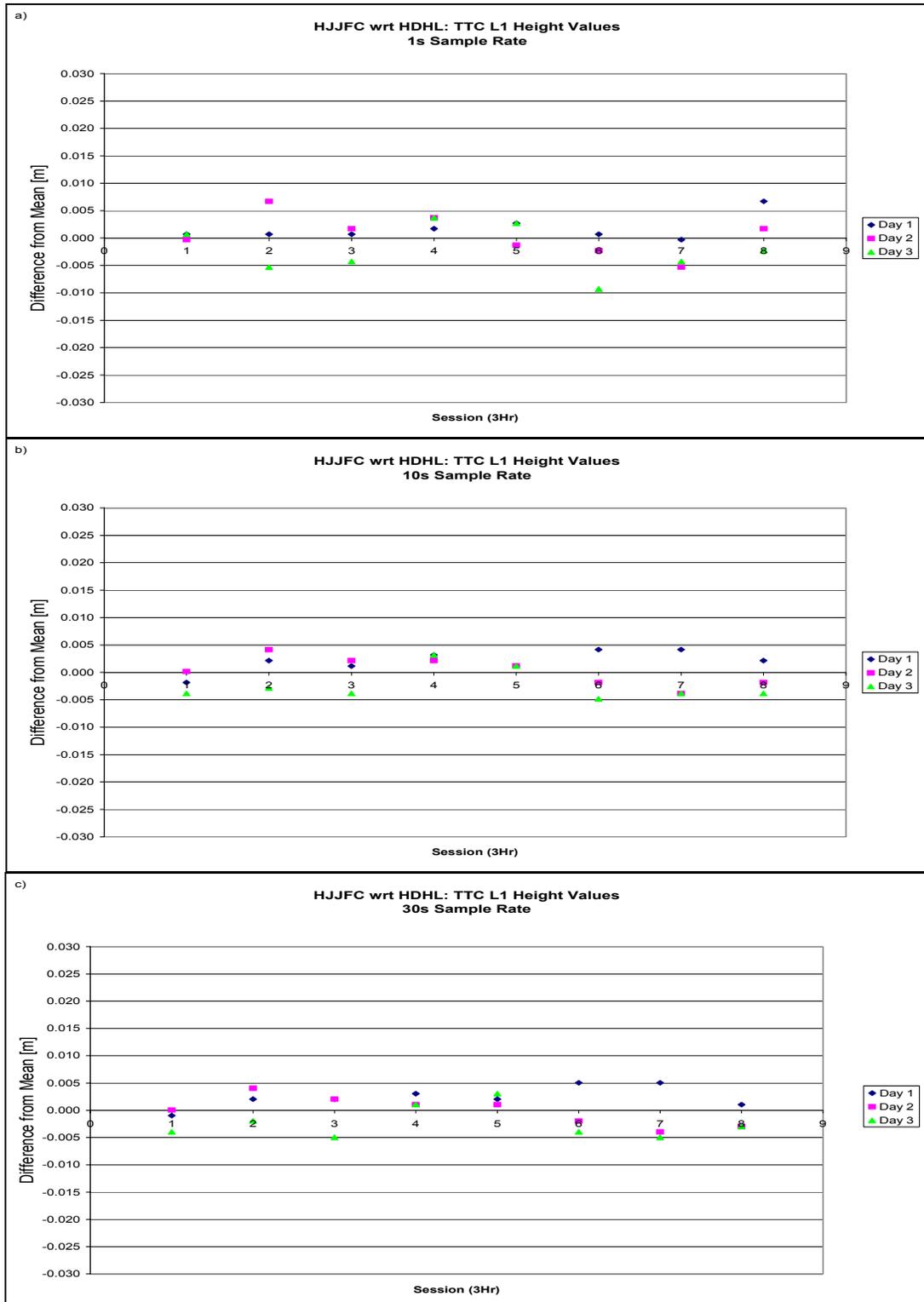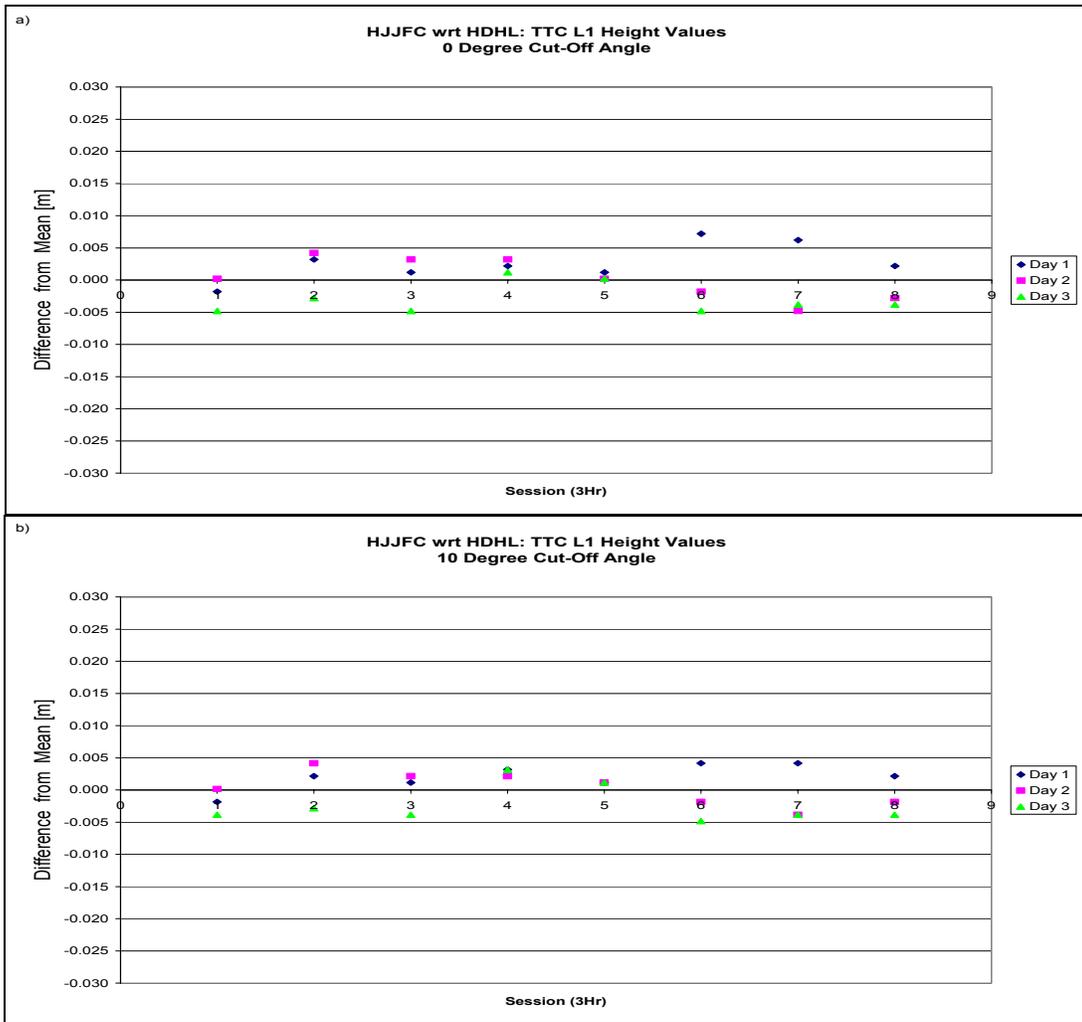

Figure 4.8 a-b: Elevation Cut-Off Angle Comparison
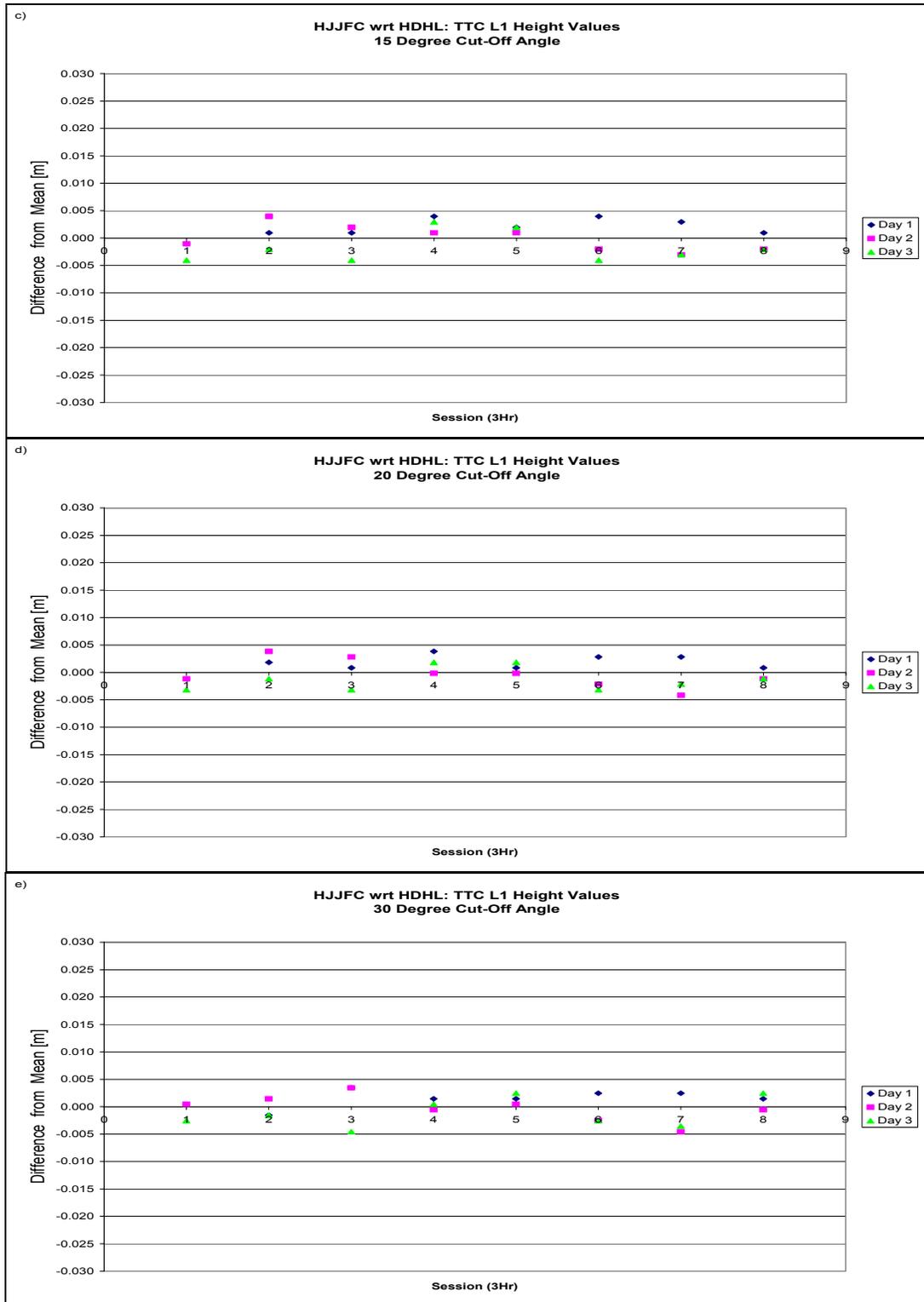
Figure 4.8 c-e: Elevation Cut-Off Angle Comparison

In processing the data, TTC reports the number of observations that are masked by the elevation cut-off angle. Table 4.2 provides an idea of the percentage of total observations that are masked at each cut-off angle.

Table 4.2   Percentage of Observations Masked at a Given Cut-Off Angle

Elevation Cut-Off	% Observations Masked
0	0
10	10
15	20
20	30
30	50

From Figure 4.8 it can be concluded that using 10,15, 20 and 30 degree elevation cut-off angles yielded similar results in the height component. The same was the case for the horizontal solutions. With no elevation cut-off angle imposed, the results were slightly worse. From Table 4.2 it is observed that setting the cut-off angle at or above 20 degrees quickly eliminates a large percentage of observations. It is therefore recommended that an elevation cut-off angle of 10 to15 degrees be imposed in processing.

4.3.3   Tropospheric Model

Tropospheric models are used to estimate the amount of tropospheric delay in a GPS range measurement. No model behaves perfectly, but some

models are more accurate than others. For this analysis, height solutions using four different tropospheric models were compared: Hopfield, Goad and Goodman, Niell and Saastamoinen. The results are presented in Figure 4.9 a-d.
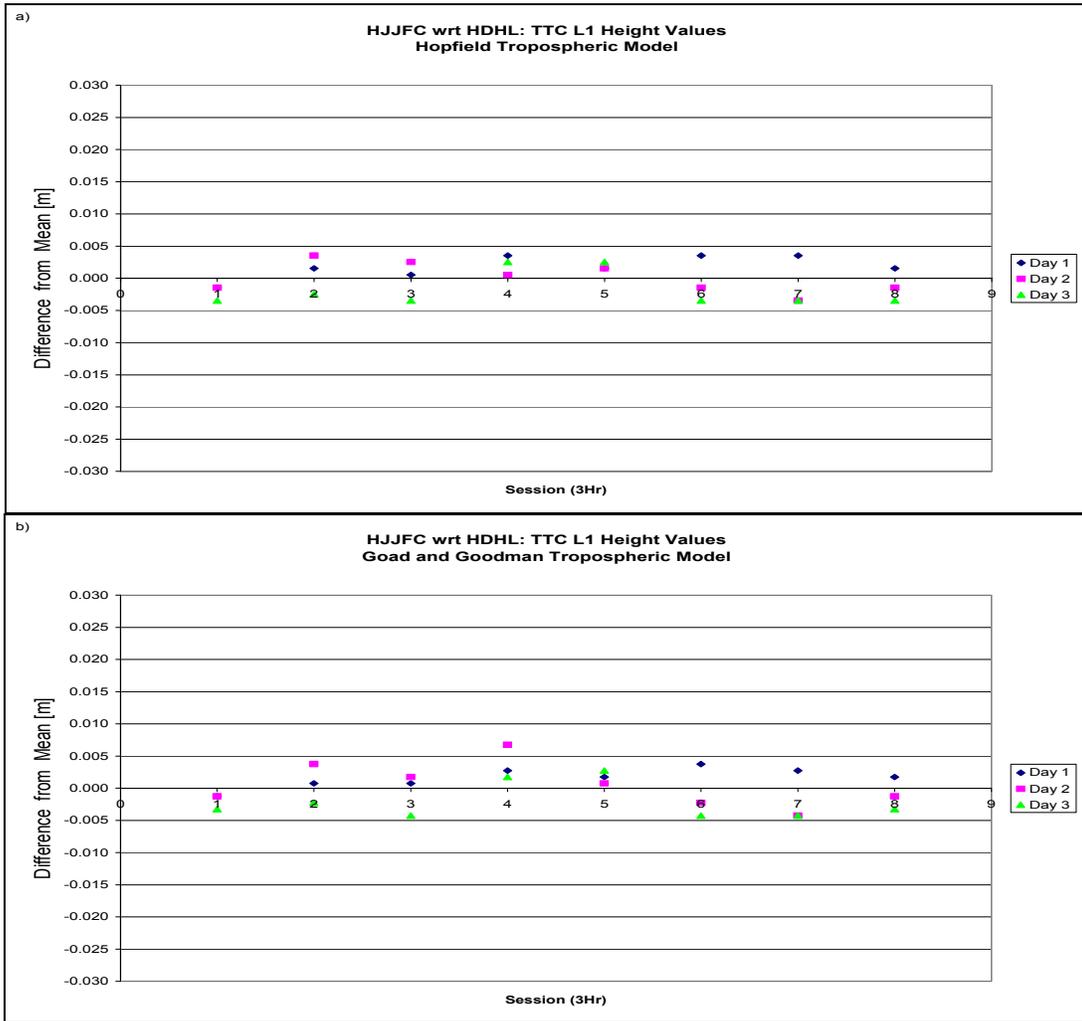
Figure 4.9 a-b: Tropospheric Model Comparison
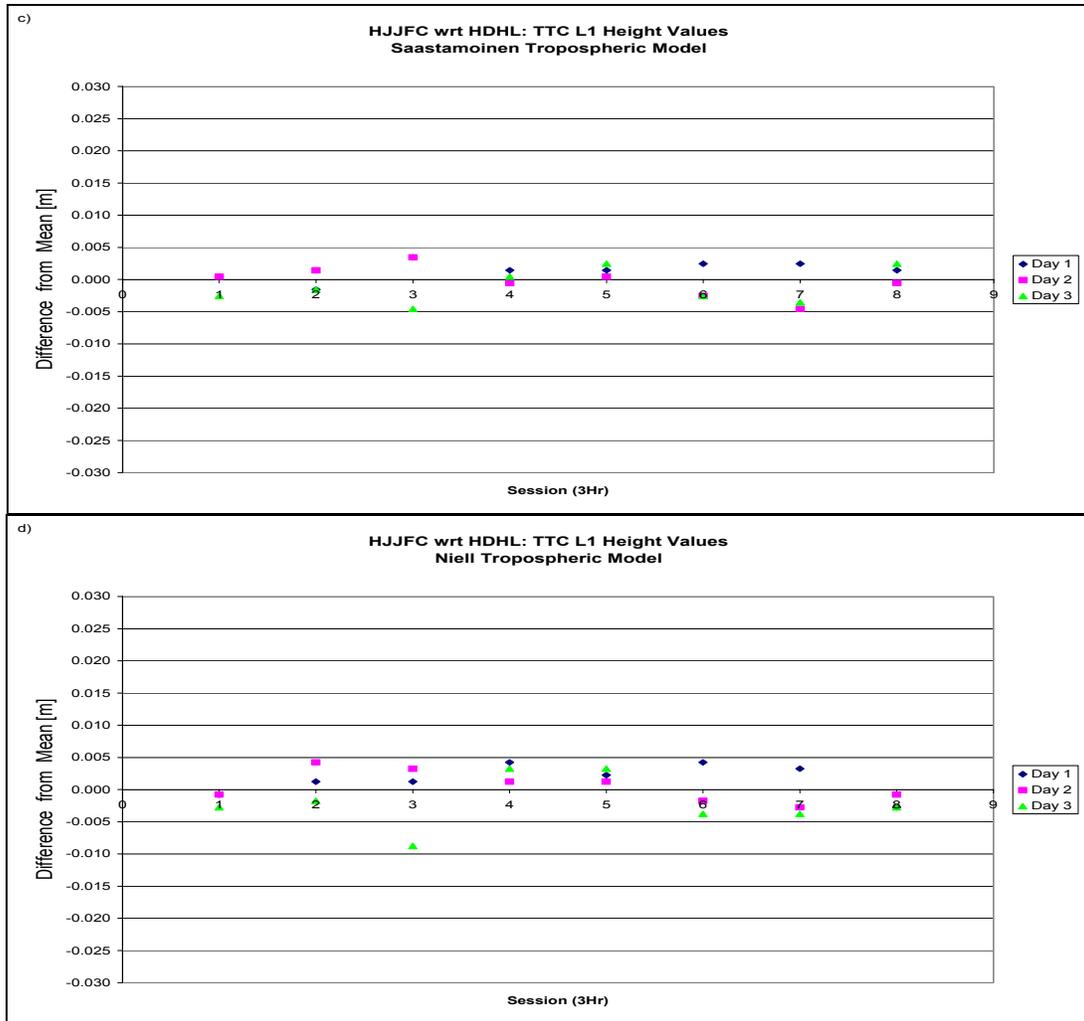
Figure 4.9 c-d: Tropospheric Model Comparison

It can be seen from Figure 4.9 that the four tropospheric models tested produced similar deviations from the mean of the height component. The Hopfield and Saastamoinen models performed best, confirming earlier findings by Janes *et al*., [1991], and their use is recommended.

4.3.4 Session Length

In this section, the impact of the duration of observation time on the GPS solution is analyzed. The idea here is that over a certain period of time, certain biases may average out (e.g., multipath). Additionally, the added redundancy in itself may lead to a more robust solution. This factor will be very much site dependent, and will have to be analyzed in each scenario.

In this investigation, session lengths of 1/2, 1, 2, 3 and 4 hours were compared. The results are presented in Figure 4.10 and the calculated standard deviations for the solution components of each sample are shown in Table 4.3.
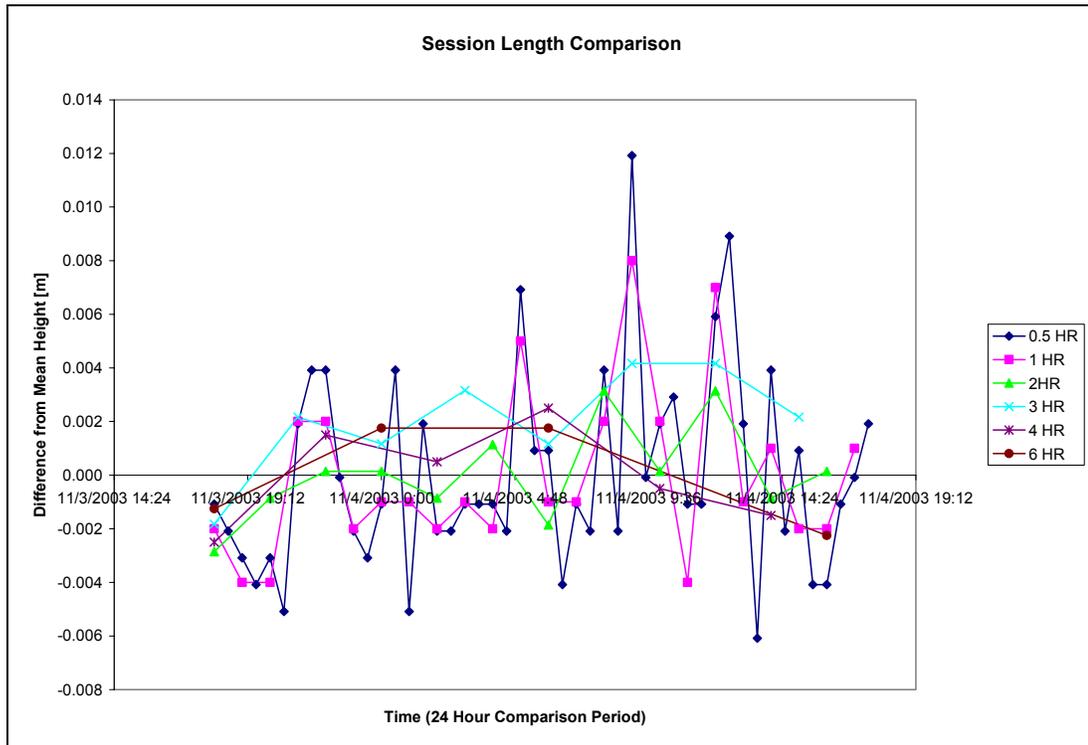
Figure 4.10   Session Length Comparison

Table 4.3   Standard Deviations of Each Solution Component

Session Length [Hrs]	σN [m]	σE [m]	σH [m]	σX [m]	σY [m]	σZ [m]
0.5	0.0030	0.0026	0.0037	0.0023	0.0035	0.0030
1.0	0.0027	0.0021	0.0031	0.0021	0.0032	0.0022
2.0	0.0023	0.0018	0.0017	0.0014	0.0024	0.0015
3.0	0.0019	0.0016	0.0018	0.0010	0.0024	0.0015
4.0	0.0022	0.0012	0.0017	0.0011	0.0024	0.0013
6.0	0.0019	0.0005	0.0018	0.0011	0.0023	0.0009

From Figure 4.10 and Table 4.3 it can be concluded that using 1 hour sessions leads to about 0.003 m standard deviation of all three components. It is not until session lengths reach the 3 hour mark that the root mean square (rms) errors of the N,E,H components drop below 0.002 m. RMS values of the solution components show some improvement as sessions increase in length. As previously mentioned, the impact of session length on the solution quality is site dependent and depends upon the project requirements. For high precision GPS surveys using short, static baselines, it appears that a session length of at least 3 hours should be used.

4.3.5   Time of Day of Observations

GPS satellites orbit such that the constellation repeats itself every 12 hours. Consequently, there are periods during the day which exhibit more

favourable conditions for obtaining robust GPS solutions. Additionally, when height differences exist between reference and rover stations, differences in atmospheric conditions between sites become important. At certain times of the day these disparities may be less pronounced. Each GPS scenario will be unique and will require an investigation as to when the best time to make observations will be.

Figure 4.11 depicts the variation in GPS solutions of the height component (using 10 s data, 10 degree cut-off angle, Saastamoinen tropospheric model and 3 hour sessions), the number of satellites visible and the time of day of the solutions (GPS Time). It should be noted that the solution is plotted at the end of the three hour session so that the satellites viewed over that session can be seen in the three hour block prior the solution. GPS Time is 4 hours ahead of local time (Atlantic Standard Time).
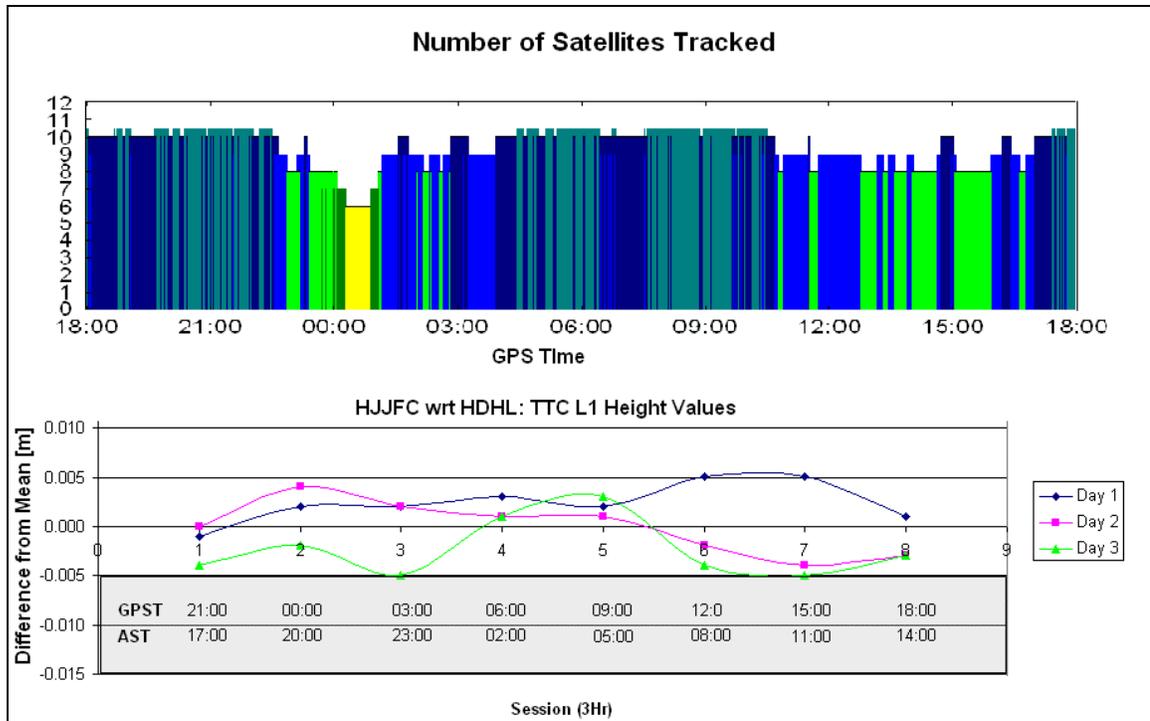
Figure 4.11   Satellite Availiability, GPS Time of Day and Solution Results

From Figure 4.11, it can be seen that when there are 10 or more satellites visible throughout the whole session, there is remarkable repeatability of the solutions from day to day (within a couple of millimetres). The results for this baseline are good throughout the duration of this observation, which can be attributed to favourable GPS conditions. It is difficult in this case to correlate poor solutions with poor satellite visibility. However, it is interesting to note that around noon the largest spread in solutions occurs and overnight the smallest spread in solutions is exhibited.

5 HVC DATA ANALYSIS

Highland Valley Copper, as was described in Chapter 3, represents a very different scenario from that just discussed. Two field tests were conducted at HVC. The first was conducted in October of 2002, using four GPS receivers. The reference station was called 424 and the rover stations were located at RTS1, RTS2 and RTS3. Analysis of data from this first test showed upward trends of the RTS stations. Since this did not make physical sense, it was hypothesized that the reference station was actually sinking. Since there was no way of confirming this hypothesis, a second field test was conducted during August and September of 2003.

In the second field test, a second reference station was added so that the stability of the reference stations could be confirmed. Figure 5.1 illustrates the distribution of the GPS points at HVC. Points 424 and 987 are reference stations, located in 'stable' conditions. RTS1, RTS2 and RTS3 are locations of combined GPS-RTS setups. Table 5.1 presents the distances between points.
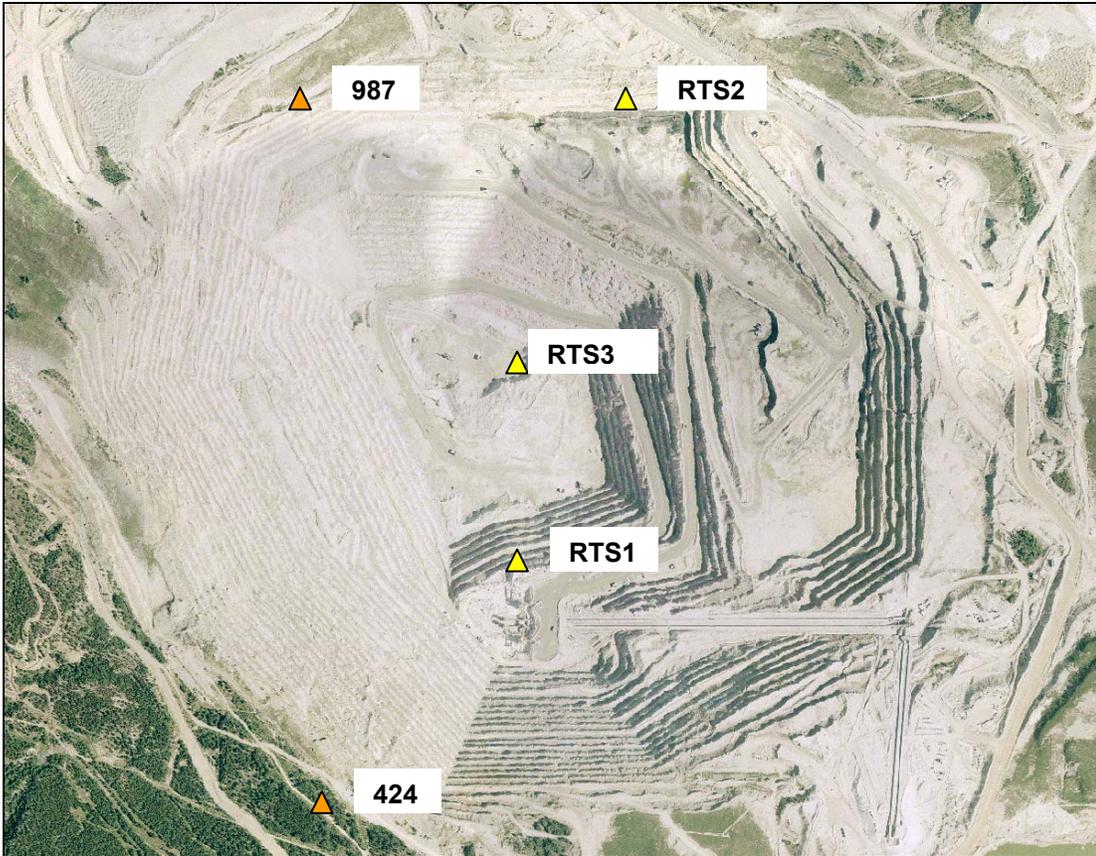
Figure 5.1   Distribution of GPS Points at HVC

Table 5.1   RTS+GPS Control Network Distances

From	To	Height Difference [m]	Slope Distance [m]	Horizontal Distance [m]
424	987	315.670	2534.328	2514.592
424	RTS1	512.374	1426.420	1331.220
424	RTS2	360.333	2537.591	2511.877
424	RTS3	676.777	1875.733	1749.385
987	RTS1	196.704	1291.390	1276.321
987	RTS2	44.663	447.442	445.207
987	RTS3	361.107	920.995	847.250
RTS2	RTS1	152.041	1200.400	1190.732
RTS2	RTS3	316.445	825.508	762.448
RTS1	RTS3	164.404	469.156	439.407

The second GPS test was conducted during the period of August 21 to September 10, 2003. Technological difficulties limited the actual amount of data collected during this period. Table 5.2 summarizes the data availability for this test where 'X' denotes available.

Table 5.2 Data Availability During the Second GPS Test

Station:	424	987	RTS1	RTS2	RTS3
Thursday, August 21, 2003				X	
Friday, August 22, 2003	X	X		X	
Saturday, August 23, 2003	X	X		X	
Sunday, August 24, 2003	X	X		X	
Monday, August 25, 2003	X	X		X	
Tuesday, August 26, 2003	X	X		X	
Wednesday, August 27, 2003	X	X		X	
Thursday, August 28, 2003	X	X	X	X	
Friday, August 29, 2003	X	X		X	
Saturday, August 30, 2003	X	X		X	
Sunday, August 31, 2003	X	X		X	
Monday, September 01, 2003	X			X	
Tuesday, September 02, 2003	X			X	
Wednesday, September 03, 2003	X		X	X	X
Thursday, September 04, 2003	X		X	X	X
Friday, September 05, 2003	X	X	X	X	X
Saturday, September 06, 2003	X	X	X	X	X
Sunday, September 07, 2003	X	X	X	X	X
Monday, September 08, 2003	X	X	X	X	X
Tuesday, September 09, 2003	X	X	X	X	X
Wednesday, September 10, 2003	X	X	X	X	X

This chapter uses the optimal settings determined in Chapter 4 to process the data collected at Highland Valley Copper mine. The objective of this chapter is to ascertain the accuracy and precision that can be achieved in a harsh GPS environment.

5.1   Processing Optimization

Data was processed in Trimble Total Control (TTC) software for analysis, using the settings determined in the previous section. Baselines have been processed from each RTS station to each reference station, as well as between reference stations. The effects of varying the session length and the time of day of the sessions were investigated. The results are presented in the following subsections.

5.1.1 Session Length

From Section 4.3.4 it is apparent that a session length of at least 3 hours is required to meet the demands of this project. Therefore, processing started with a session length of 3 hours, which was then increased to 6, 12 and 24 hours. The standard deviations of the baseline components which have been computed for each sample are presented in Table 5.3.

Table 5.3   Standard Deviations of Solution Components as
Session Length Varies

From	To	Session Length [Hrs]	Duration [Days]	Sample Size	σN [m]	σE [m]	σH [m]
987	424	3	15	118	0.0035	0.0034	0.0071
987	RTS1	3	5	40	0.0024	0.0023	0.0036
987	RTS2	3	13	103	0.0010	0.0016	0.0014
987	RTS3	3	5	38	0.0020	0.0032	0.0059
424	RTS1	3	7	57	0.0026	0.0031	0.0136
424	RTS2	3	19	145	0.0037	0.0043	0.0093
424	RTS3	3	7	55	0.0035	0.0060	0.0107
987	424	6	5	20	0.0030	0.0029	0.0059
987	RTS1	6	5	20	0.0022	0.0020	0.0028
987	RTS2	6	5	20	0.0007	0.0011	0.0013
987	RTS3	6	5	20	0.0019	0.0030	0.0078
424	RTS1	6	5	20	0.0026	0.0019	0.0064
424	RTS2	6	5	20	0.0029	0.0029	0.0061
424	RTS3	6	5	20	0.0027	0.0030	0.0082
987	424	12	15	28	0.0027	0.0026	0.0040
987	RTS1	12	5	10	0.0028	0.0022	0.0030
987	RTS2	12	15	28	0.0007	0.0016	0.0017
987	RTS3	12	5	10	0.0023	0.0025	0.0059
424	RTS1	12	7	13	0.0020	0.0019	0.0046
424	RTS2	12	19	38	0.0029	0.0033	0.0042
424	RTS3	12	7	13	0.0025	0.0020	0.0112
987	424	24	15	15	0.0019	0.0024	0.0032
987	RTS1	24	6	6	0.0019	0.0009	0.0018
987	RTS2	24	16	16	0.0009	0.0018	0.0020
987	RTS3	24	6	6	0.0017	0.0023	0.0040
424	RTS1	24	6	6	0.0015	0.0015	0.0042
424	RTS2	24	18	18	0.0017	0.0026	0.0037
424	RTS3	24	6	6	0.0018	0.0014	0.0034

From Table 5.3, some interesting observations can be made. First, to point out the obvious, it can be seen that in most cases, having a longer session length improves the quality of results. The biggest improvement can be seen in

the height component of the solution. This is particularly true for baselines having height differences of a couple hundred metres. For baselines with stations having roughly the same height (987 to RTS2), the improvement in the quality of the solutions is slight, if there is any improvement at all, when session length is increased above 3 hours.

Increasing the session length increases the redundancy of the problem. For baselines having restricted satellite visibility, longer session lengths allow better satellite geometry to be viewed, thus providing a better quality solution. Additionally, erratic meteorological variations caused by microclimates have a less pronounced impact on the solution when they are averaged out over longer periods. That is, the longer the observation period, the more likely the troposphere is to behave as modelled.

The problem with increasing session length is that it reduces the ability of the deformation monitoring system to provide 'real-time' results. Having to wait 24 hours for an update may not satisfy the requirements of the system. More frequent sessions are preferable.

To summarize the results in Table 5.3, the following points are noted:

1. For baselines having height differences of less than 100 m, standard deviations of 2 mm or better are achievable in all three solution components when using 3 hour solutions.

2. The baseline components of 987 to RTS1 can be determined to better than +/- 3 mm in all solution components using 6 hour sessions.

3. The baseline components of all baselines can be determined to better than +/- 5 mm in all solution components using 24 hour sessions.

4. The height component can only be determined to +/- 5 mm between 424 and RTS3 or 987 and RTS3 by using session lengths of 24 hours.

5. Unmodelled tropospheric biases resulting from the large height differences between 424 and the RTS stations make it an unfavourable reference station. It may be used to confirm the stability of 987. If the tropospheric biases can be modelled, it may become a viable reference station. An alternative location for 424 would be a location further away from the pit but at an elevation similar to 987's.

5.1.2 Time of Day of Observations

In an environment such as that at HVC, satellite availability becomes an important issue. Certain periods of the day will provide more favourable conditions for achieving quality solutions. For example, Figure 5.2 shows the number of satellites visible at RTS3 over a 24 hour period. It can be seen that there are periods of the day during which a GPS solution is not even possible due to limited satellite availability. Figure 5.3 illustrates the variation of the height

component of RTS3 over 5 consecutive days using 3 hour session lengths. Session 1 solutions in Figure 5.3 used the number of satellites illustrated from 18:00 to 21:00 hours in Figure 5.2 and so on.
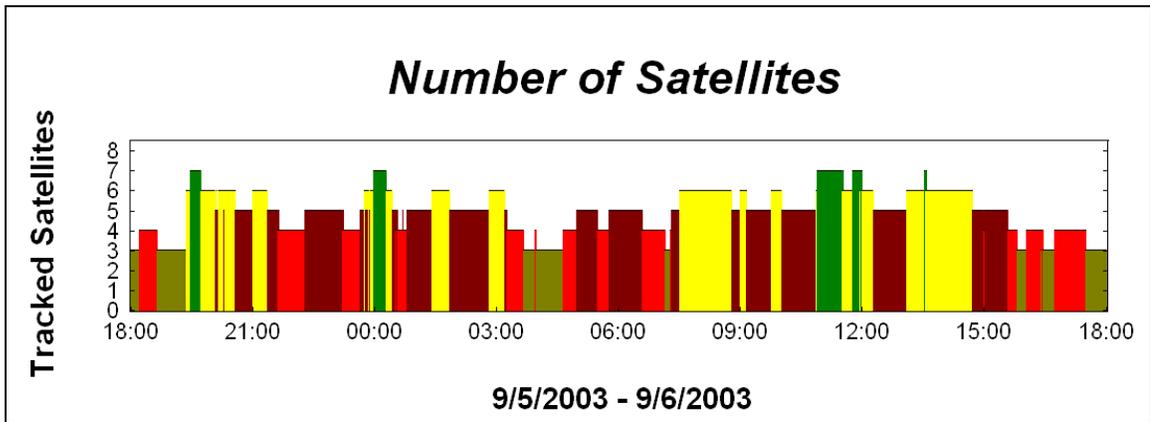
Figure 5.2   Number of Satellites Visible at RTS3
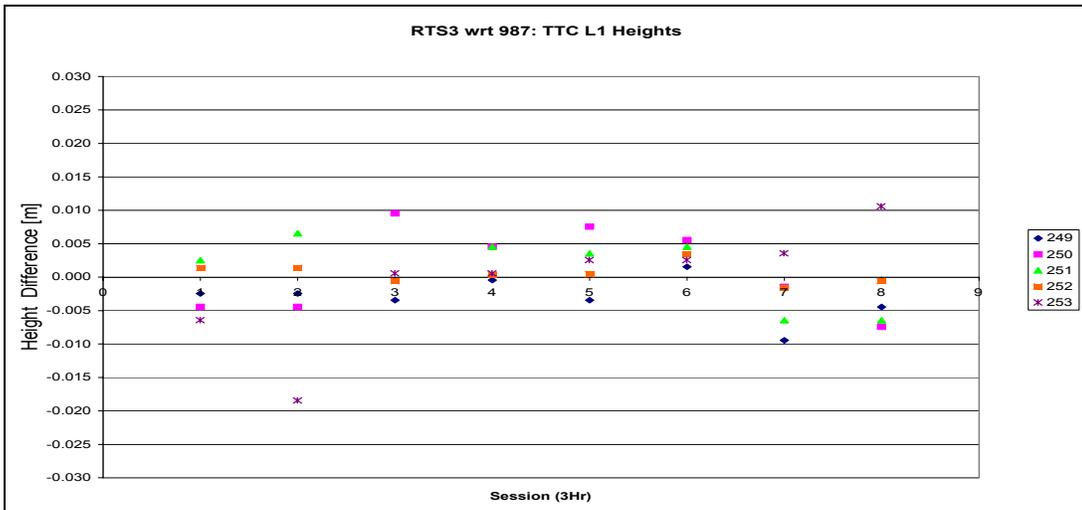
Figure 5.3   Height Variation from 5 Day Mean at RTS3

It is difficult to show any correlation between Figures 5.2 and 5.3. Session 4, which views 3, 4 and 5 satellites, actually has one of the most consistent solutions. Unfortunately, plotting the number of satellites that are visible does not tell us anything about satellite geometry. A more useful plot for analyzing the relationship between satellite availability, satellite geometry and quality of solutions is a polar plot of satellite orbits.

Figures 5.4 and 5.5 are polar plots for sessions 2 and 4 respectively, having the worst and best results. An elevation mask of 15 degrees has been set to mimic conditions in the pit. Additionally, an obstacle causing a 30 degree elevation mask has been set in the south, representing the steep pit wall.
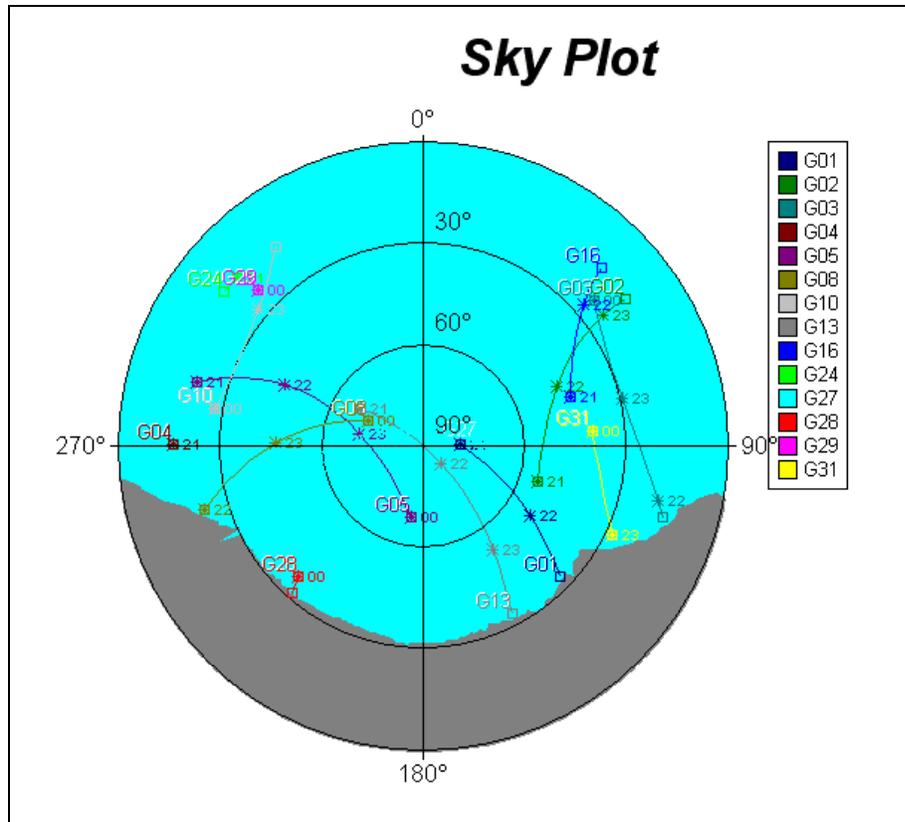
Figure 5.4 Polar Plot of Satellite Orbits for Session 2
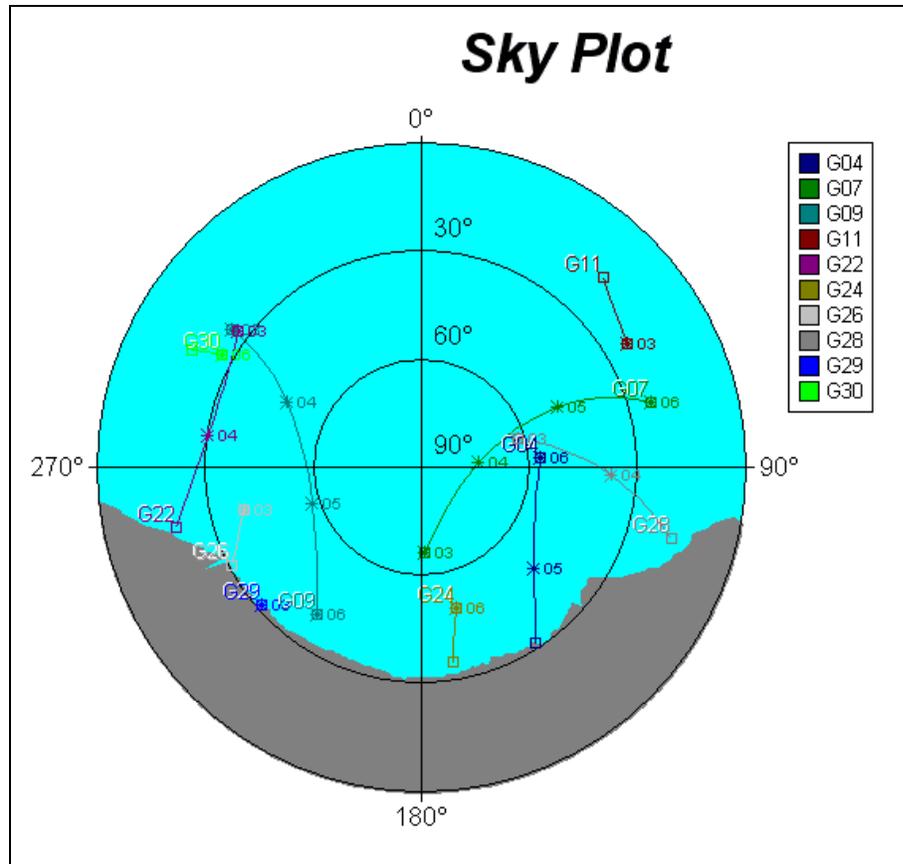
Figure 5.5   Polar Plot of Satellite Orbits for Session 4

Again, it is not apparent whether satellite visibility or geometry is significantly better in one scenario than the other. A closer look at Figure 5.3 reveals that the repeatability from session to session is good, except for the occasional outlier that makes the results look much worse than they really are. There appears to be some other factor that biases the results every so often.

It is highly suspected that residual tropospheric delay still biases the results. This bias becomes more pronounced with baselines having large height differences such as this one. Unfortunately, meteorological sensor data was not

available at stations 987 and RTS3. This does not allow for analysis of variations of atmospheric conditions and position solutions for this baseline. MET sensor data was available for stations 424 and RTS2. An investigation into the use of meteorological data is presented in Section 6.3.

With regard to the time of day that these variations are occurring, there is a 7 hour time difference between Pacific Daylight Savings Time and GPS Time. Therefore, Session 1 in Figure 5.3 begins at 18:00 − 7:00 = 11:00. Similar to what was found in Section 4.1.2.5, the sessions with highest repeatabilities (4, 5 and 6) occur overnight.

5.2   Implications of Findings

From the previous discussion, it is apparent that one would be hard pressed to obtain standard deviations of better than +/- 2 mm in the GPS solution components. Consequently, due to limitations of the GPS system and in the achievable accuracies of RTSs, at the present time, the ultimate goal of +/- 5 mm at 95% confidence is not attainable.

It also becomes apparent that Scenario I from the pre-analysis performed in Section 3.6 will not be a viable approach unless residual tropospheric delay biases are accurately estimated. From Table 3.4, then, it can be expected that sub-centimetre level displacements can be detected at HVC through the

implementation of Scenario II. The stipulation is that proper measures must be taken to achieve the cited RTS accuracies, as discussed in Section 3.4.2 and sight lengths must be restricted to less than 500 m. By using sight lengths of 400 m or less, accuracies of +/- 7 mm at 95% confidence can be achieved in all three solution components. For further discussion on implementing a combined RTS+GPS system at HVC, see A. Chrzanowski & Associates [2004].

6 TECHNIQUES FOR IMPROVING GPS RESULTS

Several processing techniques have been devised for improving the quality of GPS position solutions. This chapter discusses the applicability of techniques which have been implemented in other research (including day-to-day correlation analysis of multipath, estimating residual tropospheric delay parameters and using meteorological data in processing). Additionally, a couple of new ideas are considered (a moving average filter and a bootstrapping method are discussed). An investigation into the potential use of augmentation systems is then presented.

6.1 Day-to-Day Correlation Analysis

In local, GPS-based, deformation surveys, multipath is commonly the largest error source, contributing errors as large as 5 cm [Radovanovic, 2000]. Multipath is caused by reflective objects in the GPS antenna environment. If this environment does not change, the multipath bias should reoccur, as the GPS satellite constellation repeats its geometry every 23 hours 56 minutes.

This bias is manifested in the double-difference residuals and is referred to as the characteristic multipath 'signature' for a satellite pair. The magnitude of the day-to-day correlation is typically around 85%, but this value will depend upon the consistency of the multipath environment [Radovanovic, 2000].

The principle behind day-to-day correlation analysis is straight forward. If coordinates are known for a point on any given day, the multipath error at every epoch can be calculated for phase data, creating the multipath signature. This signature can be subtracted from data collected on subsequent days to mitigate the effects of multipath. Epoch-to-epoch position accuracies at the 5 mm (1 σ) level have been reported [Radovanovic, 2000].

There are two conditions that must be met in order for this to be a viable approach. The first is that the principle error source is, in fact, multipath. If, for example, residual tropospheric delay is contaminating the results, one would be hard pressed to find any day-to-day correlation. The second condition is that the multipath originates from a specular source, which causes high repeatability from day-to-day. Multipath caused by diffraction or diffusion is not so predictable. Diffraction and diffusion (similar to multiple specular reflections) may cause the GPS receiver to track the composite GPS signal of a direct and (multiple) reflected signal(s) with different multipath characteristics every day [Kim *et al*., 2003].

The potential for using day-to-day correlation analysis was investigated after the first GPS field test [Kim *et al*., 2003]. Figure 6.1 shows the double difference residuals for the satellite pair PRN 15 and 18 for the 424-RTS2 baseline. The plot illustrates that the effects of multipath are not diurnally correlated. The residuals are not clean multipath observables. Unmodelled

effects are still present. Similar results were observed for the other baselines investigated.
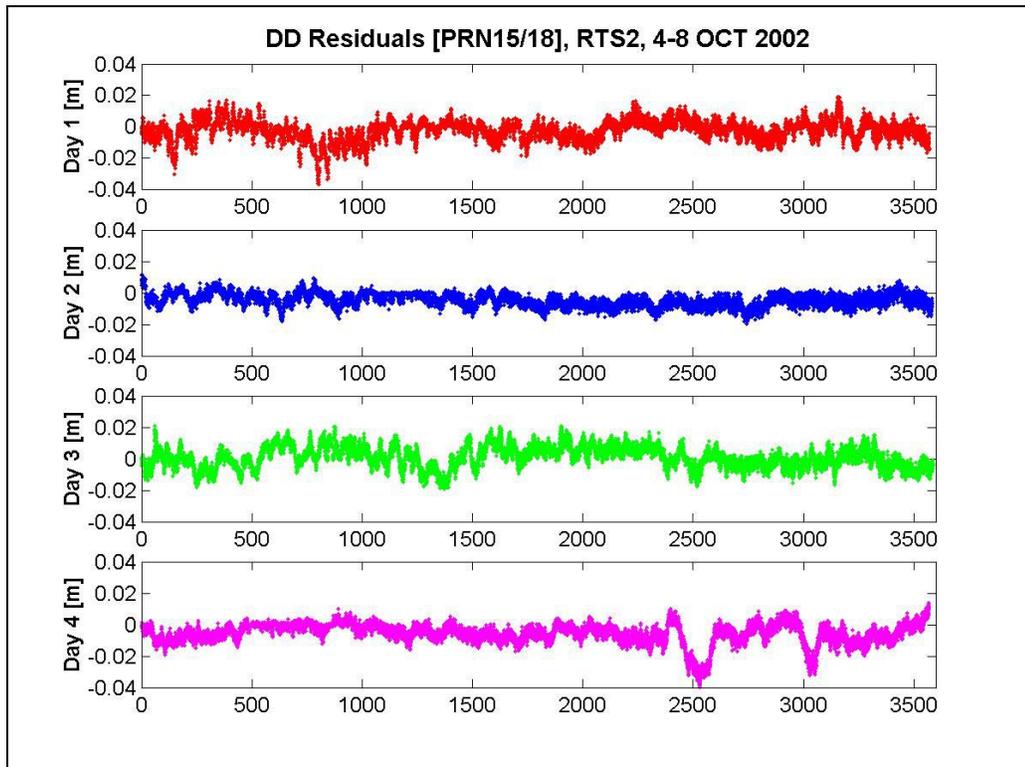
Figure 6.1   Double-Difference Residuals for the Same 1 Hour Session Over 4 Days [Kim *et al*., 2003]

6.2 Estimation of a Residual Tropospheric Delay Parameter

This technique was discussed in Section 2.1.2.1. In order to test the effectiveness of this strategy, a modified version of DIPOP, produced within the

CCGE, was used for processing. TTC and most other commercial software do no offer this option.

The baseline from 424 to RTS2 is presented here, since it has a large height difference and the benefits of estimating a residual tropospheric delay parameter are more apparent. The results are presented in Figure 6.2. Each grid column in the plot contains 4, 6-hour solutions. The top plot does not make use of a tropospheric parameter whereas the bottom estimates one every half hour.

From Figure 6.2, it can be seen that there is a definite improvement in the accuracy of the solutions when a tropospheric parameter is estimated. Except for a few outliers, most of the solutions fall within +/- 5 mm at the standard confidence level. The effectiveness of this technique reaffirms the suspicion that tropospheric delay is the major contaminant in the results. It should be pointed that for baselines where low elevation satellites are not tracked (e.g., to RTS3), this strategy may not be as useful.
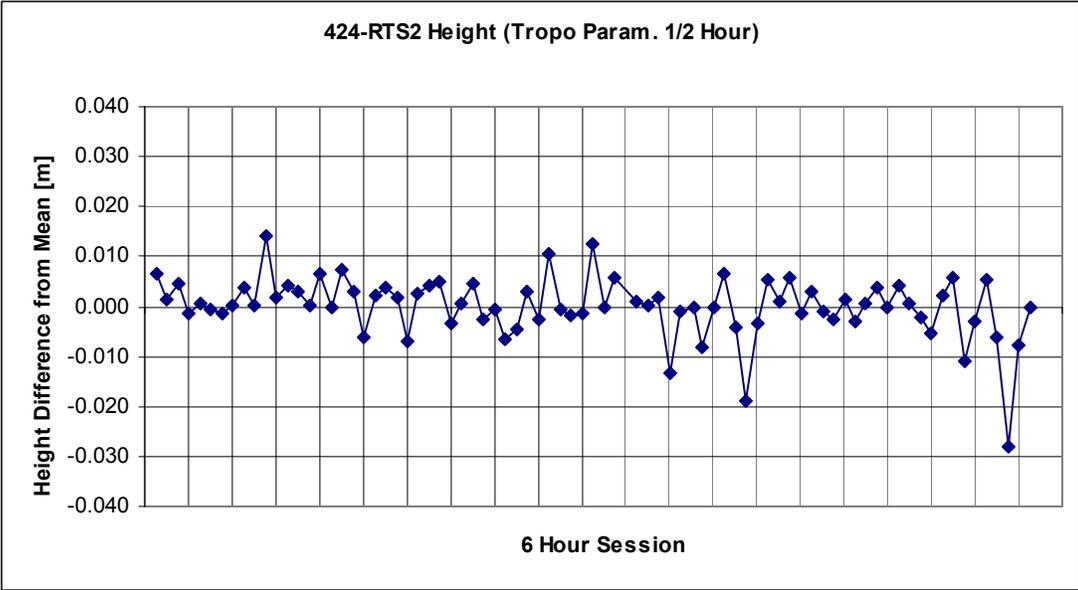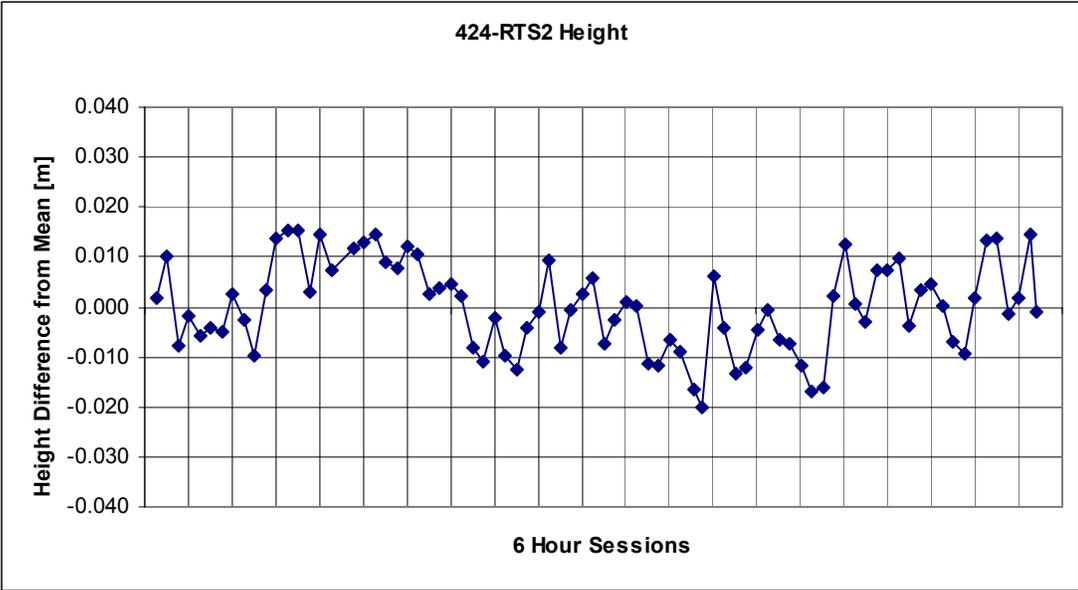
Figure 6.2   Tropospheric Parameter Estimation [Wilkins, 2004]

6.3 Use of Meteorological Data

During the second GPS field test at HVC, meteorological data (temperature, pressure and relative humidity) was recorded at stations 424 and RTS2. Meteorological data was collected approximately every 10 minutes at both stations and hourly averages were computed. TTC allows for meteorological data to be input for each session for a baseline. It was desired to determine whether or not using this information would lead to any improvement in baseline results.

Figure 6.3 shows the height component results of the baseline between 424 and RTS2, which has been processed with and without meteorological data. Three hour sessions have been used. It can be seen that the use of meteorological data does not improve the results, and actually makes them worse, as was pointed out by Rizos [2001] and Janes *et al*., [1991].
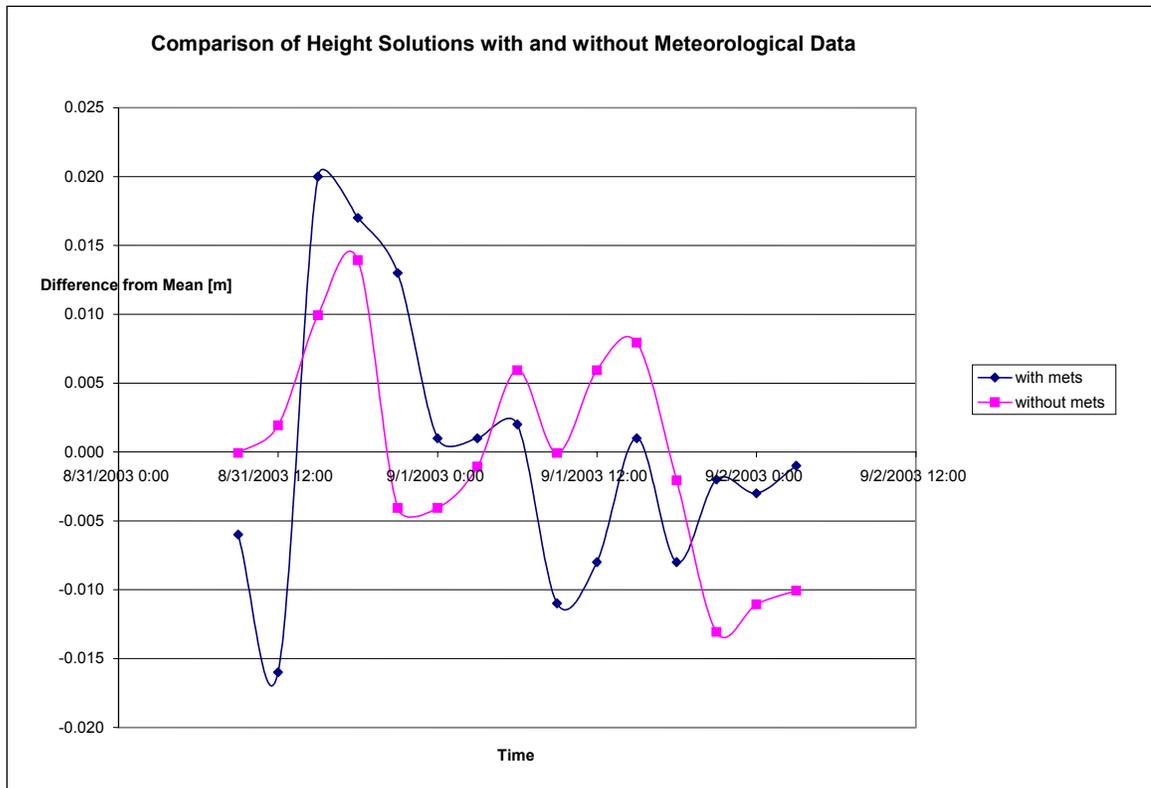
Figure 6.3   Use of Meteorological Data in GPS Processing

It was also desired to determine whether or not there was any correlation between the variations in meteorological conditions and the variations in height solutions. This investigation provides some insight into how well the tropospheric model reflects actual conditions at the mine site.

To accomplish this task, the temperature, pressure, relative humidity and refractive indices of each station were calculated using the profile functions presented in Section 2.1.1. The refractive index was calculated at each station using the Hopfield model (representing values used by the software model). The difference in these values between stations was then calculated. Similarly, using

the actual meteorological data, differences in temperature, pressure, relative humidity and the refractive index between stations were calculated.

Table 6.1 presents the *differences in the differences* between observed and modelled met values (and calculated refractive indices, based upon these values) between 424 and RTS2, shown for every hour over the 24 hour period tested above. Since a difference in the difference in refractive indices between stations translates directly into a relative zenith tropospheric delay error, the approximation of Beutler *et al*. [1988] can be used to determine the relative height error (*a 1 mm differential tropospheric bias causes a height error of about 3 mm,* see Section 2.1.1*)*. This is reflected in the last column of Table 6.1.

The relative height error caused by the tropospheric delay bias was approximated by multiplying the height difference between the two stations (361 m) by δΔn and then multiplying the result by the factor of 3 (section 2.1.1). For this particular baseline, it can be seen that biases of about one centimetre can enter into the solution.

Based upon these values, it was attempted to apply a correction term to the height values obtained using TTC, mimicking the approach used by Rothacher *et al*. [1986], discussed in Section 2.1.2.3 (although not rigorously implemented since the correction term was not calculated for every satellite range). The correction term was determined by first calculating the refractive index values for both stations as would have been done in the software (the Hopfield model was used for ease of calculation). Secondly, the average

103

refractive index value between stations was then computed. The refractive index

at each station was calculated using the meteorological data, and the average

value between stations was also computed.

Table 6.1   Differences (δ) in the Differences (Δ) in Meteorological Values and
Refractive Indices between Modelled Values and Measured Values, and the
Resulting Relative Height Error.

δΔn (ppm)	δΔT (C)	δΔP (mbar)	δΔH (%)	Δh$_e$ (mm)
3.5	1.9	2.0	4.6	4
4.4	1.2	2.1	6.8	5
3.7	1.4	2.0	5.6	4
3.6	2.1	1.8	4.3	4
0.0	2.6	1.6	-2.0	0
0.6	2.1	1.6	0.3	1
2.9	1.0	1.6	5.0	3
5.7	-0.8	1.5	9.9	6
7.4	-2.7	1.6	12.8	8
7.6	-3.4	1.4	13.1	8
9.7	-3.1	1.0	13.5	11
8.7	-1.6	1.4	10.4	9
9.6	-1.4	2.1	10.3	10
9.1	-1.8	3.1	9.4	10
9.2	-1.3	3.1	10.1	10
7.5	-0.1	3.4	8.8	8
7.7	-0.8	3.6	10.0	8
8.3	-1.4	3.3	12.5	9
8.8	-1.9	2.8	14.8	9
7.4	-1.1	2.5	13.2	8
5.6	-0.4	2.3	10.9	6
4.1	0.5	2.1	7.7	4
4.0	0.9	2.0	6.8	4
3.5	0.7	1.9	6.6	4

The correction term was calculated both with and without Beutler's factor

of 3. To obtain the correction term, the difference in the difference in refractive

indices was multiplied by: a) just the height difference b) the height difference and then by 3 (Beutler's approximation). Figure 6.4 shows the uncorrected results and the corrected results using a and b.
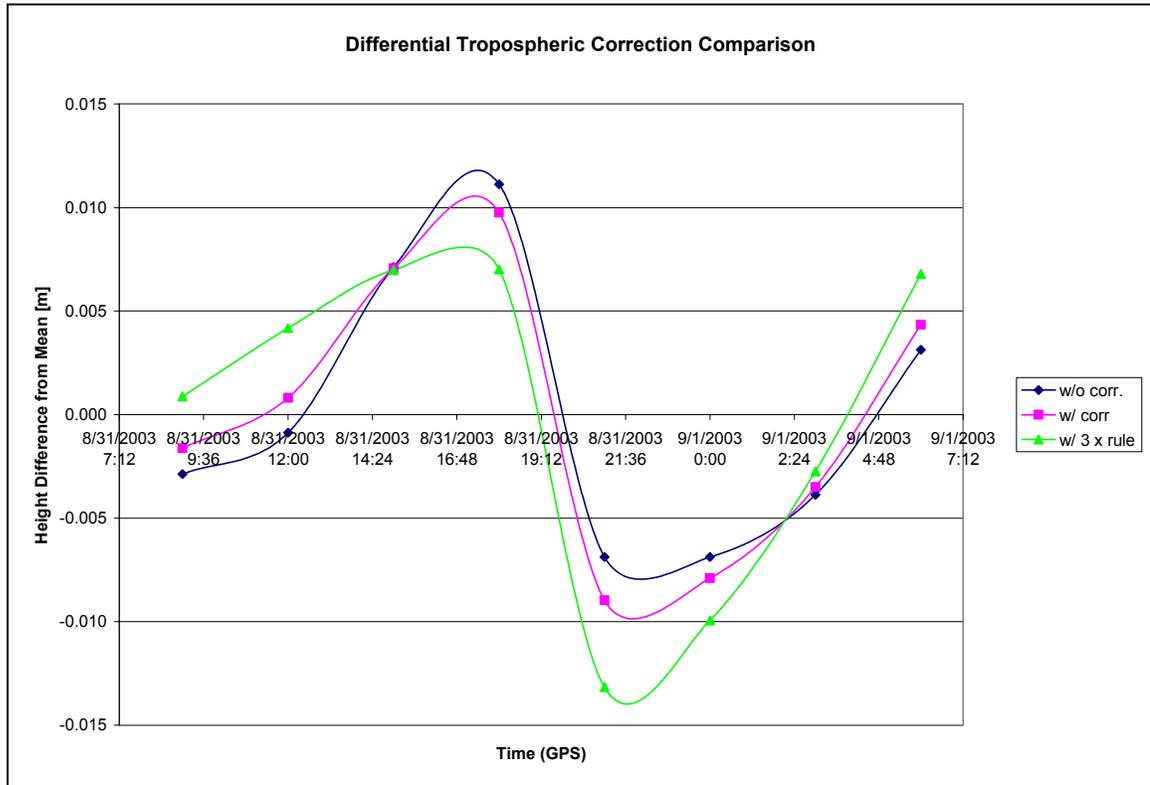
Figure 6.4   Meteorological Correction Implementation

From Figure 6.4, it can be seen that neither correction term caused any significant improvement in results. This does not imply that meteorological data cannot be used to improve solutions, even though Rothacher et al. [1986] have shown otherwise. Following this more rigorous approach, in which each satellite range is corrected using meteorological data, improved results may be attained.

6.4 Filtering

In Section 4.2.1.1 it was determined that 24 hour session lengths provide the best accuracy, but are too long to offer 'real-time' results. As a compromise, a simple moving average filter has been tested to see if 24 hour solutions, which are processed every three hours, offer any advantage [Chrzanowksi, 2004]. The concept is illustrated in Figure 6.5. The initial position solution is a 24 hour solution, which can be thought of as consisting of 8 x 3 hour blocks of data. After the next three hours of GPS data is collected, a new 24 hour solution is collected, consisting of 7 blocks of 3 hour data from the old solution, and 1 new block.
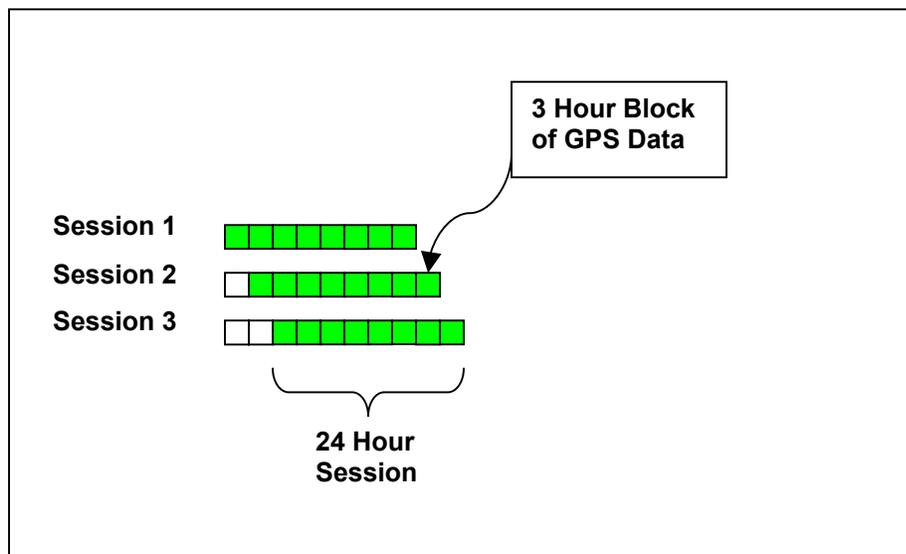
Figure 6.5 Moving Average Concept

This technique was tested on the 987-RTS1 and 987-RTS3 baselines. The results are presented in Figures 6.6 and 6.7, and Tables 6.2 and 6.3
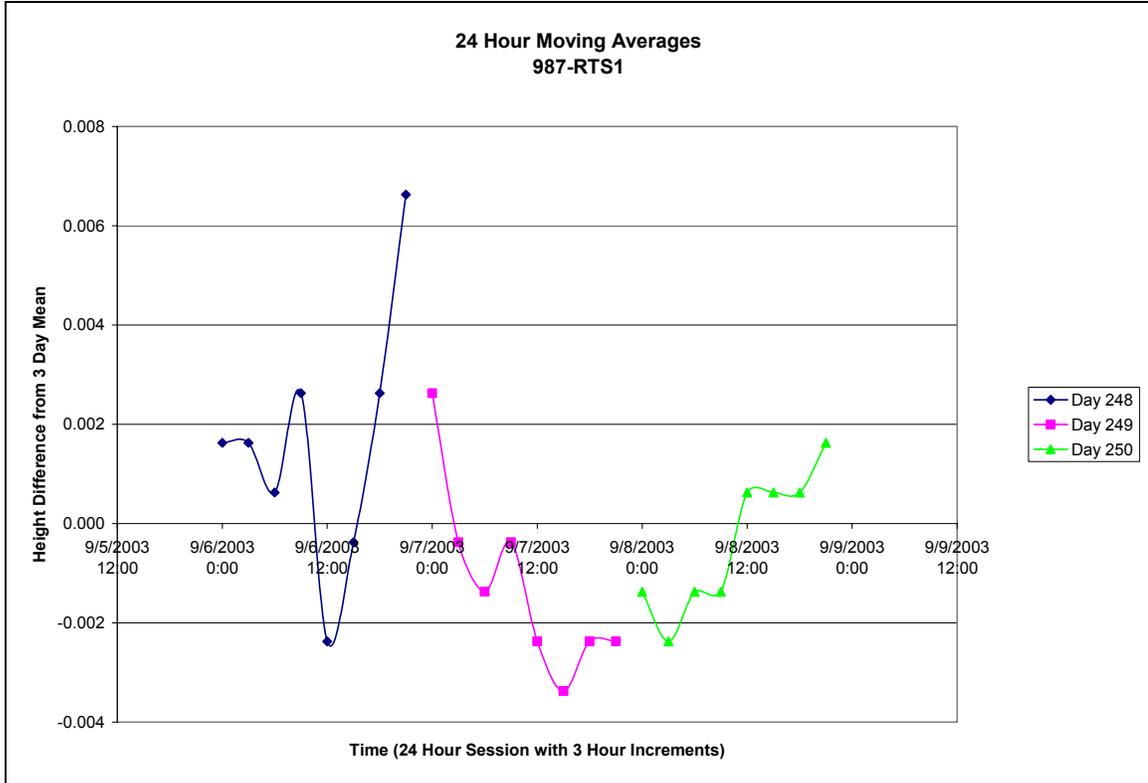
Figure 6.6   24 Hour Moving Average Filter over Baseline 987-RTS1

Table 6.2   Standard Deviations of Solution Components using Moving Average Filter, 987-RTS1

σN [m]	σE [m]	σH [m]
0.0015	0.0019	0.0023

107
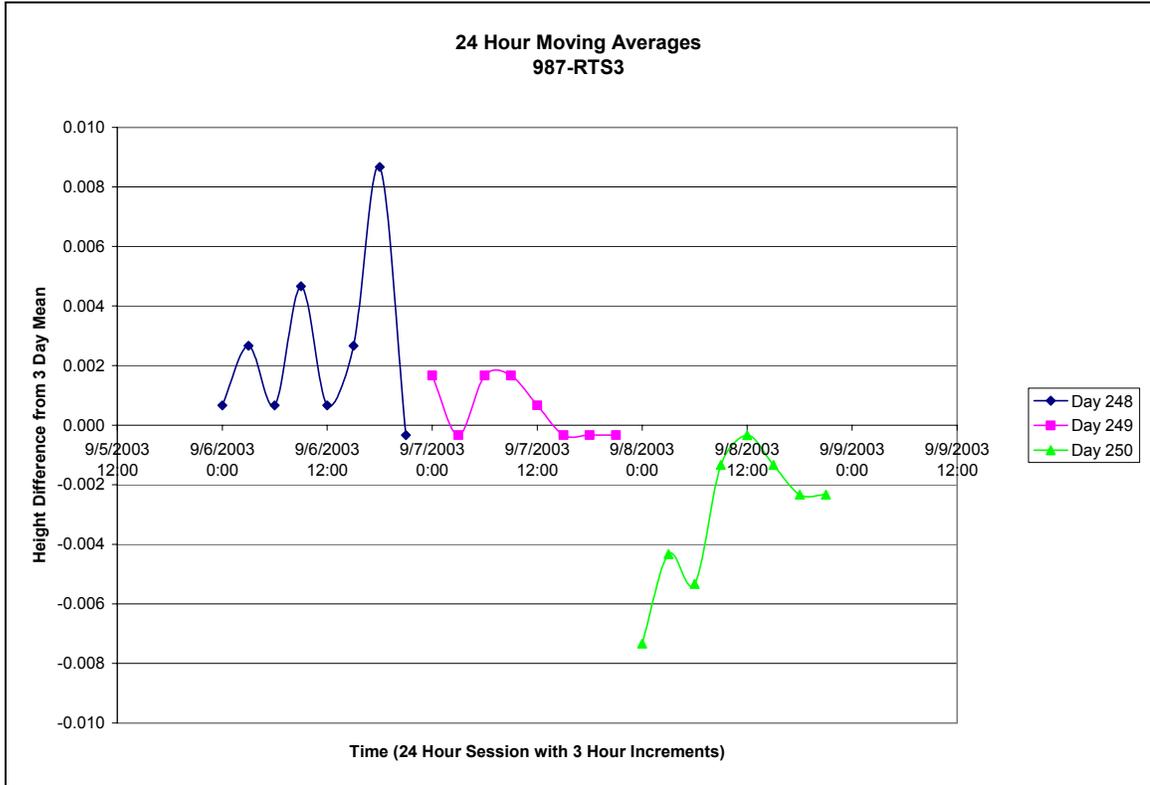
Figure 6.7   24 Hour Moving Average Filter over Baseline 987-RTS1

Table 6.3   Standard Deviations of Solution Components using Moving Average
Filter, Baseline 987-RTS3

σN [m]	σE [m]	σH [m]
0.0012	0.0027	0.0032

The results using this technique are good. For baselines having similar heights, accuracies of 2 mm in horizontal and about 3 mm in the vertical components can be expected. For baselines having larger height differences (as in the case of 987-RTS3), accuracies of 3 mm in horizontal and vertical components can be expected. It is interesting to note the jump in the vertical solution for both baselines during the 7th session of the first day. The cause is uncertain.

Although this technique offers high precision GPS results after every block of GPS data is collected, it is not a true 'real-time' system. If a displacement occurs it will not be fully detected until the weight of the new position is larger than that of the old. If the displacements are plotted from one epoch to the next, a gradual trend toward the new position will be seen. The full displacement will not be seen until each of the 8, 3-hour blocks indicates the new position, which will occur 24 hours after the displacement has occurred.

Recently, the CCGE has implemented a 'smarter' filtering approach for obtaining GPS solutions. The current strategy uses an optimized filter to estimate the change in baseline components of each RTS relative to a base station [Wilkins, 2004]. Depending on the conditions and the situation, either triple or double differencing of observations can be utilized in the solution.

Figure 6.8 a-c illustrates some preliminary results obtained using the triple difference (TD) mode to obtain the changes in the baseline components of an RTS with a length and height difference of 1291.390 m and 196.704 m

respectively (987 to RTS1). Clearly, trends in the RTS position can easily be identified at the millimetre level. Research at the CCGE is ongoing in the testing and implementation of this technique for use in their automated displacement monitoring software, ALERT [Wilkins *et al*., 2003a], but the initial results are very encouraging.
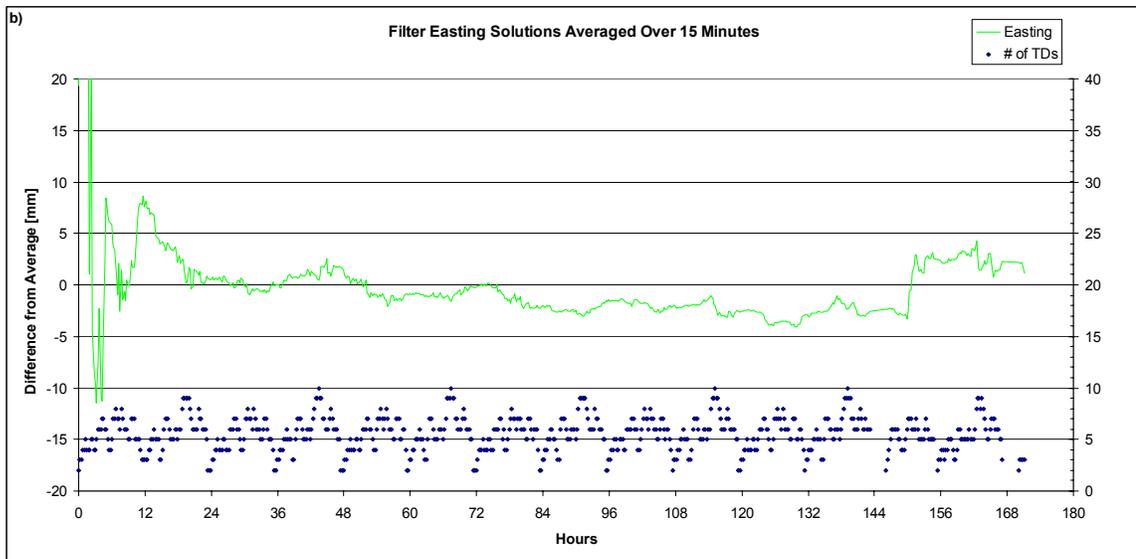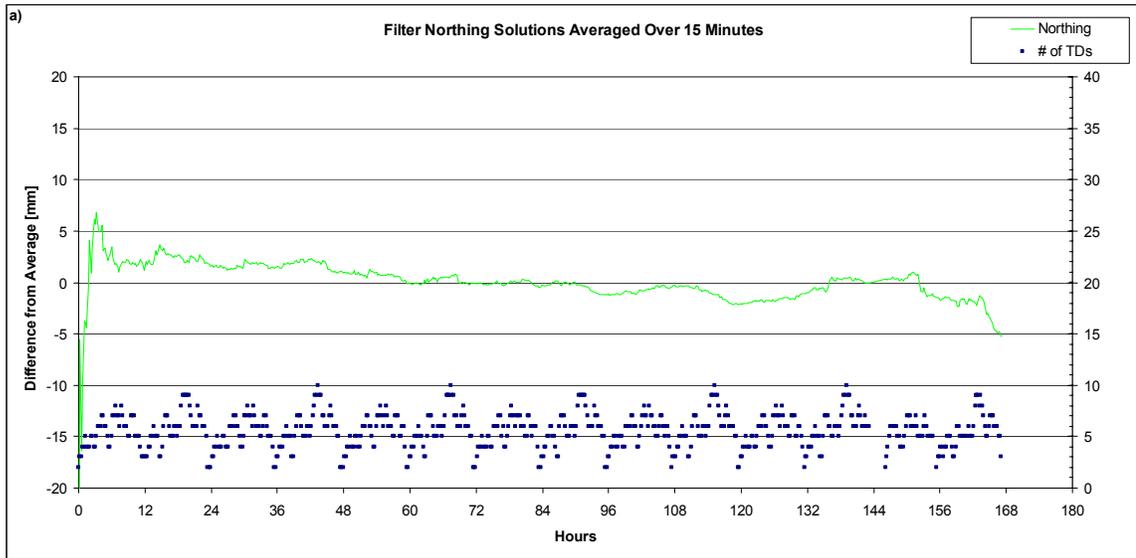
Figure 6.8 a-b   Filter Solutions Averaged Over 15 Minutes
[Wilkins, 2004]
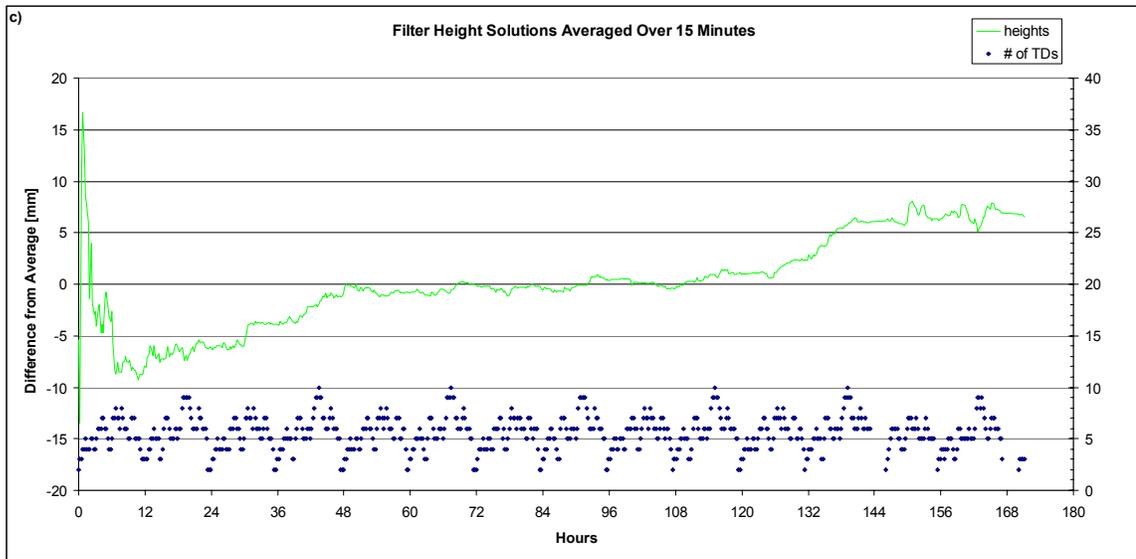
Figure 6.9 c   Filter Solutions Averaged Over 15 Minutes [Wilkins, 2004]

6.5   Bootstrapping to the Bottom

In Section 4.2.1.1 it was seen that only when height differences between baseline stations are about 150 m or less, can accuracies of a couple of millimetres be achieved with session lengths less than 12 hours. This approach, proposed by the author, utilizes this information to implement a technique to achieve millimetre level accuracies at all stations with shorter session lengths.

This strategy can be thought of as building a stairway down to the bottom of the pit. Each step is a short baseline with a height difference of about 150 m or

less. The purpose of each step in the descent is to confirm the stability of the next higher GPS point.

It was shown that accuracies of 2-3 millimetres can be achieved over such baselines with session lengths of 3 – 6 hours. An initialization period will be needed (a 24 hour solution should suffice) so that a base or reference session is obtained for all GPS stations. At each step in the descent, a test is conducted to see if the position calculated from GPS is statistically the same as that determined in the reference session.

It is not desired to use the calculated coordinates for positioning purposes in the descent, as error propagation would quickly degrade the quality of the results. It is desired to start from the top and bootstrap to the bottom station to confirm that nothing has moved. For each baseline, the coordinates determined during the reference session will be held fixed, and not the coordinates determined for that session (assuming nothing has moved).

In the event that something has moved, then a longer session length will be required to confirm the displacements of all GPS stations. A 24 hour session would be used to achieve this. Although the confirmation process is still a day long, at least the system has been able to give warning to within 3-6 hours of the displacement.

This technique is illustrated in Figure 6.9 and summarized in Figure 6.10. Each station is separated by a height difference of less than 150 m and the baselines are less than 2500 m. A 24 hour session will be used to determine

reference coordinates of all rover stations. After the first monitoring session, the baseline between Master (reference) and GPS 1 (rover) will be processed. If GPS 1 is determined to be in the same location as in reference session, it becomes the new reference station. The baseline between GPS 1 (reference) and GPS 2 (rover) is processed holding the reference coordinates for GPS 1 as fixed. If GPS 2 is determined to be in the same location as in the reference session, it becomes the new reference station and so on. If at any point in this process one of the points is determined to be unstable, then a longer session length will be required to confirm the displacements of all rover stations.
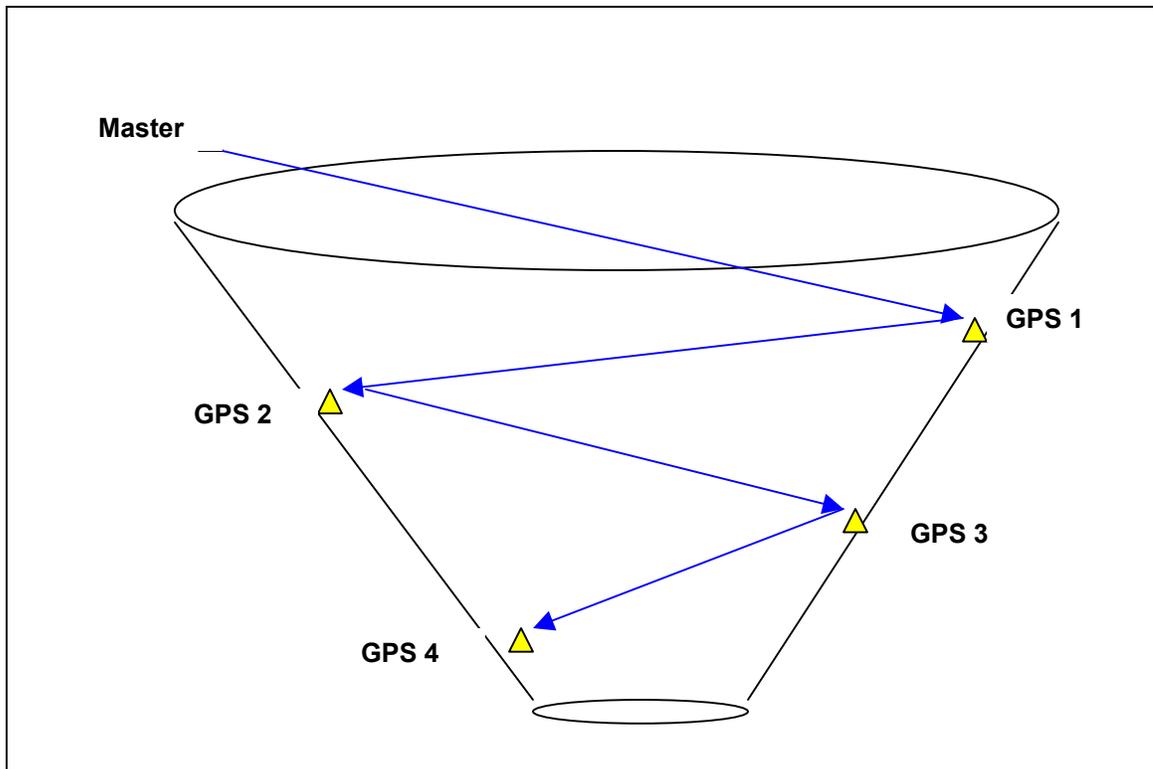
Figure 6.10   Bootstrapping to the Bottom of the Pit with GPS
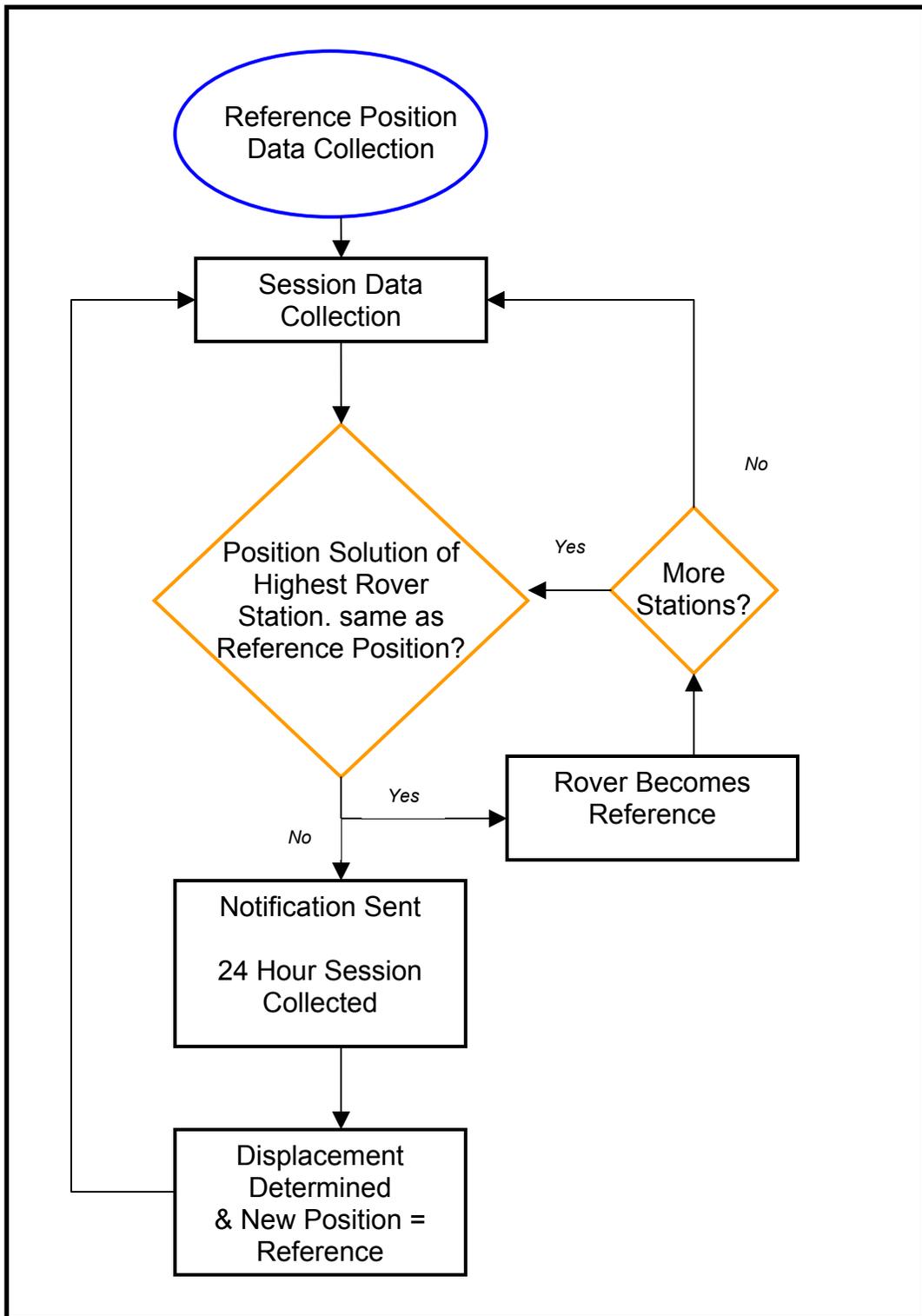
Figure 6.11   Bootstrapping to the Bottom Logistics

114

To determine the potential of this technique, a test was conducted using the HVC data. Unfortunately, the location of the GPS stations was such that it was not possible to abide by the 150 m height difference restriction between stations 424 and 987. Consequently, 424 had to be omitted from this analysis. Three baselines were used to bootstrap to the bottom of the pit: 987-RTS2 (dH = 45 m) RTS2-RTS1 (dH = 152 m) and RTS1-RTS3 (dH = 164 m). Figures 6.11 a-c illustrate the potential accuracy in the height component of the three baselines.
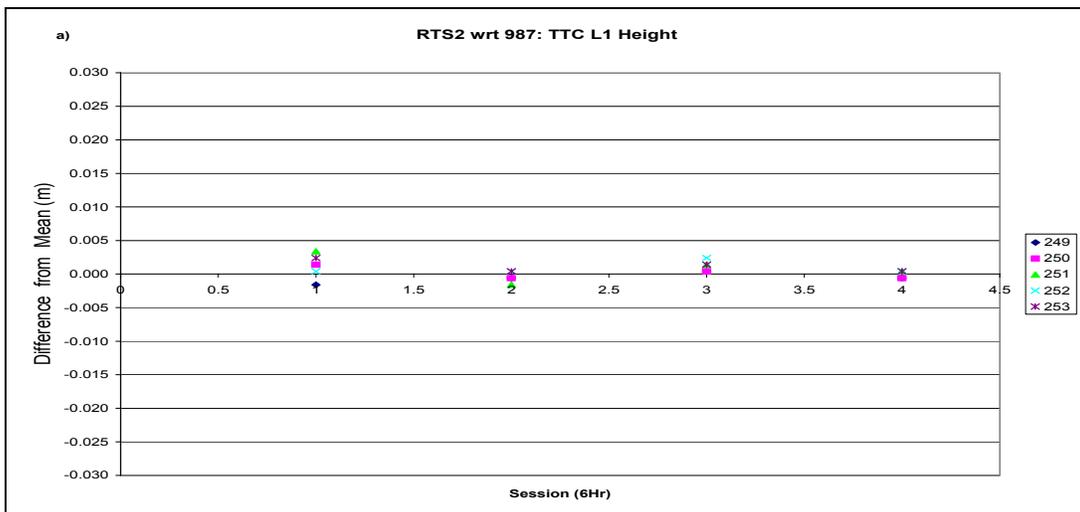
Figure 6.12 a   Accuracy in the Height Component using the Bootstrapping Method
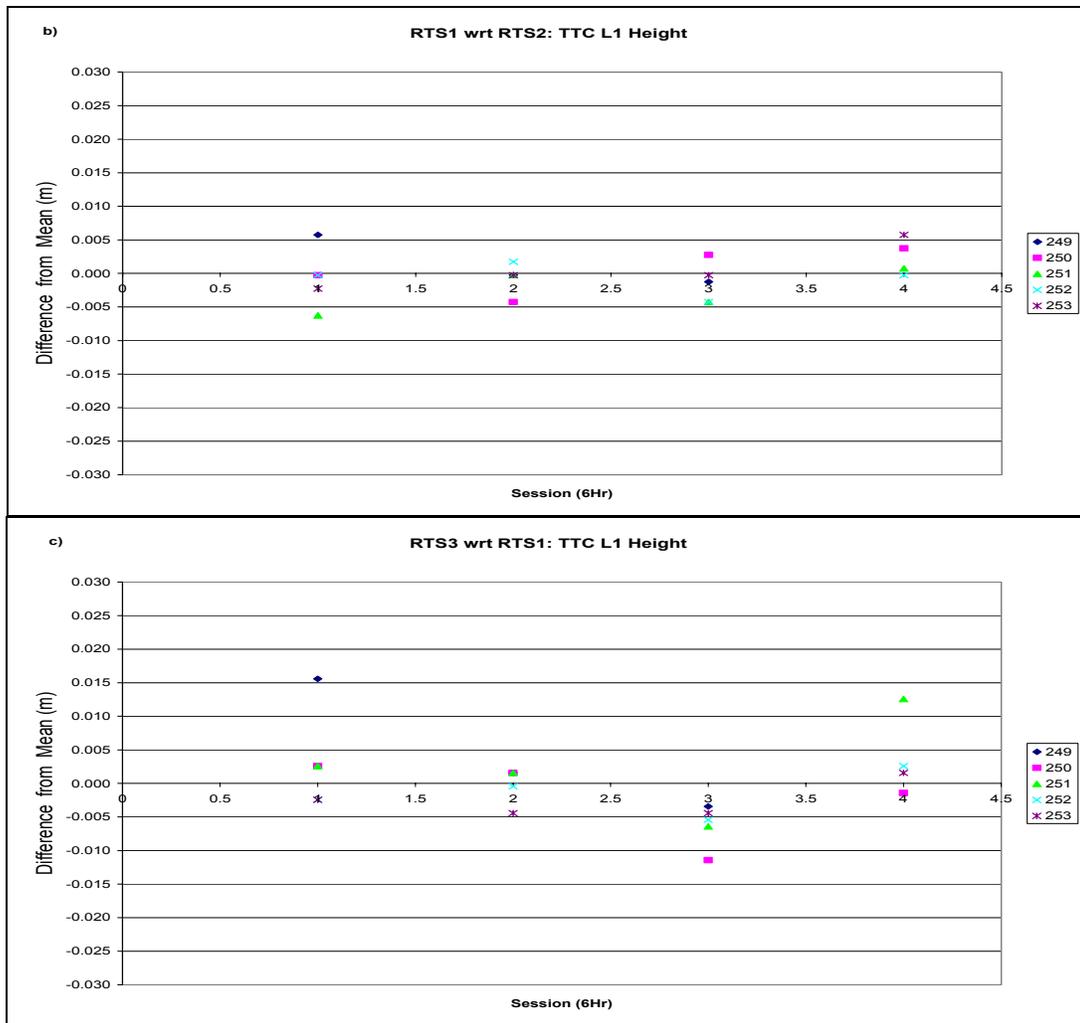
Figure 6.13 b-c   Accuracy in the Height Component using the Bootstrapping
Method

From Figure 6.10a it can be seen that there is no difficulty in achieving

millimetre accuracies between 987 and RTS2. In Figure 6.10b, the accuracy is

slightly worse (the height difference is 3 times larger and satellite visibility is more

restricted than with 987-RTS2), however, accuracies of 2-3 millimetres are still

being attained.

In Figure 6.10c there are two outliers visible. In this case where satellite visibility is highly restricted, it seems more practical to compare repeatabilities with solutions for a particular session. It can be seen that the second and third sessions offer solutions that are repeatable to within 2-3 millimetres from day-to-day. After removing the two outliers, the first and fourth sessions offer the same accuracy. If sessions are to be compared from day-to-day, reference solutions for the baseline should be calculated individually for each particular session, so that the daily variations are taken into account.

From these plots, it does appear as if this technique can be built upon to provide frequent and precise updates to the deformation monitoring system using GPS. These results could perhaps be further enhanced by having an additional GPS receiver to cut down on the large height differences between the RTS stations.

It is important to point out that this approach provides the required precision for each baseline and not necessarily the required accuracy. Since tropospheric delay is a systematic bias, it will add to the same amount whether or not several baselines or one baseline is used. The advantage of this approach is that it can confirm the stability in each step of the descent with a precision comparable to the accuracies found in the near ideal scenario. The disadvantage of this approach is that if the displacements of each station are slightly less than what can be detected, the total displacement will remain hidden. The risk of this

occurring increases with the number of steps. Further research must be conducted to verify the applicability of this technique.

6.6 GLONASS

Although, strictly speaking, the GLObal NAvigation Satellite System (GLONASS) is not an augmentation system for GPS since it was designed as a stand alone system, its principle function today can be considered as such. Hardships in the Russian economy have resulted in a depletion of the 24 satellite constellation to only 11 satellites [Russian Federation Ministry of Defense, 2004]. Although this discussion has been limited to GLONASS, its applicability to other global navigation satellite systems (e.g., Europe's Galileo Satellite Navigation System) is just as relevant. The only condition being that receiver technology must be developed to handle these additional satellite signals in order to benefit from them.

6.6.1 Purpose

The purpose of this investigation was to assess the potential benefit of using a combined GPS+GLONASS system over stand alone GPS in an open pit

environment. It was desired to determine whether or not such a system could improve the accuracies achieved at HVC. Figures 6.12 and 6.13 show the potential improvement in satellite visibility at RTS3 using GLONASS.
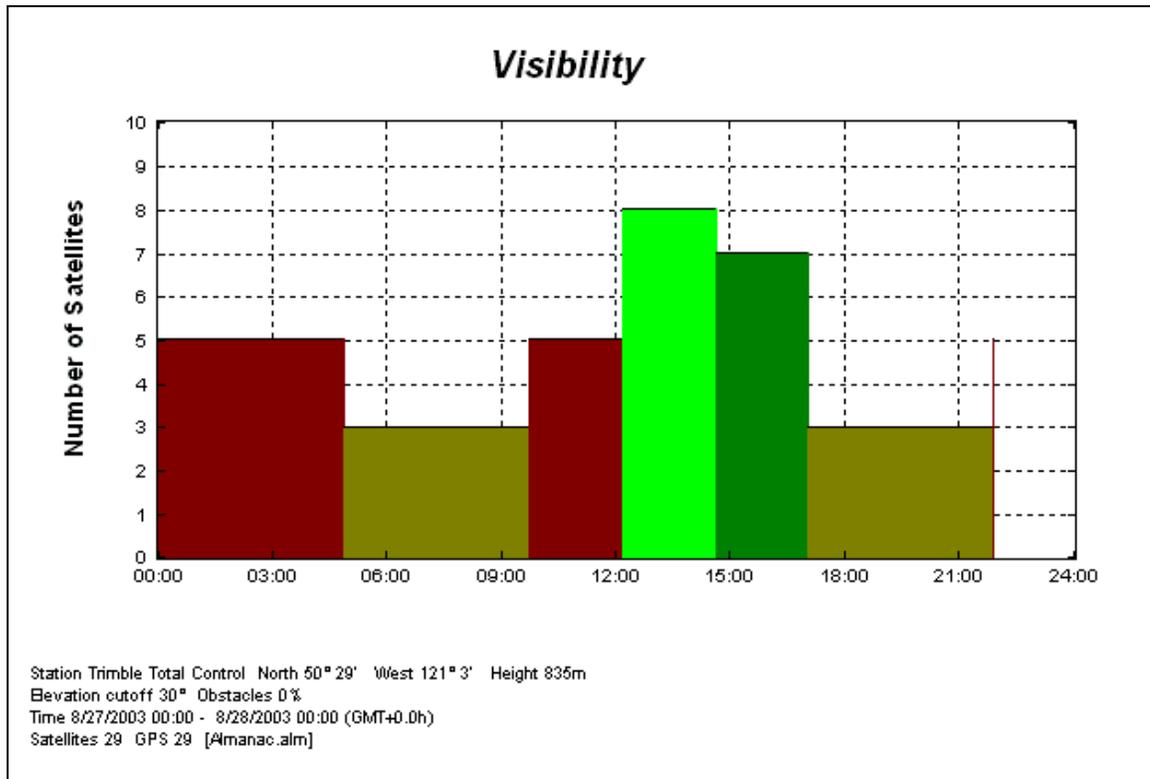
Figure 6.14   GPS Satellite Availability at RTS3, HVC
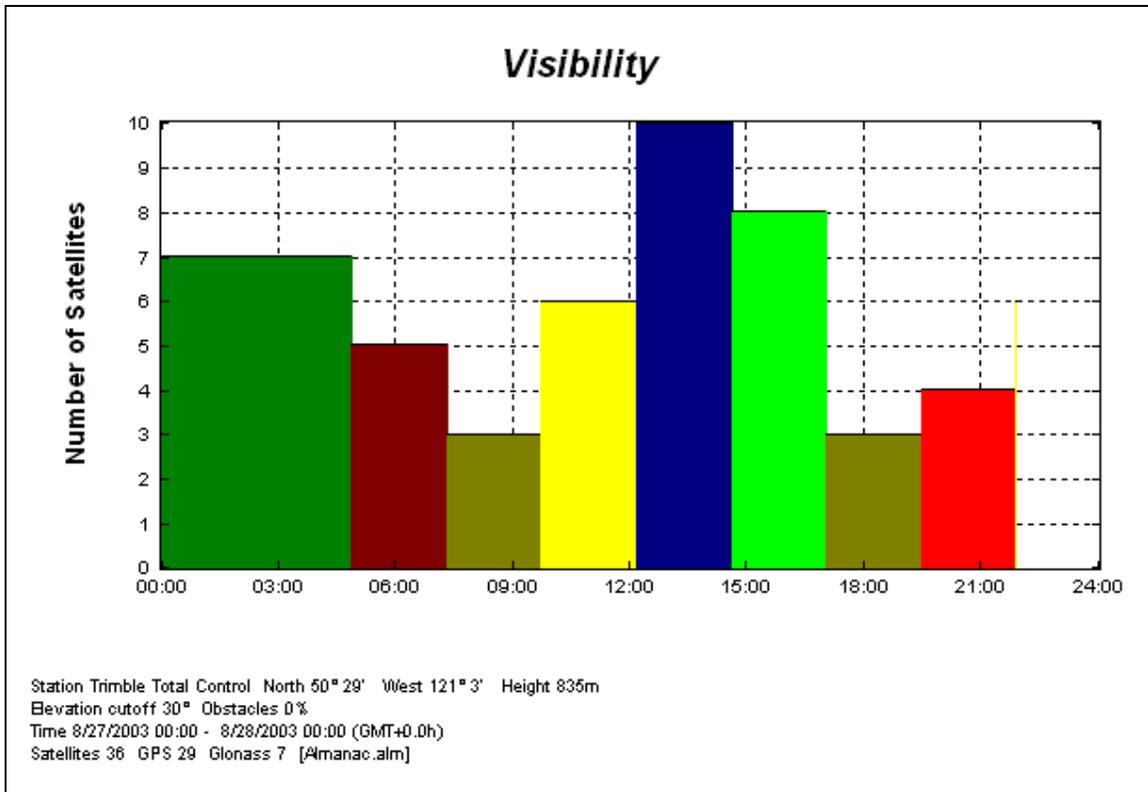
Figure 6.15   GPS+GLONASS Satellite Availability at RTS3, HVC

6.6.2 Equipment

For this experiment, two Javad Legacy receivers with Dual Depth Regant antennas were used to observe a baseline (Figure 6.14). Data was processed using Topcon's Pinnacle software.

Figure 6.16   Javad Legacy Receivers with Dual Depth Regant Antennas

6.6.3 Procedure

Because one of the antennas is permanently mounted on the roof of Head Hall at UNB (IGS station UNB1), it was not possible to observe a baseline at HVC with this equipment. Alternatively, a baseline was observed at UNB campus and a simulation of the open pit mine was performed. The second antenna was located on the roof of Gillin Wing, as illustrated in Figure 6.15. The baseline length for this experiment is 46 m. A pre-analysis of satellite visibility is shown in Figure 6.16.
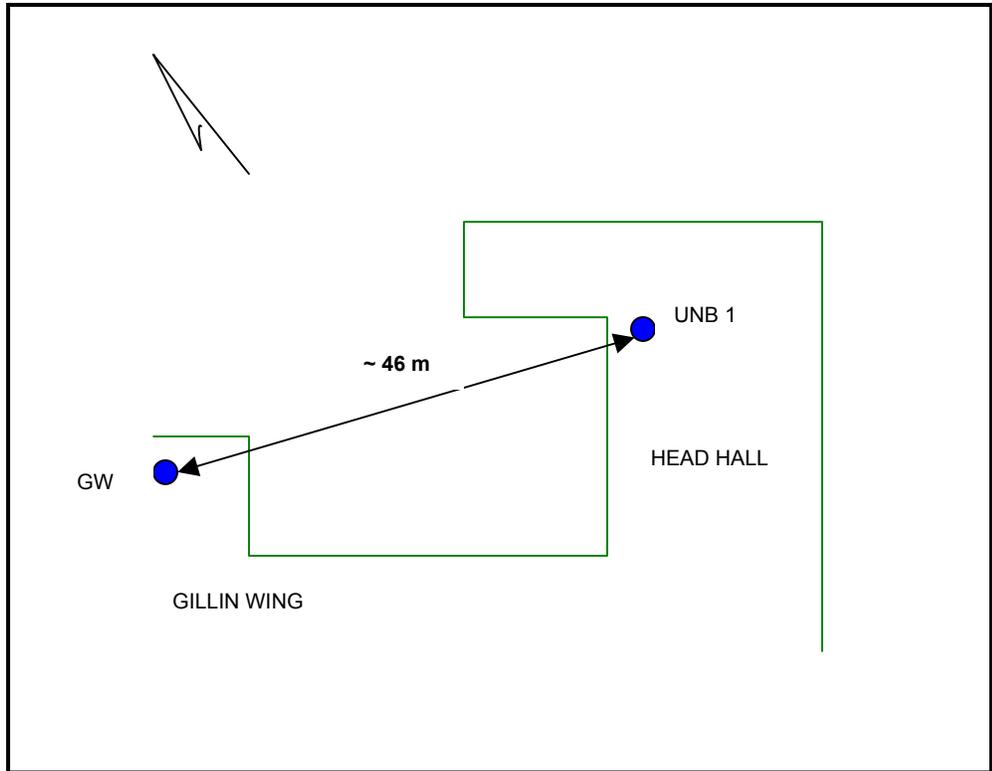
Figure 6.17   GLONASS+GPS Observed Baseline
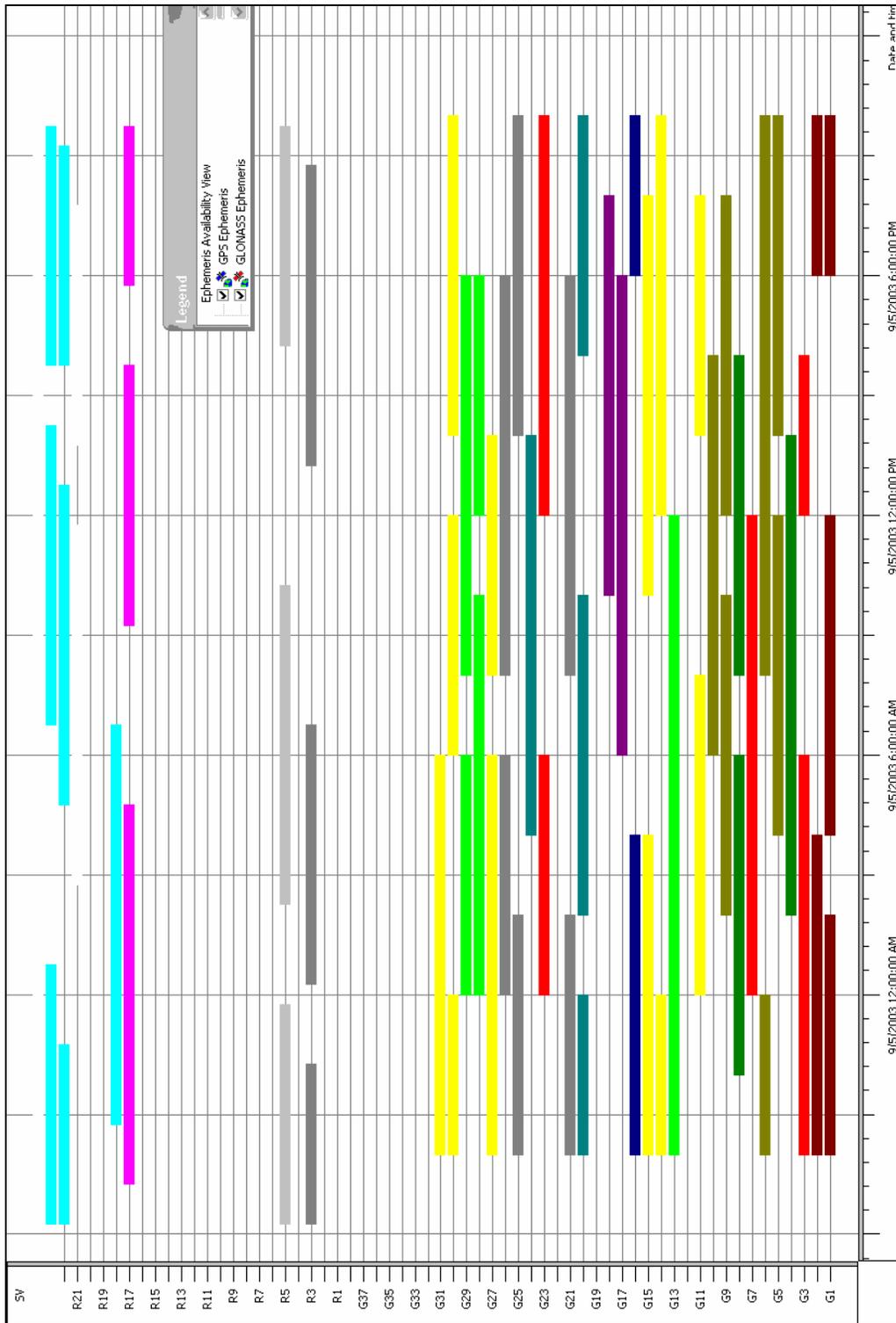
Figure 6.18   GPS & GLONASS Satellite Availability

To simulate the open pit mine environment, a 35 degree elevation cut off angle was imposed in processing, as illustrated in Figure 6.17. Hourly sessions were processed over a 24 hour period using GPS+GLONASS and stand alone GPS.
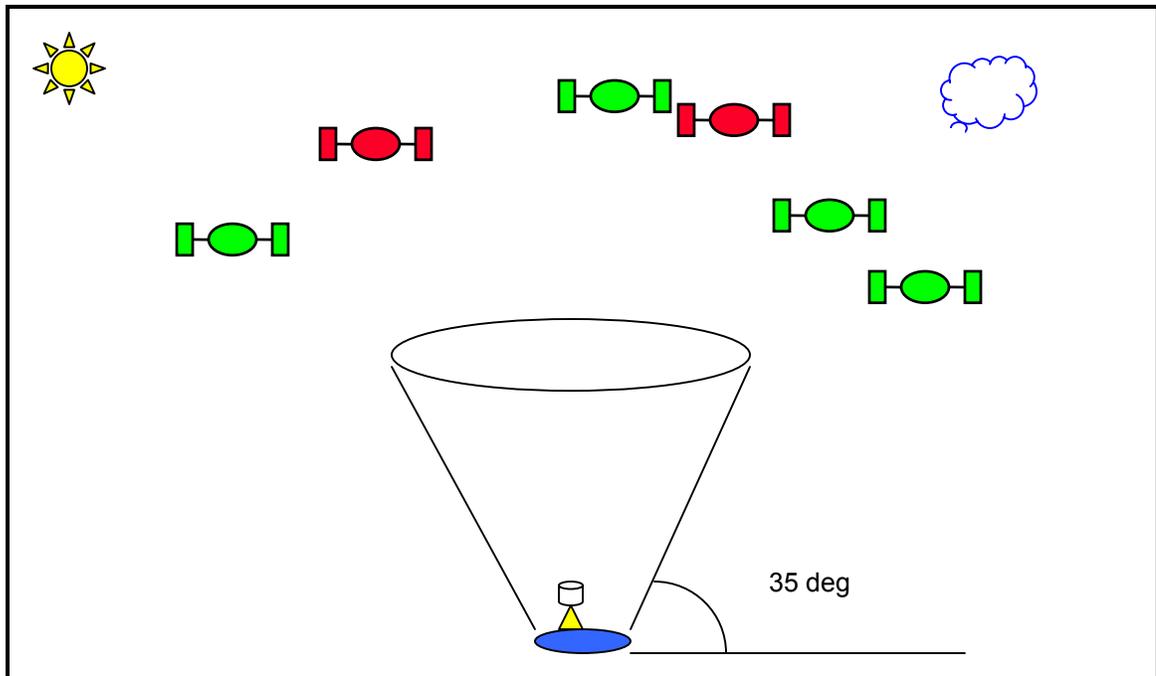
Figure 6.19   Open Pit Mine GPS+GLONASS Simulation

6.6.4   Findings

A plot of the height solutions using GPS+GLONASS and stand alone GPS is found in Figure 6.18. It can be deduced that the combined GPS+GLONASS solution is more consistent than stand alone GPS. In the 5th hour, it can be seen

that the combined solution offers a much better solution than stand alone. Table 6.4 also illustrates that higher accuracy can be achieved using a combined system.
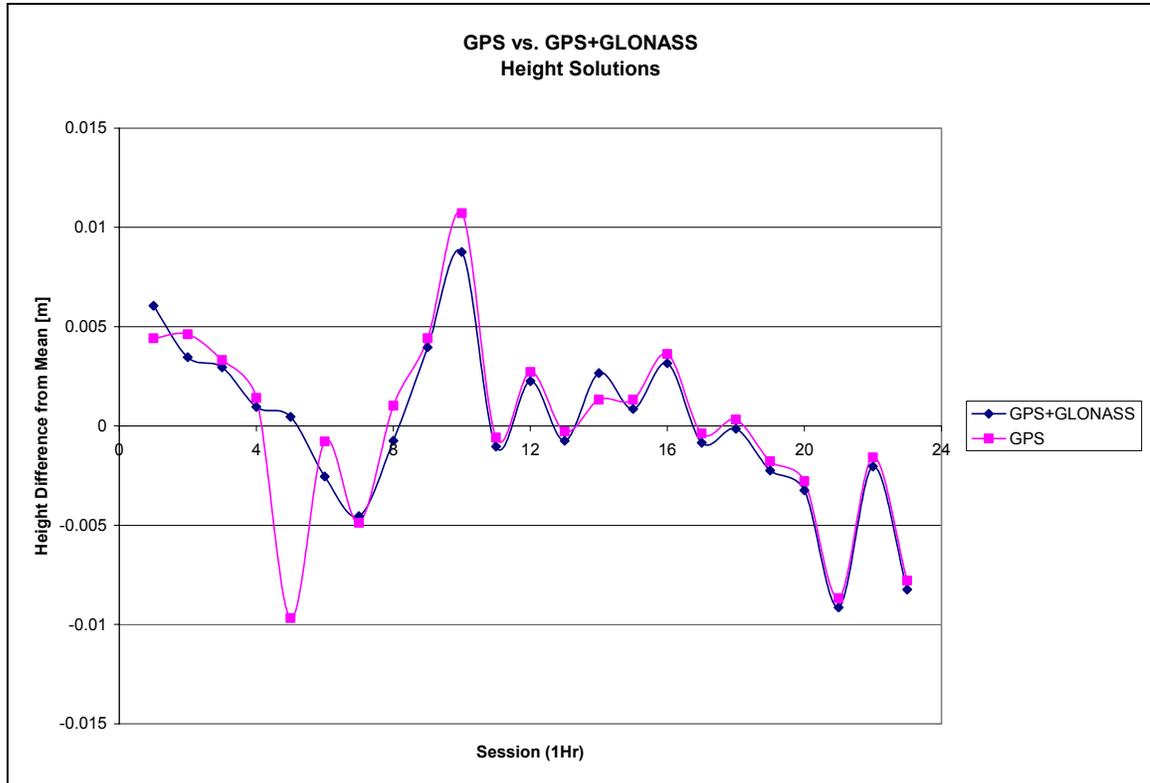
Figure 6.20   Comparison of Height Solutions between GPS and GPS+GLONASS

Table 6.4   GPS vs. GPS+GLONASS Baseline Component Standard Deviations

System	σN	σE	σH
GPS+GLONASS	0.001	0.001	0.004
GPS	0.002	0.001	0.005

125

Thus, there are accuracy improvements associated with enhancing GPS with GLONASS. For areas with restricted satellite visibility, the increased number of satellites is also a benefit, as was found in Johnson and van Diggelen [1999]. This becomes even more important in real-time kinematic applications.

6.7   Pseudolites

Suppose that terrestrial based, local satellites could provide the same information as a GPS satellite. Not only would a continuous supply of signals be available, but a predetermined geometric strength could be assigned to the solution. This is the concept of using pseudolites for precise positioning.

Pseudolites, or PLs, (from "pseudo-satellite") are ground based transmitters which can be used as a substitute for or to supplement GPS satellites [Dai *et al.*, 2001]. Pseudolites typically transmit signals using the GPS frequency bands (L1 = 1575.42 MHz and L2 = 1227.6 MHz) [Dai *et al.*, 2001]. Both pseudo-range and carrier phase measurements can be made using pseudolite signals. The first application of pseudolites was to test the GPS system in the late 1970s before the launch of the first GPS satellites [Dai *et al.*, 2001]. Recent advances in GPS user equipment have brought pseudolite applications from testing devices to clever augmentation tools.

6.7.1 Purpose

The purpose of this investigation was to assess the benefit of using pseudolites to augment GPS in an open pit environment through a simulation exercise. It was desired to determine whether or not such a system could help improve the accuracies achieved at HVC.

6.7.2 Procedure

To gain an appreciation for the magnitude of accuracy improvement that could be expected using pseudolites, a pre-analysis of the HVC scenario was performed. Using GPS data collected during the October 2002 field test, it was possible to determine which satellites were actually viewed from the RTS3 station. SP3 files containing coordinate information for the satellites were downloaded from the International GPS Service (IGS) so that design matrix of double-difference observations could be populated for each session. Potential PL locations were chosen and used to augment the design matrix to simulate pseudolite observations.

A local coordinate system was established with control station 424 at the origin so that coordinate values for the pseudolite locations could be determined. Four pseudolite locations were chosen in the north, south, east and west

quadrants of the pit (Figure 6.19). To determine the impact of vertical location of the pseudolite, different heights were assigned to each horizontal location. An initial height value of 0 was assigned to the pseudolite location so that it was at the same height as 424. Then, heights 400, 800 and 12000 m above and below 424 were considered. Local coordinates were scaled off a map and then converted to WGS84 geocentric coordinates.

Figure 6.21   Pseudolite Locations and Local Coordinate System

6.7.3 Findings

Relative horizontal dilution of precision values (RHDOP) and relative vertical dilution of precision values (RVDOP) were calculated for hourly sessions over a 12 hour period. For each 1 hour session, Table 6.5 presents the RVDOP value with stand alone GPS and the amount of improvement in RVDOP values associated with having a pseudolite in the indicated location. Table 6.6 presents a summary of the data in Table 6.5.

Table 6.5   Pseudolite Improvements in RVDOP values for each Session

Location	Height	Hour: 1	2	3	4	5	6	7	8	9	10	11	12
	RVDOPS:	1.5	1.5	1.1	0.9	0.9	0.9	1.0	1.2	1.4	1.4	2.7	2.0
North	0	0.2	0.4	0.0	0.0	0.0	0.0	0.1	0.1	0.2	0.1	0.1	0.1
	-400	0.5	0.6	0.1	0.1	0.1	0.0	0.2	0.2	0.4	0.2	0.4	0.5
	-800	0.7	0.8	0.2	0.2	0.2	0.2	0.3	0.4	0.6	0.3	1.1	1.0
	-12000	1.1	1.1	0.6	0.5	0.5	0.5	0.6	0.7	1.0	0.9	2.2	1.6
	400	0.1	0.2	0.0	0.0	0.0	0.0	0.0	0.0	0.1	0.1	0.3	0.0
	800	0.1	0.1	0.0	0.0	0.0	0.0	0.0	0.0	0.0	0.1	0.5	0.1
	12000	0.3	0.2	0.1	0.1	0.1	0.1	0.1	0.1	0.3	0.3	0.9	0.3
East	0	0.1	0.1	0.0	0.0	0.0	0.0	0.0	0.0	0.1	0.1	0.5	0.3
	-400	0.4	0.2	0.0	0.1	0.1	0.1	0.1	0.2	0.4	0.2	1.1	0.7
	-800	0.7	0.5	0.2	0.2	0.2	0.2	0.2	0.4	0.6	0.5	1.6	1.0
	-12000	1.1	1.1	0.6	0.5	0.5	0.5	0.6	0.7	1.0	0.9	2.2	1.6
	400	0.1	0.1	0.0	0.0	0.0	0.0	0.0	0.0	0.0	0.1	0.1	0.1
	800	0.1	0.1	0.1	0.0	0.0	0.0	0.0	0.0	0.0	0.2	0.2	0.0
	12000	0.3	0.2	0.1	0.1	0.1	0.1	0.1	0.2	0.3	0.3	0.9	0.3
South	0	0.1	0.1	0.1	0.0	0.0	0.1	0.0	0.0	0.0	0.2	1.2	0.8
	-400	0.2	0.3	0.2	0.1	0.1	0.1	0.0	0.1	0.0	0.4	1.5	1.0
	-800	0.4	0.5	0.3	0.2	0.1	0.2	0.1	0.2	0.2	0.6	1.8	1.2
	-12000	1.0	1.1	0.7	0.5	0.5	0.5	0.6	0.7	1.0	0.9	2.2	1.6
	400	0.1	0.1	0.0	0.0	0.0	0.0	0.0	0.0	0.1	0.1	0.9	0.6
	800	0.1	0.1	0.0	0.0	0.0	0.0	0.1	0.1	0.2	0.1	0.5	0.3
	12000	0.3	0.2	0.1	0.1	0.1	0.1	0.1	0.2	0.4	0.3	0.8	0.2
West	0	0.1	0.5	0.1	0.0	0.0	0.1	0.0	0.0	0.0	0.1	1.0	0.7
	-400	0.2	0.7	0.3	0.1	0.1	0.1	0.2	0.2	0.1	0.3	1.5	1.1
	-800	0.4	0.8	0.4	0.2	0.1	0.3	0.4	0.4	0.4	0.5	1.9	1.3
	-12000	1.0	1.1	0.7	0.5	0.5	0.5	0.6	0.7	1.0	0.9	2.2	1.6
	400	0.1	0.3	0.0	0.0	0.0	0.0	0.0	0.0	0.1	0.1	0.4	0.3
	800	0.1	0.2	0.0	0.0	0.0	0.0	0.0	0.0	0.2	0.1	0.1	0.1
	12000	0.3	0.2	0.1	0.1	0.1	0.1	0.1	0.2	0.3	0.3	0.9	0.2

Table 6.6   Summary of Improvements in RVDOP Values Associated with PLs

Location		Average	Max	Min
North	**0**	0.1	0.4	0.0
	-400	0.3	0.6	0.0
	-800	0.5	1.1	0.2
	-12000	0.9	2.2	0.5
	400	0.1	0.3	0.0
	800	0.1	0.5	0.0
	12000	0.2	0.9	0.1
East	**0**	0.1	0.5	0.0
	-400	0.3	1.1	0.0
	-800	0.5	1.6	0.2
	-12000	0.9	2.2	0.5
	400	0.0	0.1	0.0
	800	0.1	0.2	0.0
	12000	0.2	0.9	0.1
South	**0**	0.2	1.2	0.0
	-400	0.3	1.5	0.0
	-800	0.5	1.8	0.1
	-12000	0.9	2.2	0.5
	400	0.2	0.9	0.0
	800	0.1	0.5	0.0
	12000	0.2	0.8	0.1
West	**0**	0.2	1.0	0.0
	-400	0.4	1.5	0.1
	-800	0.6	1.9	0.1
	-12000	0.9	2.2	0.5
	400	0.1	0.4	0.0
	800	0.1	0.2	0.0
	12000	0.2	0.9	0.1

Additional analysis was performed on the improvement of RDOP values using 2 and 3 pseudolites. To summarize the findings of this pre-analysis the following conclusions are drawn:

1. Pseudolites do improve RDOP values. The amount of improvement will depend upon how restrictive the environment is on GPS satellite

visibility and how strategically the PLs can be placed to account for these restrictions.

2. Additional pseudolites do not significantly improve RDOP values in each session. If it were possible to move one pseudolite around from one session to the next, one would be able to attain nearly as good a result as using multiple PLs. The major advantage of deploying several PLs is that it increases the chance of having one in a location that will produce the most benefit.

6.7.4 Further Investigation

In the spring of 2003, the CCGE purchased an IN200–D pseudolite kit [IntegriNautics 2002]. An additional IN1200 receiver was purchased and 2 more pseudolites were leased for the purpose of testing a pseudolite system at HVC. Following the GPS field test in 2003, a pseudolite field test was conducted (Figure 6.20). However, there are significant differences in processing pseudolite and GPS data (e.g., pseudolite navigation messages do not contain location information, pseudolite range values are biased, tropospheric modelling is unique, multipath effects do not tend to average out). The processing and analysis of this data will be the focus of further work by the author.

Figure 6.22   Pseudolite Field Test at HVC

7 CONCLUSIONS AND RECOMMENDATIONS

In favourable GPS conditions for short, static baselines, it is possible to achieve solutions for the position components of +/- 2 mm at standard confidence level. In order to achieve these results, it is recommended that:

1. Quality software is used (Trimble Total Control performed the best of the commercial software tested);

2. A sample rate of 30 seconds or higher is implemented;

3. An elevation cut-off angle of 10-15 degrees is imposed;

4. The Saastamoinen or Hopfield tropospheric models be used;

5. A session length of at least 3 hours is observed;

6. Sessions are observed when satellite visibility is the best; and

7. Sessions are observed at night.

In unfavourable GPS conditions for short, static baselines, the height difference between stations directly affects the achievable accuracy. Height differences tend to cause residual tropospheric delay biases. For height differences less than 150 m, session lengths of 6 hours produced results with accuracies of +/- 3 mm or better in all three components at the standard confidence level. For height differences of up to 650 m, session lengths of 24 hours produced results with accuracies of +/- 5 mm or better in all three components at the standard confidence level.

Longer session lengths tend to produce better results with large height differences. Increasing the session length increases the redundancy of the problem. For baselines having restricted satellite visibility, longer session lengths allow better satellite geometry to be viewed, thus providing a better quality solution. Additionally, erratic meteorological variations caused by microclimates have a less pronounced impact on the solution when they are averaged over longer periods. That is, the longer the observation period, the more likely the troposphere is to have behaved as modelled. The length of the session that can be observed will be dictated by the project requirements.

With the level of accuracy presently achievable with GPS, it was determined that sub-centimetre level displacements can be detected at HVC through the implementation of a system similar to Scenario II described in Section 3.6. If appropriate measures are taken to achieve the cited RTS accuracies, displacements can be detected within +/- 7 mm at 95% confidence in all three solution components of the target points.

There is still room for improvement in the GPS results achieved in this analysis. Several methods were presented which potentially can be used for obtaining more accurate results. Depending on the project scenario, any or all of the following techniques may be used.

Although multipath was not a major error source in the results at HVC, it could be in other mining environments. In such cases, day-to-day correlation analysis may be applied to enhance position solutions.

Estimation of a tropospheric delay parameter was also shown to improve the accuracy of the solution. This strategy was not available in processing in Trimble Total Control. Therefore, the results presented may be improved by implementing this technique. Although not evaluated here, the Kalman filter approach to stochastically estimating zenith path delays (discussed in section 2.1.2) could also be used to improve the results.

The use of meteorological data in GPS processing (as conventionally implemented in tropospheric modelling) does not improve the accuracy of the results. However, it is has been shown [Rothacher *et al*., 1986] that the use of meteorological data in differential tropospheric modelling can be beneficial. It was not possible to verify these findings due to time constraints. This technique warrants further investigation, especially if tropospheric biases can be mitigated over baselines having large height differences.

A simple moving average filter was tested and shown to yield accuracies of +/- 3 mm in solution components. This technique satisfies project needs by providing more frequent displacement updates, but is not a true 'real-time' system. The full displacement will not be revealed until the moving average filter has all of its 'session blocks' based upon the new displaced position.

A bootstrapping method was proposed to implement a series of steps to the bottom of the pit to confirm the stability of each point. This strategy was demonstrated to potentially provide accuracies of 2 to 3 mm in each solution

components. Even at RTS3 such accuracies could be achieved by observing at favourable periods during the day.

The potential of a combined GPS+GLONASS system was investigated. It was shown that the results obtained from the combined system were more accurate than a stand alone GPS system. The benefits of such a system will be more apparent in areas of restricted satellite visibility.

A pre-analysis of implementing a pseudolite system at HVC was conducted. It was found that pseudolites do improve relative dilution of precision values. Several field tests have also been conducted using pseudoliltes. Processing software for the GPS+PL data remains to be developed, which will be used to confirm theoretical findings.

The effect of refraction was one of the main limitations of the RTS-based deformation monitoring system used at HVC. While investigating the potential of GPS for augmenting the RTS-based system, refraction again surfaced as the major restriction on the achievable accuracy of the system. This time it was introduced in the form of a residual tropospheric delay bias.

Over baselines with small height differences (i.e., less than 150 m) the impact of residual tropospheric delay is generally small, and GPS can effectively be used to obtain millimetre level displacement detection. When baselines have larger height differences, this bias becomes more pronounced. However, the nature of GPS makes this bias more quantifiable than with conventional RTS

measurements. If correctly modelled, estimated or filtered out, similar accuracies can be expected as for baselines having small height differences.

The accuracy that can be expected with GPS makes it a viable option for augmenting the CCGE's current deformation monitoring system. GPS allows high accuracy coordinate information to be obtained for the RTS+GPS control stations within the pit, without having to worry about instrument instability. With advances in satellite navigation technology and processing strategies, GPS biases (such as tropospheric delay) can be more readily accounted for, allowing for a more flexible deformation monitoring system.

REFERENCES

A. Chrzanowski and Associates, 2004. *Highland Valley Copper: The Use of GPS in Pit Wall Stability Monitoring in the Valley Pit*. Project Report, A. Chrzanowski & Associates, Frederiction, NB, Canada.

Bern, 2003. *Antenna Phase Centre Variation Values.* Astronomical Institute of the University of Bern, ftp://ftp.unibe.ch/aiub/BSWUSER/GEN/, accessed 12 July 2003.

Beutler, G., I. Bauersima, W. Gurtner, M. Rothacher, T. Schildknecht and A. Gieger, 1988. "Atmospheric refraction and other important biased in GPS carrier phase observations." *Atmospheric Effects on Geodetic Space Measurements*, Monograph 12, School of Surveying, University of New South Wales, pp.15-43.

Beutler, G., W. Gurtner, M. Rothacher, U. Wild, and E. Frei, 1989. "Relative Static Positioning with the Global Positioning System: Basic Technical Considerations." *Global Positioning System: An Overview*, Symposium No. 102, Edinburgh, Scotland, August 7-8, 1989.

Black, H.D. 1978. "An easily implemented algorithm for the tropospheric range correction." *Journal of Geophysical Research*. No. 83(B4), pp.1825-1828.

Braasch, M.S. and A.J. Van Dierendonck, 1999. "GPS receiver architectures and measurements." Proceedings of the *IEEE*, Vol. 87, No.1, January 1999, pp. 48-64.

Brunner, F.K. and S. McCluskey, 1991. "Tropospheric Zenith Delay Parameters: How Many Should Be Estimated in GPS Processing?" *Aust, J. Geod. Photogram. Surv*., No.55, pp.67-75.

Collins, J.P. and R.B. Langley, 1997. *Estimating the residual tropospheric delay for airborne differential GPS positioning (A Summary)*. http://gauss.gge.unb.ca/papers.pdf/iag97.tropo.pdf, accessed on: 28 Nov. 2003.

Chrzanowski, A., Y. Chen, R. Leeman and J. Leal, 1989. "Integration of the Global Positioning System with Geodetic Leveling Surveys in Ground Subsidence Studies." *CISM* Journal, Vol. 43, No.4, Winter 1989, p.377.

Chrzanowski, A., 1999. *Effects of Atmospheric Refraction on Monitoring Vertical Displacements*. Report submitted to Geometronic section of the Metropolitan Water District of Southern California, February, 1999.

Chrzanowski, A., 2002. GGE 6001: Advanced Engineering and Mining Surveys Lecture Notes. Department of Geodesy and Geomatics Engineering, University of New Brunswick, Fredericton, New Brunswick, Canada.

Chrzanowski, A., 2004. Personal Communciation. Director, Canadian Centre for Geodetic Engineering, University of New Brunswick, Fredericton, New Brunswick, Canada.

Dai, L., J. Wang, C. Rizos and S. Han, 2001. *Applications of Pseudolites in Deformation Monitoring Systems*. www.gmat.unsw.edu.au/snap/publications/dai_etal2001a.pdf. Accessed on: 23 October 2002.

Duffy, M., C. Hill and C. Whitaker, 2001. "An Automated and Integrated Monitoring Program for Diamond Valley Lake in California." Paper presented at the *10th FIG International Symposium on Deformation Measurements*, Orange, CA, March 19-22, 2001. http://ccge.unb.ca/publications/downloads/ accessed on: 9 January 2004.

Essen L., and K.D. Froome, 1951. "The refractive indices and dielectric constants of air and its principal constituents at 24 000 Mc/s." Proceedings of *Physical Society*, Vol. 64(B), pp. 862-875.

Goad, C.C., and L. Goodman, 1974. "A modified Hopfield tropospheric refraction correction model." Presented at the *Fall Annual Meeting of the American Geophysical Union*, San Francisco, December 1974.

Gurtner, W., G. Beutler, S. Botton, M. Rothacher, A. Geiger, H.G. Kahle, D. Schneider and A. Wiget, 1989. "The use of the Global Positioning System in mountainous areas." *Manuscripta Geodaetica*, Vol. 14, No. 1, pp. 53-60.

Hofmann-Wellenhof, B., H. Lichtenegger and J. Collins , 2001. *Global Positioning System: Theory and Practice*, 5th rev. ed., Springer-Verlag, New York.

Hopfield, H.S., 1969. "Two-quadratic tropospheric refractivity profile for correcting satellite data." *Journal of Geophysical Research*, No. 74, pp. 4487-4499.

IntegriNautics, 2002. IntegriNautics Corporation, 1505 Adams Drive, Menlo Park, CA. www.IntegriNautics.com accessed on: 19 April 2004.

Janes, H.W., R.B. Langley and S.P. Newby, 1991. "Analysis of tropospheric delay prediction models: comparisions with ray-tracing and implications for GPS relative positioning." *Bulletin Geodesique* No. 65, pp.151-161.

Johnson, L., F. van Diggelen, 1998. "Advantages of a Combined GPS+GLONASS Precision Sensor for Machine Control Applications in Open Pit Mining." http://products.thalesnavigation.com/assets/techpapers/14_Advantages_GPSGlonass.pdf, accessed on 20 Jan. 2004

Kim, D., R.B. Langley, J. Bond and A. Chrzanowski (2003). "Local deformation monitoring using GPS in an open pit mine: Initial Study." *GPS Solutions*, in press. Presented at IUGG 2003, Sapporo, Japan, July.

Kleusberg A. and R.B. Langley, 1990. "The Limitations of GPS". Reprint from *GPS World,* March/April 1990.

Langley, R.B., 1995. *Propagation of the GPS Signals*. Chapter 3 of *GPS for Geodesy*, Proceedings of the *International School of GPS for Geodesy*, Delft, the Netherlands, March 26 - Aprils 1, 1995.

Leica GeoSystems, 2002. GPS Newsletter- General. *A One Page Newsletter On System 500 GPS, Vol. 01, No. 12*. http://www.leicaatl.com/support/gps/gps_faqs/PDF_Vol_01/GPS01%20No.%2012%20General%20GPS.pdf , accessed on: 12 November 2002.

Leica GeoSystems, 2004. "Leica TC1800 / TCA1800." *TPS System 1000 Total Stations*. http://www.leica-geosystems.com/surveying/product/totalstations/tc1800.htm, accessed on 06 Jan 2004.

Leick, A., 1995. *GPS Satellite Surveying*. 2nd ed., A Wiley-Interscience Publication, New York.

Mader, G.L., 2002. GPS Antenna Calibration at the National Geodetic Survey. http://www.ngs.noaa.gov/ANTCAL/Files/summary.html, 07 November 2002.

Mining Technology, 2003. "Highland Valley Copper Mine, Canada." *The Website for the Mining Industry.* http://www.mining-technology.com/projects/highland/index.html, accessed on: 12 December 2003.

MiStupid Online Knowlege Magazine, 2003. *Layers of the Atmosphere*. http:///www.mistupid.com/science/images/ atmosphere.gif. Accessed on: 27 November 2003.

Newcomen, H.W., C.S. Maggs and L. Shwydiuk, 2003. *Managing Pit Slope Displacements: Highland Valley Copper's Lornex Pit Southwest Wall*. Canadian Institute of Mining, Metallurgy and Petroleum (CIM) Bulletin, Volume 96, No.1071.

NGS, 2003. Antenna Phase Centre Variation Values. National Geodetic Survey, http://www.ngs.noaa.gov/ANTCAL/index.shtml. accessed on 12 July 2003.

Radovanovic, R. 2000. "High Accuracy Deformation Monitoring Via Multipath Mitigation by Day-To-Day Correlation Analysis." Proceedings of the *13th International Technical Meeting of the Satellite Division of the Institute of Navigation* (ION GPS 2000), 19-22 September 2000, Salt Lake City, UT.

Rizos, C. 2001. *Principles and Practice of GPS Surveying*. http://www.gmat.unsw.edu.au/snap/gps/gps_survey/principles_gps.htm, accessed on: 09 February 2003.

Rothacher, M., G. Beutler, W. Gurtner, A. Geiger, H.G. Kahle, and D. Schneider, 1986. "The 1985 Swiss GPS Campaign." *Fourth International Geodetic Symposium on Satellite Positioning*, Austin, Texas, 979-991.

Rüeger, 1990. *Electronic Distance Measurement*. 3rd ed., Springer-Verlag, Berlin Hiedelberg.

Russian Federation Ministry of Defense, 2004. "History." *Coordinational Scientific Information Center.* http://www.glonass-center.ru/frame.html, accessed on: 20 January 2004.

Saastamoinen, J., 1972. "Atmospheric correction for the troposphere and stratosphere in radio ranging of satellites." *Use of artificial satellites for geodesy*, Geophysical Monograph 15, American Geophysical Union, Washington, D.C.

Seeber, G., 1993. *Satellite Geodesy: Foundations, Methods, and Applications*. Walter de Gruyter, Berlin, NewYork.

Tralli, D.M. and S.M. Lichten (1990). "Stocastic estimation of tropospheric path delays in Global Positioning System geodetic measurements." *Bulletin Geodesique*, Vol. 64, pp127-159.

Venture Kamloops. *Kamloops and Area Maps*.
http://www.venturekamloops.com/SiteCM/U/D/CC62B3D5E07F301A.pdf,
accessed on: 03 April 2004.

Wang, J., 2002. "Pseudolite Applications in Positioning and Navigation: Progress and Problems." *Journal of Global Positioning Systems*, Vol. 1 No.1, pp. 48-56.

Ware, R., 2004. Personal Communication. Customer Support Representative, Radiometrics Corporation, 2840 Wilderness Place Unit G, Boulder, Colorado. http://www.radiometrics.com.

Weill, L.R., 2003. "Multipath Mitigation. How Good Can It Get with New Signals?" *GPS World Innovation Column*, June 2003. http://www.gpsworld.com, accessed on 20 August 2003.

Wells, D.E., N. Beck, D. Delikaraoglou, A. Kleusberg, E.J. Krakiwsky, G. Lachapelle, R.B. Langley, M. Nakiboglu, K.P. Schwarz, J.M. Tranquilla and P. Vanicek ,1987. *Guide to GPS Positioning*. Canadian GPS Associates, Fredericton, N.B., Canada.

Wert, T. 2003. Personal Communication. MScE Candidate, Department of Geodesy and Geomatics Engineering, University of New Brunswick, Fredericton, New Brunswick, Canada, December.

Wilkins, R., G. Bastin, A. Chrzanowski, W. Newcomen and L. Shwydiuk, 2003a. *A Fully Automated System for Monitoring Pit Wall Displacements*. Paper presented at: *SME 2003*, Cincinnati, OH, February 24-26, 2003. Available at: http://ccge.unb.ca.

Wilkins, R., G. Bastin and A. Chrzanowski, 2003b. *ALERT—A fully automated displacement monitoring system*. Proceedings of *CAMI 2003,* Sept. 8-10, 2003, Calgary, Canada.
Available at: http://ccge.unb.ca/publications/all_publications.php.

Wilkins, R., 2004 Personal Communciation. Senior Engineer, Canadian Centre for Geodetic Engineering, University of New Brunswick, Fredericton, New Brunswick, Canada.

Wubbena, G., A. Bagge, G. Boettcher, M. Schmitz, and P. Andree, 2001. "Permanent Object Monitoring with GPS with 1 Millimeter Accuracy." Proceedings of *ION GPS 2001*, Salt Lake City, UT, 11-14 Sept., 2001.

VITA

Candidate's full name:

Donald Jason Bond

Universities attended:

University of New Brunswick, B.Sc.E., 2002

Publications:

Bond, J. 2004. "Demographic Study of Licensed Land Surveyors in the Maritimes." *Geomatica,* Summer 2004 (in press).

Bond, J., D. Kim, R.B. Langley and A. Chrzanowski, 2003. "*An investigation on the use of GPS for deformation monitoring in open pit mines.*" Proceedings of the Fourth International Conference on Computer Applications in the Minerals Industries (CAMI 2003), September 8-10, 2003, Calgary, Alberta, Canada.

Kim, D., R.B. Langley, J. Bond and A. Chrzanowski, 2003. "*Local deformation monitoring using GPS in an open pit mine: Initial study.*" Presented at IUGG2003, Sapporo, Japan, July. GPS Solutions, September 2003, 7:176-185.